CFTR GATING MECHANISM: THE ROLE OF DIMERIZATION OF NUCLEOTIDE BINDING DOMAINS

A Dissertation
Presented to
The Faculty of the Graduate School
University of Missouri

In Partial Fulfillment
of the Requirements for the Degree
of Doctor of Philosophy

By

XIAOHUI WANG

Dr. Tzyh-Chang Hwang, M.D., Ph.D. Dissertation Supervisor

Dec 2009

The undersigned, appointed by the Dean of the Graduate School, have examined the dissertation entitled:

CFTR GATING MECHANISM: THE ROLE OF DIMERIZATION OF NUCLEOTIDE BINDING DOMAINS

presented by Xiaohui Wang

a candidate for the degree of Doctor of Philosophy

and hereby certify that in their opinion, it is worthy of acceptance.

_____

Dr. Tzyh-Chang Hwang

_____

Dr. Kevin D. Gillis

_____

Dr. Mark A. Milanick

_____

Dr. Liqun (Andrew) Gu

_____

Dr. Xiaoqin Zou

ACKNOWLEDGEMENTS

Many people contribute to my dissertation, without their help and supporting, I couldn’t finish my work today. My supervisor, Dr. Tzyh-Chang Hwang, guided me all these years; I really appreciate his time, his intelligent ideas, his support and all his help.

I would like to extend my thanks to all my committee members, Dr. Xiaoqin Zou, Dr. Mark Milanick, Dr Kevin Gillis and Dr. Andrew Gu. They are not only helping me on research work, but also help me on study and life. I want especially thanks Dr. Zou because she brought me to the research field, provided the beginning opportunities for me to work and study in this field.

My laboratory collegues are gratefully acknowledged: Dr. Zhen Zhou, Dr. Yoshiro Sohma, Dr. Min Li, Dr. Silvia G Bompadre, Dr. Tomohiko Ai, Dr. Hao-Yang Liu, Dr. Zoia Kopeikin, Cindy Chu, Shenghui Hu, Dr. Hiroyasu Shimizu, Dr. Jeong Han Cho, Mingfeng Tsai , Haruna Miki and Yonghong Bai, all of their contributions, discussions, and helps are very appreciated.

I would also thank my family, my parents and my friends for their support.

TABLE OF CONTENTS

LIST OF FIGURES

FIGURE **PAGE**

CFTR GATING MECHANISM: THE ROLE OF DIMERIZATION OF NUCLEOTIDE BINDING DOMAINS

Xiaohui Wang

Tzyh-Chang Hwang, M.D., Ph.D. Dissertation supervisor

Abstract

The chloride channel, cystic fibrosis transmembrane conductance regulator (CFTR) belongs to ATP-binding cassette (ABC) transporter superfamily. As a member, the CFTR has two membrane spanning domains (MSD), forming the channel pore, and two nucleotide binding domains (NBD), controlling the channel gating (opening and closing). The CFTR also has a unique regulatory (R) domain. After the CFTR is phosphorylated at R domain, gating of the phosphorylated CFTR is coupled to ATP binding and hydrolysis at CFTR's two NBDs. Recent studies present evidence that the open channel conformation reflects a head-to-tail dimerization of CFTR's two NBDs with two ATP molecules sandwiched at the interface of the dimer, forming two ATP binding sites. However, the role of dimerization in channel gating is unknown. Furthermore, how does conformation change of NBD dimerization transmit to channel opening is unclear.

We first investigated whether two ATP binding sites play an equivalent role in the dynamics of NBD dimerization, therefore in gating CFTR channels. By identifying two critical aromatic amino acids (W401 in NBD1 and Y1219 in NBD2) that coordinate the adenine ring of the bound ATP, we are able

to study the distinct roles of these two binding sites, without disturbing the ATP hydrolysis. Mutations of these two equivalent residues result in two channels with totally different gating behavior. W401G has little effect on the sensitivity of the opening rate to [ATP], but Y1219G dramatically lowers the apparent affinity for ATP by more than 50-fold. On the other hand, W401G shortens the open time constant, while Y1219G has little effect on channel open time. We conclude that opening of the channel is initiated by ATP binding at the NBD2 site, and tighter binding at W401 at the NBD1 site prolongs channel open time.

We then studied the role of signature sequence in channel gating. We found that micromolar [Cd^{2+}] can dramatically increase the activity of G551D-CFTR, whose activity is insensitive to [ATP]. By mutations changing individual residues from signature sequence, a specific region of the signature sequence is found to result in positive response to Cd^{2+}. We thus conclude that signature sequence serves as a switch that transmits the signal of Cd^{2+} binding to the gate opening. The Cd^{2+} effect is found to work through forming a metal bridge connecting G551D/C to unknown cysteine residue in CFTR. Surprisingly, the cysteine is identified to be 832C in R domain, which can not fit to the NBD dimerization idea. This challenges whether NBD dimerization is absolutely required for channel gating. We propose that R domain, especially around 832, mediates the signal transmission of ligand binding to channel opening. Our data provide the first evidence that R domain is involved in the CFTR channel opening, besides its role in PKA-dependent phosphorylation.

Chapter I: Overview of the CFTR chloride channel

I.1 Introduction of CFTR and CF

The cystic fibrosis transmembrane conductance regulator (CFTR) is a transmembrane protein found in epithelial cells in tissues that produce mucus, sweat, saliva, tears and digestive enzymes. CFTR plays an important role in Cl^- conductance and regulates other protein. Its gene is located on the long (q) arm of chromosome 7 at position 31.2, from base pair 116,907,253 to base pair 117,095,955. The mature CFTR protein is composed of a single polypeptide chain with 1480 amino acids and has a molecular weight of 168,173 Da (Rowe et al., 2005). CFTR belongs to the ABC (ATP Binding Cassette) super family or traffic ATPase. This protein family members transport molecules such as sugars, peptides, inorganic phosphate, chloride, and metal ions across the cell membrane.

There are more than 1,500 mutations in the CFTR gene (Rowe et al., 2005) and mutation of CFTR is the fundamental cause for Cystic Fibrosis. The mutations can be grouped into four classes: defective protein production, defective processing, defective regulation and defective conduction (Welsh and Smith, 1993). The most common mutation that causes a processing defect, called ΔF508, or a deletion (Δ) of one amino acid at position 508 in the CFTR protein, has been found in 70% of CF patients. Most of the altered proteins never reach the cell membrane because they are degraded shortly after protein synthesis. Another very common mutation that causes a regulation defect, G551D, is carried by one sixth of CF patients. This altered protein assumes very low channel activity.

With an incidence of 1 in 2000 live births, cystic fibrosis is the most common lethal genetic disease that affects Caucasian populations worldwide. About 5% of white Americans are carriers who have one defective and one normal copy of the gene. Only individuals with a defective mutation in both alleles show the severe symptoms of the disease.

Normally, epithelial cells that line the lumen of the airway secrete mucus to trap and kill bacteria and the cilia on the surface constantly sweep away the debris. When those disease-related mutations in the CFTR gene prevent the channels from properly functioning, this process is less efficient due to a blockage of the movement of salt and water into and out of cells. As a result of this blockage, airways in patients with CF produce abnormally thick, sticky mucus. This highly concentrated mucus obstructs the airways and glands, causing the characteristic signs and symptoms of cystic fibrosis. Meanwhile, it traps bacteria that give rise to chronic infections. Usually, CF patients show recurrent pulmonary infections, pancreatic insufficiency, hepatic cirrhosis, intestinal obstructions, and male infertility (Rowe et al., 2005). So this disease usually manifests itself as severe chronic airway disease, exocrine pancreatic insufficiency, and high Cl^- concentration in the sweat.

Currently, there is no cure for CF. CF patients are treated by relieving their symptoms routinely, for example, by treating lung infection by antibiotics, removing the thick mucus with maneuvers that help airway clearance, lessening digestive problem by nutrition therapy, or even lung transplantation. All these methods of treatment are not targeted to the patients' fundamental problem. We try to understand the mechanism by

which CFTR channels are regulated, comprehend the structure-function relationship, and thereby provide information for future drug design. Below is the overview of the CFTR function which was well established in this field.

I.2 CFTR's Physiological functions

CFTR works as a chloride channel across the cell membrane. After being phosphorylated with cAMP-dependent protein kinase A or C, Wild Type (WT) CFTR channel activity is increased by >100 fold in the present of ATP. The transport of chloride helps control the movement of water (osmosis) in tissues and maintains the fluidity of mucus and other secretions. Normal function of these channels ensures the digestive system, reproductive system, and other organs and tissues function properly (Vankeerberghen et al., 2002). The CFTR protein may also regulate the function of other channels. One example is a type of channel that transports sodium across cell membranes (Vankeerberghen et al., 2002). CFTR has been called a conductance regulator and multifunctional molecule instead of Cl channel due to a series of defects in cellular functions found in CF epithelia. These "secondary" defects included dysfunction of a separate class of Cl channels, K^+ channels, overactive Na^+ channels, and defective exocytosis and endocytosis in CF cells. As a result, these "secondary" effects may further lead possibly to "tertiary" consequences within CF cells (Vankeerberghen et al., 2002). All the facts spotlight the significance of CFTR in cellular activity and the necessity of CFTR research.

I.3 CFTR's structure

Crystallographic structural information of CFTR protein is helpful for our functional studies. Unfortunately, the full length structure of CFTR is not available. Currently, the crystal structures of isolated human and mouse NBD1 and NBD2 have been solved (Lewis et al., 2004, 2005; Zhao et al., 2008). In addition, several crystal structures of other ABC transporters can also serve as a guide to study CFTR. Typical ABC transporters possess four subunits: two nucleotide-binding domains (NBD1 and NBD2) where ATP binding and hydrolysis drive the transport cycle, and two membrane spanning domains (MSD1 and MSD2) which provide the pathway for substrate transport. In addition to these common subunits seen with other ABC proteins, CFTR contains a unique regulatory (R) domain located between the NBD1 and MSD2 (see figure I.1). Phosphorylation of many of the consensus serine residues in the R domain is a prerequisite for CFTR to function. After the channel is phosphorylated by protein kinase A (PKA) and ATP, gating of phosphorylated CFTR is controlled by ATP. Protein kinase C-dependent phosphorylation was also found to modulate CFTR (for a review, Gadsby and Narin, 1999; Hanrahan and Wioland, 2004; Seibert et al., 1999; Sheppard and Welsh, 1999; Zhou and Hwang, 2009; Chen and Hwang, 2008; Hwang and Sheppard, 2009; Muallem and Vergani, 2009).

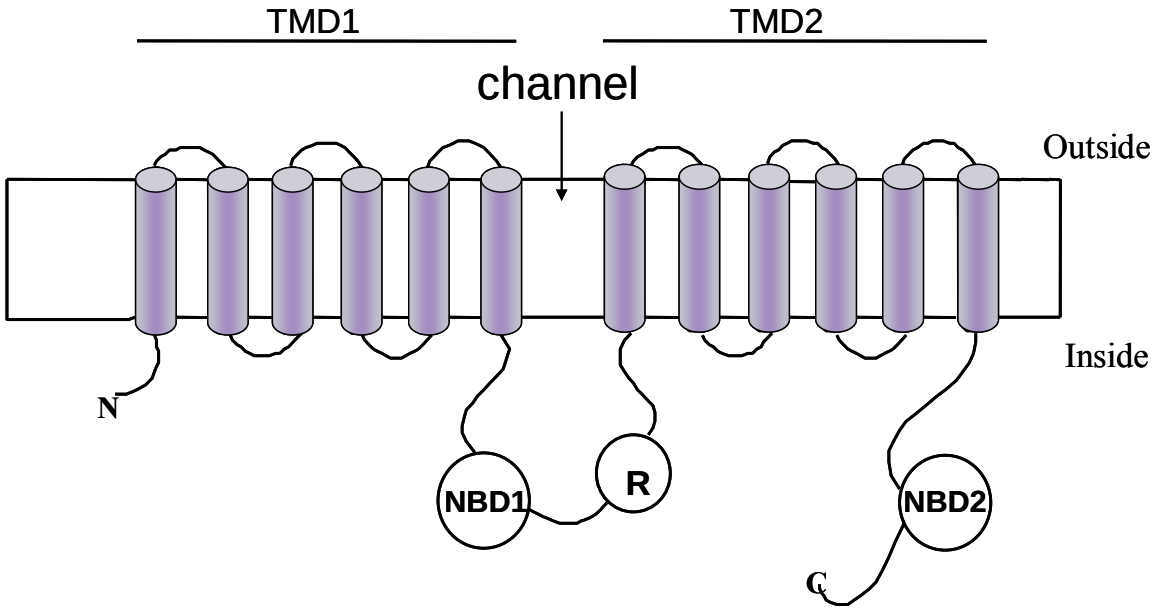

Chapter I Figure I.1 Topology of CFTR. The CFTR consists of 5 domains, 2 nucleotide binding domains (NBD1 and NBD2), 2 membrane spanning domain (MSD1 and MSD2) and 1 regulatory domain (R domain).

Conserved in all ATP binding proteins, CFTR's NBD contain the characteristic Walker A motif (GxxGxGKS/T, x represents any amino acid) and Walker B motif (hhhhD, h represents a hydrophobic amino acid) (Walker et al., 1982). The ATP binding to the protein is characterized structurally by the Walker A lysine, which coordinates the γ- and β- phosphates of the bound ATP, the Walker B aspartate, which coordinates Mg2+, and the catalytic glutamate. Moreover, unique in ABC transporters, there is a signature sequence (LSGGQ) which is believed to participate in ATP binding (Davidson and Chen, 2004). Various experimental evidences suggest that the two NBDs form a dimer. When an NBD dimer is formed, two ATP molecules are buried at the dimer interface, and recently solved structures of NBD dimers like E.c Malk and MJ0796 show a head-to-tail configuration (Chen et al., 2003; Smith et al., 2002; Zaitseva et al., 2005). Once the NBDs dimerized in this head-to-tail configuration, the ATP binding pocket is composed of the Walker A and B motifs from one NBD and the signature motif from the partner NBD. It is thus more convenient to define the two ATP binding pockets (ABP), rather than referring to two NBDs. ABP1 is formed by the Walker A and B motifs of NBD1 and the signature sequence of NBD2; ABP2 is formed by the Walker A and B motifs of NBD2 and the signature sequence of NBD1 (Figure I.2). The head-to-tail NBD dimerization is also consistent with many biochemical data (Moody et al., 2002; Smith et al., 2002; Lu et al., 2005; Higgins and Linton, 2004), as well as the full length crystal structure of several ABC transporters (Locher et al., 2002; Hollenstein et al., 2007; Pinkett et al., 2007; Dawson and Locher, 2006).

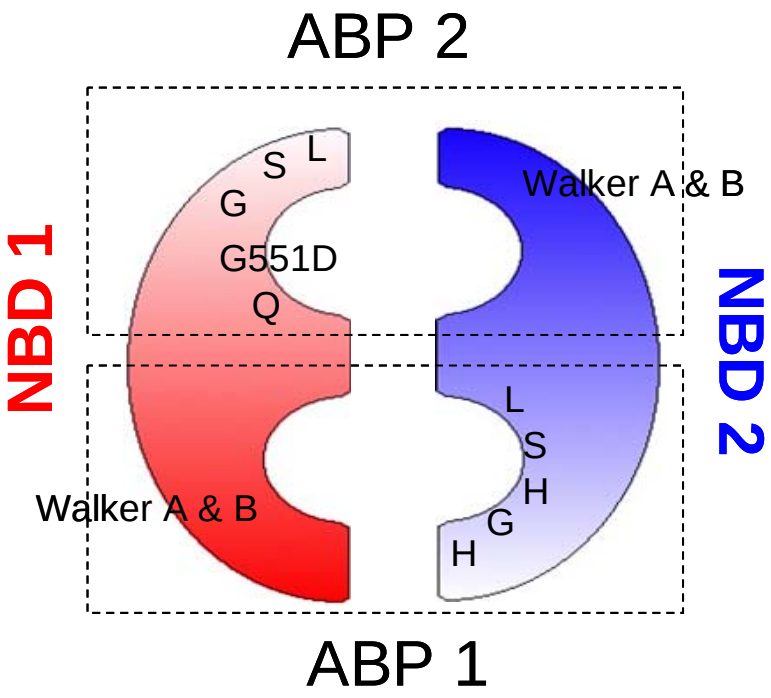

Chapter I Figure I.2 Cartoon showing the two ATP binding sites. The NBD1 and NBD2 are colored in red and blue, respectively. ATP binding pocket 1 (ABP1) is formed by residues from Walker A and B motifs of NBD1 and signature sequence of NBD2. ATP binding pocket 2 (ABP2) is formed by residues from Walker A and B motifs of NBD2 and signature sequence of NBD1. The mutant I studied in this dissertation, G551D-CFTR, is located at the signature sequence on NBD1.

Not only the isolated NBDs shows dimerization configuration, other full length ABC transporter protein crystal structures also provide similar information about the assembling of the NBDs' dimer. For example, at least four ABC protein crystal structures are available: the vitamin B12 transporter BtuCD from E. coli (Locher et al., 2002); a putative molybdate transporter, ModBC, from Archaeoglobus fulgidus (Hollenstein et al., 2007); a metalchelate transporter, HI1470/1, from Haemophilus influenza (Pinkett et al., 2007); and a drug exporter, Sav 1866, from Staphylococcus aureus (Dawson and Locher, 2006). In all these structures, the NBDs arrangement is similar, while the MSDs interact with the NBDs differently.

Isolated human and mouse NBD1 structures were solved by Lewis et al (2004, 2005). The overall folding of these two structures is very similar to what we learned from NBD of other ABC transporters. CFTR NBD1 contains a core subdomain, including the Walker A and Walker B motifs, and a helical subdomain, including the signature motif. The ATP molecule interacts with the NBD mainly through residues in the Walker A and Walker B motifs. The aromatic residue interacting with the adenine ring of ATP is different in mouse NBD1 and human NBD1. In the structure of mouse NBD1, three residues (W401, L409 and F430) interact with ATP's adenine ring. No ring-ring stacking is found. While in structure of human NBD1, W401 interacts with the adenine ring through stacking. Comparing the sequences between CFTR NBD1 and NBD2, there are two unique regions in NBD1: the regulatory insertion (RI, residues 404-435) and the regulatory extension (RE, residues 639-670). The difference between mouse and human NBD1 is around the RI region. One should be aware that each crystal structure only

reflects a snapshot of the protein, the differences between these two structures might be partly due to crystallization condition or different state of the protein.

The preliminary crystal structure of NBD2 was released by Zhao et al. (2008). In this structure, Y1219 interacts with the adenine ring of the bound ATP analog through ring-ring stacking. No crystal structure of CFTR NBDs' dimer is available. Effort to put the crystal structures of NBD1 and this preliminary NBD2 directly to form a modeled dimer was also failed mainly due to the following two reasons. One is that the overall folding of NBD2 is twisted and thus shows discrepancy when compared the NBDs dimer from other ABC proteins. The other is that the RE (regulatory extension) region of NBD1 protrudes to the dimer interface hindering the dimer formation. Instead, the modeled dimer structure is obtained by a protein-protein docking approach (Huang et al., 2009), or it can also be modeled based on the NBD dimer structure of other ABC transporters, such as MalK, which is shown below (Figure I.3).

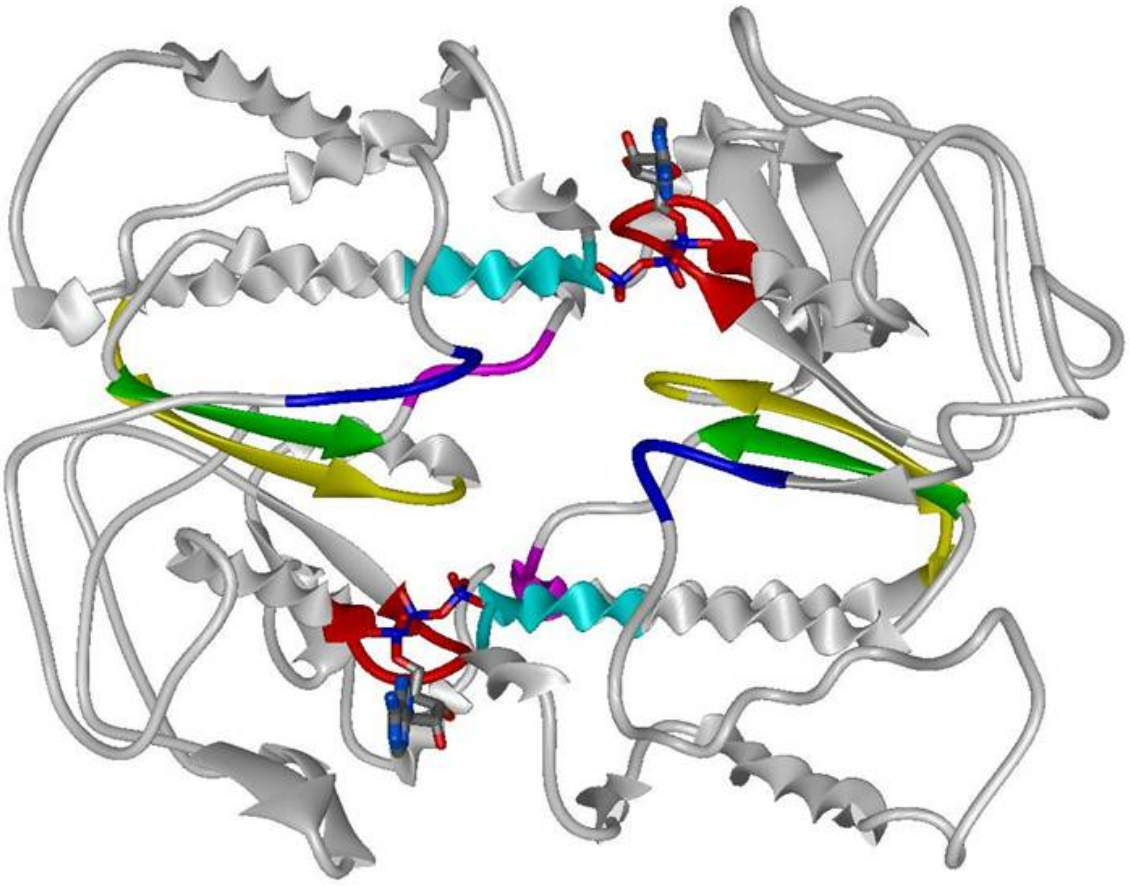

Chapter I Figure I.3 Modeled NBDs' dimer of the CFTR. The structure is based on dimer structure of MalK. The protein is shown in ribbon and two ATP molecules located at the interface are shown in sticks. The important motifs are shown in colors as following: Walker A motif, red; Walker B motif, green; Q loop, blue; H region, yellow; D loop, magenta; and signature sequences, cyan.

I.4 CFTR gating

The structural information described above has helped us understand the CFTR gating mechanism. Activation of CFTR requires phosphorylation by cAMP-dependent protein kinase A (PKA) or protein kinase C (PKC). Once the WT-CFTR channels are phosphorylated, ATP binding and hydrolysis drive NBD dimerization and dissociation, and control the gating. The phosphorylation step can be skipped by deletion of the R domain. Bompadre et al (2005a) had shown the ΔR-CFTR, whose R domain is completely removed, is very useful to study CFTR gating mechanism. In this work, the ATP-dependent gating was characterized. The phosphorylation step is bypassed in ΔR-CFTR. Since the deletion of entire R domain might introduce a substantial conformational change, the gating information deduced from this construct requires extreme caution when applied to wild type channels.

After the WT-CFTR is phosphorylated, the channel is controlled by ATP binding and hydrolysis (Zou and Hwang, 2001; Hwang and Sheppard, 2009). However, the mechanism of gating remains elusive and is under extensive investigation. We should note that the CFTR NBDs form a heterodimer. For most of the ABC transporters, their NBDs' sequences are identical. However, CFTR NBD1 and NBD2 only share 33% of sequence similarity. The two ATP binding pockets (ABPs) are asymmetric. Not only for CFTR, in several other eukaryotic ABC transporters (ABCC subfamily, MRP1-9, SUR1 and SUR2 (Dean et al., 2001)), only ABP2 presents conserved consensus residues in the motifs involved in ATP binding and hydrolysis. In contrast, some key residues are replaced in ABP1. These residues are listed as following: on NBD1 side, the glutamate residue adjacent to the Walker B motif is replaced by a serine residue. A histidine residue

that has been shown to play an important role in ATP hydrolysis in other ABC proteins (e.g., HlyB) (Zaitseva et al., 2005) is also replaced by a serine; on NBD2 side, the signature sequence is LSHGH, instead of LSGGQ. Those replacements probably account for the very low ATP dissociation rate of radioactive ATP at ABP1 (Cui et al, 2006). In addition, they may explain why biochemical studies demonstrate that ATP is hydrolyzed in ABP2 but not in ABP1 (Aleksandrov et al., 2002; Basso et al., 2003; Stratford et al., 2007).

As CFTR NBD1 and NBD2 are different, it is natural to ask if the two ATP binding sites play equal roles in gating. There are numerous questions about how channels open and close. Increased ATP induces a higher opening rate which follows a dose response curve, but how and where ATP binding leads to channel opening is unclear. Experiments suggest that ATP hydrolysis at ABP2 controls channel closure (Gadsby et al., 2006; Chen and Hwang, 2008; Hwang and Sheppard, 2009; Muallem and Vergani, 2009). How ATP binding affects channel closing is also mysterious. Besides, how the conformation change in NBD dimerization/dissociation transmits to the conformation change in MSDs to open/close the channel is the least clear issue in the field. The structure models of CFTR with NBDs and MSDs based on Sav1866 (Serohijos et al., 2008; Mornon et al., 2008) might provide insight into the coupling interface between NBDs and MSDs. The R domain is not present in the modeled structure, since it's unique to CFTR. The possibility that the interaction of RD with NBDs might play a role in channel gating cannot be excluded. Baker et al. (2007) demonstrated that dephosphorylated R domain might inhibit ATP-driven NBD dimerization by binding to NBD1, using NMR spectroscopy. All these questions highlight the importance of two NBDs interaction and dimerization, we choose

to study dimerization, not only because there are many challenging questions, but it is also the first step for proper channel gating.

I.5 Objective and outline

The main objective of the present study is to investigate the role of NBD dimerization in CFTR gating. We either perturb the protein structure by site directed mutagenesis or perturb the binding partner by using different ligands. Since dimerization is essential for CFTR channel function and previous work illustrated that NBDs' dimer generates two distinct ATP binding sites (Hwang and Sheppard, 2009), we first studied the asymmetric functional roles of each ATP binding site. The residues that contribute to the ATP binding site from the Walker A and B motifs had been extensively studied. As the binding partner, residues from the signature sequence also participate in binding with ATP. However, their roles are unclear and are studied in this thesis. Furthermore, the conformational change in dimerization of NBDs has to be transmitted to the physical gate to open the channel. The signal transmission of dimerization to channel opening was also studied in this thesis.

In Chapter II, the asymmetric roles of two ATP binding pockets are presented. We found that ATP binding at the NBD2 site initiated channel opening, while ATP binding at the NBD1 site modulated channel closing by stabilizing the open state.

In Chapter III, the roles of the signature sequences were studied. We found that mutations at the signature sequence of NBD1 create a Cd^{2+}-gated chloride channel. The effect of Cd^{2+} is mediated by a metal bridge formation between an endogenous cysteine residue(s) and the engineered aspartate or cysteine in the signature sequence. We propose that the signature sequence serves as a switch that transduces the signal of ligand binding to the channel gate.

In Chapter IV, the cysteines coordinating Cd^{2+} are identified. A residue in the R domain was found to coordinate with Cd^{2+}. We propose that the region of the R domain around residue 832 interacts with NBD1 through the signature sequence and mediates the signal transduction of ligand binding to channel opening.

In the Appendix, materials and methods used to carry out our experiments and data analysis are described. Also, the energetic analysis used to study if mutations are independent of ligand binding in Chapter II is presented.

Chapter II: Two ATP binding sites of the CFTR play distinct roles in gating kinetics and energetics.

This chapter has been revised and modified from my manuscript published in J. Gen Physiol. 128:413-22 2006, by Zhou, Z., Wang, X., Liu, H.-Y., Zou, X., Li, M. & Hwang, T.-C. (Zhen Zhou and Xiaohui Wang are equally contributing first authors). According to their web site, http://jgp.rupress.org/misc/terms.shtml, I retain the copyright for this work and am allowed to alter and build upon this work.

The goal of this chapter is to demonstrate that two ATP binding sites play distinct roles in CFTR channel gating. ATP binding at the NBD2 site initiates channel opening, while ATP binding at the NBD1 site modulates the rate of channel closing. Opening and closing (gating) of the phosphorylated CFTR is coupled to ATP binding and hydrolysis at CFTR's two nucleotide binding domains (NBD1 and NBD2). Whether these two ATP binding sites play an equivalent role in the dynamics of NBD dimerization, therefore in gating CFTR channels, remains unsettled. Based on the crystal structures of NBDs from other ABC transporters, sequence alignment, and homology modeling, we have identified two critical aromatic amino acids (W401 in NBD1 and Y1219 in NBD2) that coordinate the adenine ring of the bound ATP. Mutations of these two equivalent residues result in two channels with totally different gating behavior. Conversion of the W401 residue to glycine (W401G) has little effect on the sensitivity of the opening rate to [ATP], but the same mutation at the Y1219 residue dramatically lowers the apparent affinity for ATP by more than 50-fold, suggesting distinct roles of these two ATP binding sites in channel opening. On the other hand, the W401G mutation, however, shortens the open time

constant, while the Y1219G mutation has little effect on channel open time. Energetic analysis of our data suggests that the free energy of ATP binding at NBD1, but not at NBD2, contributes significantly to the energetics of the open state. This kinetic and energetic asymmetry of CFTR's two NBDs suggests an asymmetric motion of the NBDs during channel gating. Opening of the channel is initiated by ATP binding at the NBD2 site and Y1219 is the most vital position to interact with ATP adenine ring. Whereas separation of the NBD dimer at the NBD1 site constitutes the rate-limiting step in channel closing, tighter binding at W401 prolongs channel open time.

II.1 Introduction

Like other members of the ABC transporter superfamily, cystic fibrosis transmembrane conductance regulator (CFTR) has two membrane spanning domains MSD1 and MSD2, two nucleotide binding domains, NBD1 and NBD2 (Riordan et al., 1989). Meanwhile, CFTR has a unique regulatory domain, R domain. For CFTR to function as a chloride channel, the CFTR protein needs to be phosphorylated in the R domain as a prerequisite; subsequent interactions of ATP with the two NBDs control the opening and closing of the channel (i.e., gating). Several properties of CFTR's two NBDs distinguish CFTR among members of the ABC family. First, CFTR's two NBDs exhibit only moderate (~33%) sequence homology. Second, biochemical studies show that NBD2, but not NBD1, hydrolyzes ATP (Szabo et al., 1999; Aleksandrov et al., 2002; Basso et al., 2003). Third, NBD1 displays a higher ATP binding affinity than NBD2 (Szabo et al., 1999; Aleksandrov et al., 2001; Aleksandrov et al., 2002; Basso et al., 2003; Zhou et al., 2005). Despite more than a decade of study, the functional significance of

this structural asymmetry of NBDs in CFTR gating remains unclear. It is generally agreed that ATP hydrolysis at NBD2 leads to channel closing since mutations (e.g., K1250A and E1371S) that abolish ATP hydrolysis at the NBD2 site drastically prolong the open time (Carson et al., 1995; Gunderson and Kopito, 1995; Zeltwanger et al., 1999; Vergani et al., 2003; Bompadre et al., 2005b). However, recent studies suggest that ATP binding at NBD1 may also modulate the closing rate (Bompadre et al., 2005a,b; Zhou et al., 2005). How ATP binding catalyzes channel opening also remains unsettled. One popular hypothesis is that ATP binding to both NBD1 and NBD2 is required for channel opening (Aleksandrov et al., 2001; Vergani et al., 2003; Berger et al., 2005; Vergani et al., 2005; for review see Gadsby et al., 2006). An alternative view is that ATP binding at NBD2 plays a major role in channel opening, whereas ATP binding at NBD1 may not be absolutely required for channel opening (Powe et al., 2002; Bompadre et al., 2005b). One probable reason for these controversies is the fact that previous studies were mostly designed with limited structural information about CFTR's NBDs. Very often, manipulations that affect ATP binding also perturb ATP hydrolysis (e.g., Gunderson and Kopito, 1995; Basso et al., 2003; Vergani et al., 2003).

Ideally, to understand the roles of CFTR's two NBDs, one needs to manipulate the ligand binding affinity at each NBD by mutating amino acid residues that interact with ATP in the binding pockets and/or on the other side, by chemically engineering the bound ligand, ATP, to alter its affinity. These strategies have been successfully employed in other ATP binding proteins (e.g., Shah et al., 1997; Gillespie et al., 1999). Recent success in solving the crystal structures of CFTR's NBD1 (Lewis et al., 2004; Lewis et al., 2005) and in designing high-affinity hydrolyzable ATP analogues for CFTR gating

(Zhou et al., 2005) has made structure-guided functional studies possible for the first time in the CFTR field. A good example is the utilization of homology modeling of NBDs and mutant cycle analysis to demonstrate that the opening of the CFTR channels is associated with the dimerization of CFTR's two NBDs (Vergani et al., 2005).

Capitalizing on the crystal structures of CFTR's NBD1, we made mutations of the aromatic residues that interact (or are predicted to interact) with the adenine ring of ATP in CFTR's NBD1 (tryptophan 401, i.e., W401) and the equivalent amino acid on NBD2 (tyrosine 1219, i.e., Y1219). Macroscopic and microscopic kinetic analyses of ATP-dependent gating reveal functional asymmetry of these two ATP binding sites. Nonconserved mutations of Y1219 cause a rightward shift of the relationship between [ATP] and the opening rate, suggesting that ATP binding at the NBD2 site plays a critical role in channel opening. Although conversion of W401 to glycine (i.e., W401G) has little effect on the sensitivity of the channel opening rate to [ATP], this mutation shortens the mean open time. The shortening of the open time by the W401G mutation is also seen with the hydrolysis-deficient mutant background (i.e., E1371S), suggesting that the effect of W401G mutation is not through a perturbation of ATP hydrolysis. Kinetic and energetic asymmetry of CFTR's two ATP binding sites will be discussed.

II.2 Results

II.2.1 Identification of W401 and Y1219 as the crucial residues that interact with ATP adenine ring.

The crystal structure of the NBD1 of human CFTR (Fig. II.1 A) reveals that W401 forms a ring–ring stacking interaction with the adenine ring of the bound ATP (Lewis et

al., 2005). Sequence analyses suggest that Y1219 at NBD2 is the equivalent amino acid residue of W401 (Fig. II.1 B). The physiological importance of Y1219 in coordinating ATP is implicated by the fact that Y1219 is perfectly conserved in CFTR from 36 different species. In fact, we collected 299 sequences of the ABC transporter proteins from the gene bank; a tyrosine residue is found at the equivalent position in 86% of these proteins (the rest are phenylalanine [12%], tryptophan [1%], and histidine [1%]). This is perhaps not surprising since the importance of aromatic residues in ligand binding has been well established in other nucleotide binding proteins (e.g., Hung et al., 1998; Gillespie et al., 1999; Hopfner et al., 2000; Huai et al., 2003, 2004; Zhang et al., 2004). Based on this sequence information, we made a homology model of CFTR's NBD2 using the coordinates of NBD1 as a template (Fig. II.1 A).

Recently, structural models of the entire CFTR protein have been developed (Serohijos et al., 2008; Mornon et al., 2008). In these structures, Y1219 indeed interacts with ATP adenine ring by stacking. Furthermore, Zhao et al (2008) had solved the CFTR NBD2 crystal structure in the presence of a high binding affinity ATP analog. In this structure, the side chain of Y1219 is also shown to form stacking interaction with adenine ring of the bound nucleotide. We thus engineered mutations at these two equivalent positions (W401 and Y1219) to study the functional consequences.

II.2.2 Y1219G changes apparent ATP binding affinity greatly, while W401G has little effect.

To examine the role of ATP binding at CFTR's two NBDs, we converted W401 or Y1219 to glycine and examined the effect of these mutations on the apparent affinity for

ATP ($K_{1/2}$). Wild-type (WT) and mutant CFTR channels in excised inside-out membrane patches were activated by the catalytic subunit of PKA plus ATP. Different concentrations of ATP were then applied to obtain a macroscopic ATP dose–response relationship. Fig. II.1 C shows three representative traces. For WT channels, 0.1 mM ATP generates a CFTR activity about half of that with 2.75 mM ATP, a saturating concentration for WT CFTR gating (e.g., Zeltwanger et al., 1999). For the W401G mutant, 0.1 mM ATP elicits a similar level of activity. However, for the Y1219G mutant, 0.1 mM hardly induces any current different from the basal activity. Unlike WT and W401G, 2.75 mM ATP does not saturate the current for Y1219G and we never reach the saturating state in our test since too high [ATP] may generate inhibition. As seen in Fig. II.1 C, 1 mM ATP, a concentration that induces ~80% of maximal current for WT, only elicits a small fraction of current compared with that by 20 mM ATP, the highest [ATP] tested. Fig. II.1 D summarizes normalized macroscopic ATP dose–response relationships of WT, W401G, and Y1219G. Although the W401G mutation does not affect the apparent affinity, converting Y1219 to glycine causes a dramatic rightward shift of the ATP dose– response curve with a $K_{1/2}$ of 4.72 ± 1.12 mM, >50-fold higher than that of WT (0.09 ± 0.02 mM).

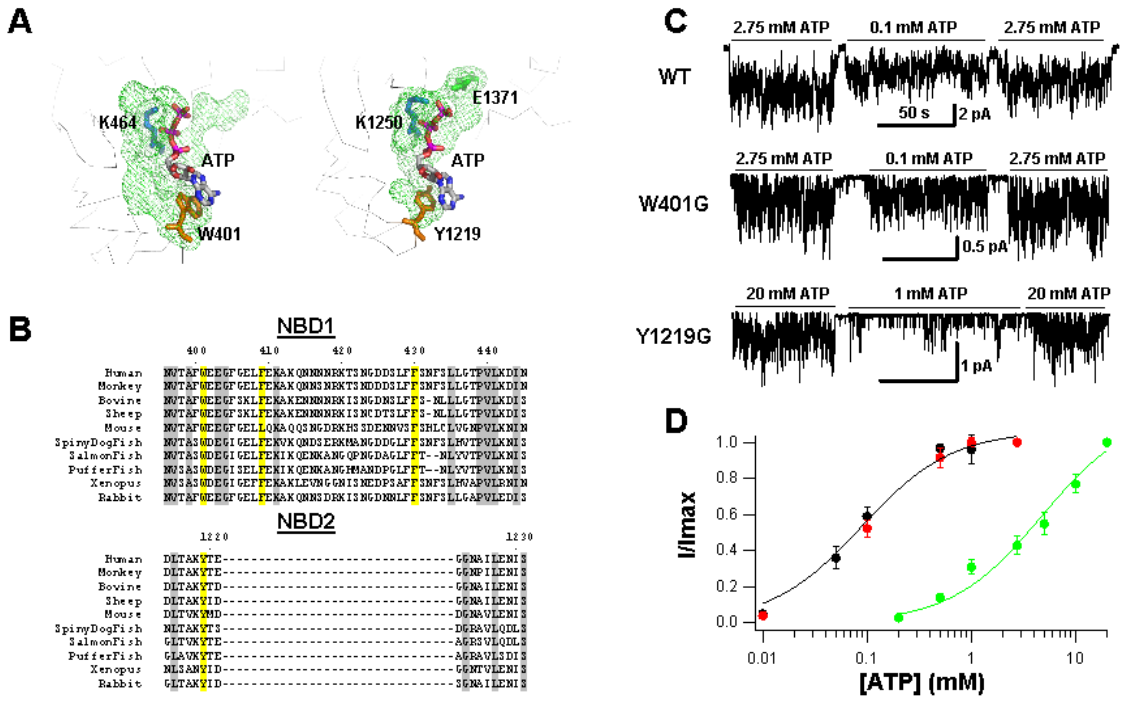

Chapter II Figure II.1. Tryptophan 401 and tyrosine 1219 residues interact with the adenine ring of ATP in the human CFTR NBD1 and NBD2 respectively. (A) Interactions between ATP and key amino acids in the NBD1 binding pocket, adopted from the monomeric crystal structure of the human F508A NBD1-ATP complexes (pdb code: 1xmi, chain A) (left). A similar picture of modeled NBD2 binding pocket is shown on the right. Residues of interest are represented by sticks, including those that interact with adenine ring (W401 in NBD1 and Y1219 in NBD2), the Walker A lysines (K464 in NBD1 and K1250 in NBD2) and the catalytic Walker B glutamate residue, E1371. The protein backbone atoms are plotted in thin lines and colored in grey. The figures were prepared by PYMOL. In other members of the ABC family, there is either an E or a D at the position equivalent to E1371 of CFTR NBD2, however, it is an serine in CFTR's NBD1, which is believed to be the structural basis for CFTR NBD1's inability to hydrolyze ATP (Lewis et al., 2004; Lewis et al., 2005). Since ATP is found to be associated with the Walker A and B motifs in all crystal structures of NBDs resolved so far (e.g., Lewis et al., 2004; Hung et al., 1998; Yuan et al., 2001; Karpowich et al., 2001), for the sake of clarity, we define the NBD1 ATP-binding site (or NBD1 site) as the binding pocket containing Walker A and Walker B motifs in the NBD1 sequence. An equivalent definition is applied to the NBD2 site. (B) Sequence alignment of the N-terminal part of the NBD1 and NBD2 of CFTR from 10 species (chosen randomly out of 36). Aromatic residues studied in this paper are highlighted in yellow. Conserved residues are highlighted in grey. Note that a stretch of ~ 30 amino acids (from 404 to 435) is present in NBD1 (i.e., regulatory insertion) but absent in NBD2 (dashed line). (C) Representative bracketed current traces at different [ATP] for constructing ATP dose-response relationships. Current induced by various [ATP] was normalized to 2.75 mM ATP in the case of WT and W401G and to 20 mM ATP in the case of Y1219G. Horizontal bars represent 50 s. (D) ATP dose-response relationships of WT (black), W401G (red) and Y1219G (green). Solid lines are Michaelis-Menten fits to the data. The $K_{1/2}$ values are 0.09 ± 0.02 mM, 0.11 ± 0.02 mM and 4.72 ± 1.12 mM for WT, W401G and Y1219G, respectively. Each data point represents the average from three to eight experiments.

II.2.3 Change of apparent ATP binding affinity of Y1219 mutation is specific to the position.

We further characterized several mutations (Y to W, F, I, G) at the Y1219 residue (Fig. II.2 A). A more conserved mutation (Y1219W) does not change the $K_{1/2}$ value significantly. The ATP dose–response relationships of Y1219F and Y1219I mutants lie between those of WT and Y1219G. These results suggest that observed changes of the ATP sensitivity are not due to a nonspecific mutational effect but due to the specific effect of site direct mutations. Since the macroscopic ATP dose–response mostly reflects the potency of ATP in opening the channel, we hypothesize that ATP binding at the NBD2 site plays a critical role in channel opening.

II.2.4 Change in apparent ATP binding affinity by Y1219G is mainly due to the change in the opening rate.

To test this hypothesis, we examined single-channel kinetics of WT, W401G, and Y1219G with saturating or the highest [ATP] we can achieve. Fig. II.2 B shows representative single-channel traces. At 2.75 mM ATP, WT and W401G channels close for hundreds of milliseconds between opening bursts. However, even at 20 mM ATP, most of the closed events for Y1219G last for several seconds. Since the opening rate of Y1219G is not saturated at 20 mM ATP, we also studied single-channel kinetics of Y1219I, which shows a smaller shift in the ATP dose–response relationship (Fig. II.2 A). The relationship between the opening rate and [ATP] reaches saturation at ~10 mM ATP. The opening rate of Y1219I at 10 or 20 mM ATP is very similar to that of WT at 2.75 mM ATP (Fig. II.2, B and C), indicating that mutations at the Y1219 residue likely affect

the ATP binding step with minimal effect on the post-binding events. Fig. II.2 C shows the relationship between the opening rate and [ATP] for WT, W401G, Y1219I, and Y1219G. It should be noted that these relationships virtually mirror the macroscopic ATP dose–response relationship (Fig. II.2 A), consistent with the notion that the opening rate is the major determinant for the macroscopic ATP dose– response curve (Zeltwanger et al., 1999; Powe et al., 2002; Vergani et al., 2003). Opening rate is the major determinant for the macroscopic ATP dose-response curve of these Y1219 mutants.

II.2.5 Decreasing opening rate of Y1219G is independent of phosphorylation.

It is known that the opening rate of CFTR is very sensitive to the influence of PKA-dependent phosphorylation (Mathews et al., 1998; Wang et al., 1998). Before we draw the conclusion that these mutational effects at the Y1219 residue result from a perturbation of ATP binding at the NBD2 site, we need to rule out the possibility that mutations at the Y1219 residue somehow hinder phosphorylation of the R domain, and thus the observed decrease of the opening rate is secondary consequence to a potential mutational effect on phosphorylation. To exclude this possibility, we introduced the mutations of interest into a CFTR construct with the entire R domain deleted (ΔR-CFTR) (Csanády et al., 2000), which we have extensively characterized its phosphorylation-independence and shown that its ATP sensitivity and single-channel kinetic parameters are very similar to those of WT CFTR (Bompadre et al., 2005a). Fig. II.2 D shows a similar rightward shift of the ATP dose–response relationships for Y1219I and Y1219G mutants under the ΔR-CFTR background. These results together strongly support the hypothesis that ATP binding at the NBD2 site catalyzes channel opening.

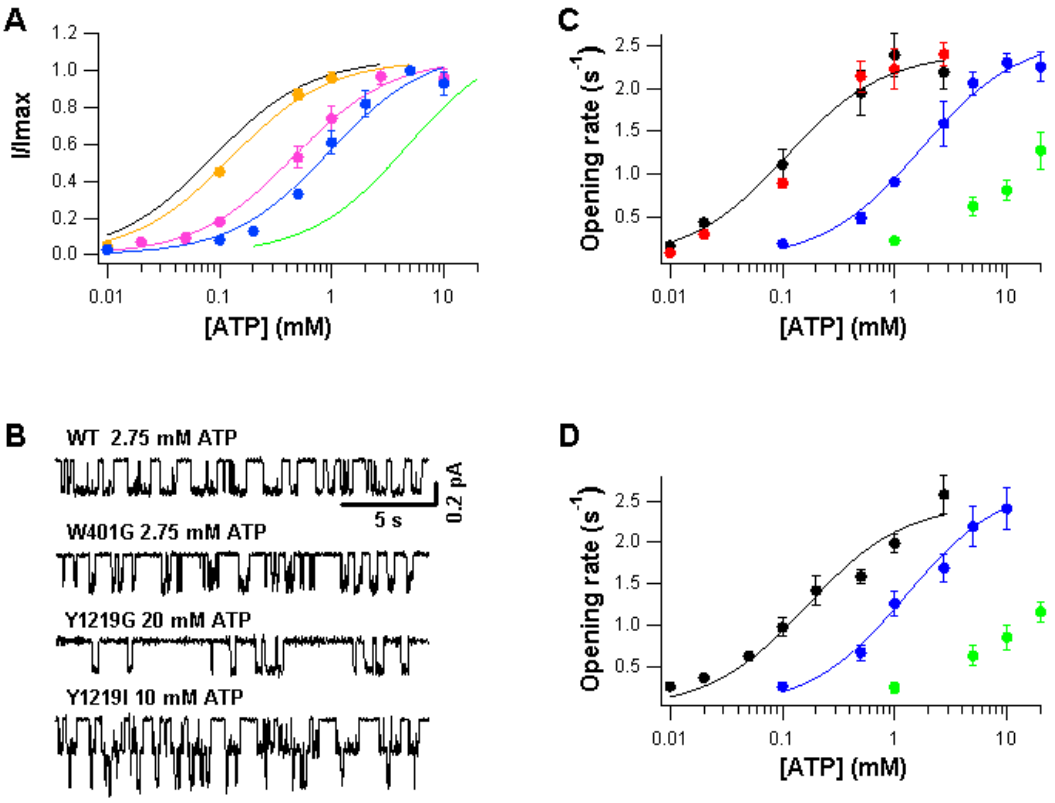

Chapter II Figure II.2. Effects of mutations at W401 and Y1219 on the opening rate. (A) Normalized ATP dose-response relationships of WT (black line, Michaelis-Menten fit from Fig. II.1d), Y1219W (brown), Y1219F (pink), Y1219I (blue), and Y1219G (green line, Michaelis-Menten fit from Fig. II.1d). Solid lines are the Michaelis-Menten fits to the data. $K_{1/2}$ values are: 0.13 ± 0.02 mM (Y1219W), 0.46 ± 0.06 mM (Y1219F), and 0.94 ± 0.20 mM (Y1219I), respectively. (B) Representative single-channel current traces of WT, W401G, Y1219G and Y1219I in response to [ATP] as marked. (C) Relationships between channel opening rates and [ATP] for WT (black), W401G (red), Y1219I (blue) and Y1219G (green). Solid lines are Michaelis-Menten fits to the data of WT (black) and Y1219I (blue). $K_{1/2}$ values are 0.11 ± 0.02 mM and 2.10 ± 0.25 mM for WT and Y1219I, respectively. (D) Relationships between channel opening rates and [ATP] for ΔR-CFTR (black), ΔR-Y1219I (blue) and ΔR-Y1219G (green). $K_{1/2}$ from Michaelis-Menten fits (solid lines) are 0.16 ± 0.04 mM and 1.27 ± 0.16mM for ΔR-CFTR and ΔR-Y1219I, respectively. (Data for ΔR-CFTR were obtained from Bompadre et al., 2005b).

II.2.6 W401G and Y1219G affect the opening time differently.

Although mutations of the W401 residue at the NBD1 site had minimal effect on the relationship between [ATP] and the opening rate (Fig. II.2, B and C), close inspection of the single-channel current trace reveals that the channel open time is shorter for the W401G mutant (Fig. II.2 B). Fig. II.3 A summarizes the mean open time for WT, W401G, and Y1219G. Even though the Y1219G mutation causes a dramatic change of the relationship between [ATP] and the opening rate, it has negligible effect on the mean open time. In contrast, W401G exhibits ~40% decrease of the mean open time, suggesting that mutations that decrease the ATP binding affinity at the NBD1 site destabilize the open channel conformation (i.e., increase the closing rate). It should be noted that this shortening of the mean open time by W401G mutant is not readily reflected in the ATP dose– response relationship (Fig. II.1 D). Indeed, according to our simulation, if the relationship between the opening rate and [ATP] remains unchanged, a 40% shortening of the mean open time only results in ~15% change of the apparent Kd, which is within the experimental error range (Fig. II.1 D).

II.2.7 W401G shortens the opening time by decreasing the stability of the NBD dimer.

We considered three possibilities for the shortened open time seen with the W401G mutation at NBD1. First, since it is established that ATP hydrolysis at NBD2 leads to channel closing during the ATP hydrolysis driven gating cycle, it is possible that the W401G mutation accelerates the ATP hydrolysis rate of NBD2. Second, it has been demonstrated that the open state of the channel corresponds to a dimer conformation of

NBDs (Vergani et al., 2005), and the two ATP molecules are sandwiched at the dimer interface as shown in other ABC family members (Smith et al., 2002; Chen et al., 2003). If this was the case, the binding energy of ATP on walker A on NBD1 could contribute to the overall stability of the dimer (or open state). It is probable then that mutating W401 in NBD1 decreases the binding energy of ATP so that the resulting dimer, thus the open state, becomes less stable. Third, the shortened open time of the W401G could be due to an allosteric effect.

To examine the potential effect of mutation in NBD1 on ATP hydrolysis at NBD2, we introduced the W401G mutation into the E1371S background, a mutant CFTR whose opening time is long due to that ATP hydrolysis is abolished (Moody et al., 2002; Tombline et al., 2004; Vergani et al., 2005). If the shortened open time seen with the W401G mutant is indeed due to an increased ATP hydrolysis rate, the effect on the open time should be at least reduced once the ATP hydrolysis is eliminated. Since the gating cycle of channels in the E1371S background is extremely long, it is technically difficult to do microscopic single-channel kinetic analysis. We, therefore, resorted to macroscopic current relaxation experiments, which has been used previously to assess the mean open time of hydrolysis deficient CFTR channels (Vergani et al., 2003, 2005; Bompadre et al., 2005a). It should be noted that the relaxation time constant upon withdrawal of ATP is determined by the channel closing rate, opening rate, and the ATP dissociation rate if a simply ligand-gated kinetic scheme is assumed. However, since the ATP dissociation rate is much faster than the channel opening rate and closing rate, this relaxation time constant reflects mainly the closing rate of the channel. Fig. II.3 B shows experiments using current relaxation analysis to estimate the open time constants for E1371S and

W401G/E1371S. Our results show that the relaxation time constant for W401G/E1371S (59.1 ± 4.6 s, n = 8) is shortened by around 50% compared with that of E1371S (111.7 ± 12.1 s, n = 15) (Fig. II.3 C), it suggested that the shorter open time of W401G is not the secondary consequence to an altered ATP hydrolysis rate. In contrast, although the Y1219G mutation greatly decreases the apparent affinity of ATP (Fig. II.2 C), introducing this mutation into the E1371S background has little effect on the relaxation time constant (107.6 ± 12.4 s, n = 7) (Fig. II.3, B and C). In addition, W401G/Y1219G/E1371S has a relaxation time constant of 49.0 ± 5.3 s (Fig. II.3, B and C), which is similar to that of W401G/E1371S, indicating that W401, but not Y1219, plays a dominant role in modulating the open time.

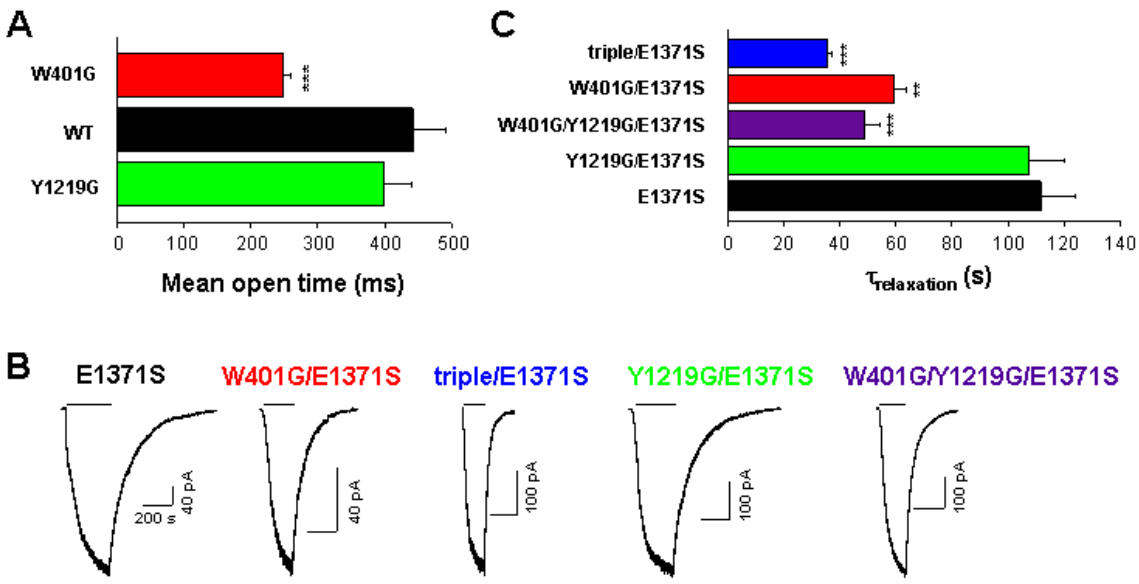

Chapter II Figure II.3. Effect of mutations at W401 and Y1219 residues on channel open time. (A) Mean open times of WT and W401G in the presence of 2.75 mM ATP are 441.3 ± 49.4 ms (n = 13) and 248.7 ± 11.3 ms (n = 22), respectively. The mean open time of Y1219G in the presence of 20 mM ATP is 399.1 ± 40.4 ms (n = 5). *** indicates $P < 0.001$ between WT and W401G. (B) Representative current relaxation traces upon withdrawal of 1 mM ATP plus PKA for E1371S, W401G/E1371S, triple/E1371S and Y1219G/E1371S. Solid lines above the traces indicate the duration of application of 1 mM ATP plus PKA. Horizontal scale bars represent 200 s. (C) Mean relaxation time constants upon withdrawal of 1 mM ATP plus PKA. ** indicates $P < 0.01$ and *** indicates $P < 0.001$ (compared to E1371S).

Although we cannot rule out the possibility of an allosteric effect of mutations on the stability of the open state, the following results are more in line with the idea that it is the binding energy of ATP on NBD1 that determines the stability of the open state. First, it has been shown that mutations at the K464 residue (Fig. II.1 A) decrease ATP binding affinity at the NBD1 site (Basso et al., 2003) and shorten the open time (Carson et al., 1995; Gunderson and Kopito, 1995; Sugita et al., 1998; Powe et al., 2002; compare with Vergani et al., 2003). Second, we have recently characterized the effects of an ATP analogue, N^6-(2-phenylethyl)-ATP (denoted as P-ATP), on CFTR gating. Not only is P-ATP >50-fold more potent than ATP in opening CFTR, it also increases the open time by ~30% (Fig. II.4 A; also see Zhou et al., 2005). Third, the shortened relaxation time constant due to the W401G mutation can be prolonged by P-ATP (see below figure II.4).

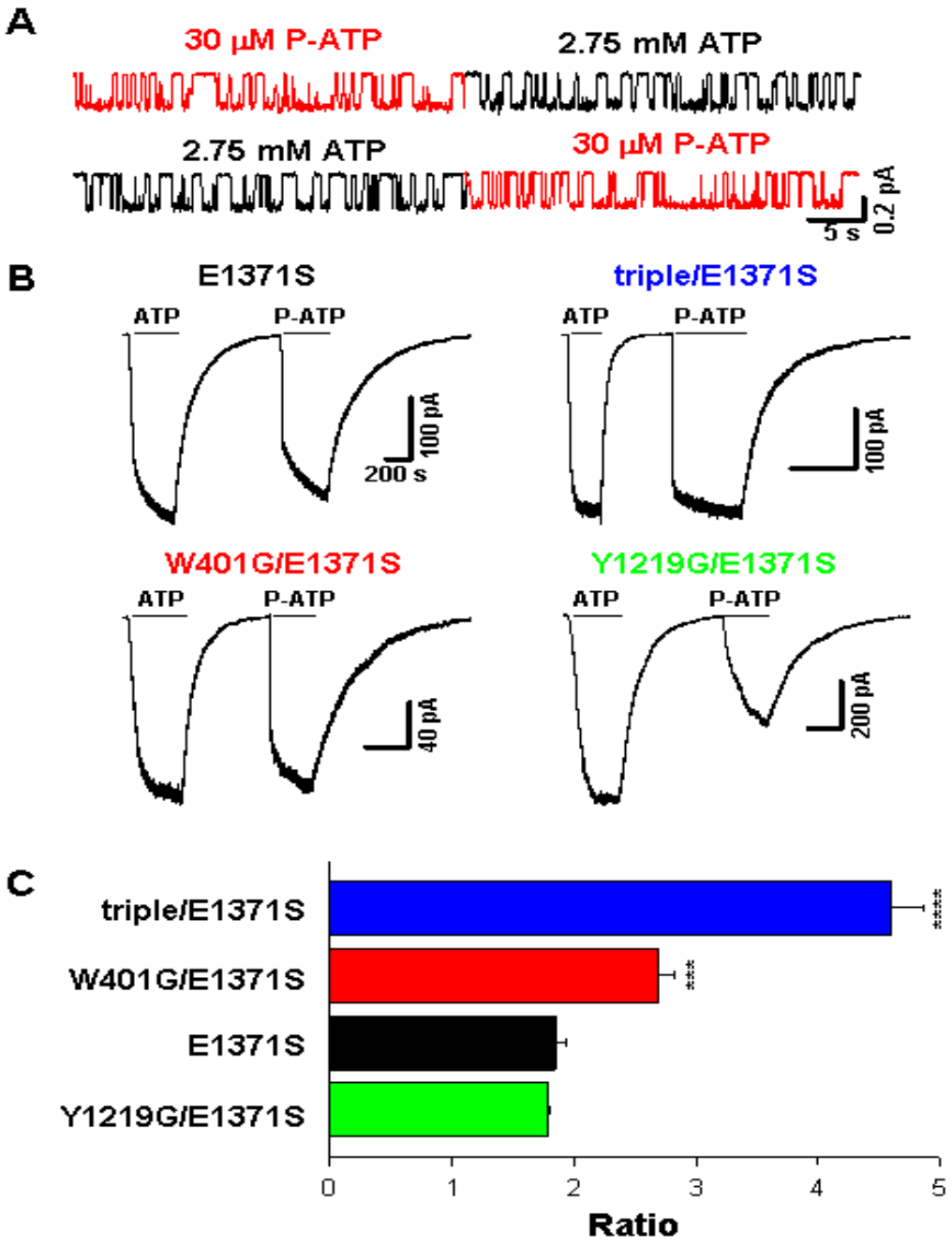

Chapter II Figure II.4. Effects of P-ATP on the relaxation time constant. (A) two representative single-channel current traces of WT-CFTR in the presence of P-ATP(red) or ATP(black). The mean open time for P-ATP or ATP opened channels are 583.9±60.6 ms(n=6) and 441.3±49.4 ms(n=13), respectively. (B) Representative current relaxation traces of E1371S, W401G/E1371S, triple/E1371S and Y1219G/E1371S after withdrawal of 1 mM ATP plus PKA or 50 μM P-ATP plus PKA. Horizontal scale bars represents 200 s. (C) The ratio of the relaxation time constant upon withdrawal of 50 μM P-ATP plus PKA to that upon withdrawal of 1 mM ATP plus PKA from the same patch was calculated for E1371S and various mutants in the E1371S background. The mean values are taken from 3 to 11 experiments. *** indicates $P < 0.001$ and **** indicates $P < 0.0001$ (compared to E1371S).

The idea that ATP binding at the NBD1 site stabilizes the open channel conformation is also supported by the recent report by Csanády et al. (2005) An interesting feature revealed by the comparison of NBD1 and NBD2 sequences (Fig. II.1 B) is that NBD1 has a "regulatory insertion" consisting of amino acids 404–435 (Lewis et al., 2004, 2005). Deletion of part of this regulatory insertion destabilizes the open state (Csanády et al., 2005). Interestingly, two additional aromatic amino acids (F409 and F430) are located in this regulatory insertion. Furthermore, the crystal structure of NBD1 from mouse CFTR shows interactions between ATP and all three amino acids including W401, F409 (leucine in the mouse NBD1), and F430. Since multiple aromatic amino acids can be used to form a high affinity nucleotide binding pocket (e.g., Gillespie et al., 1999; Huai et al., 2003, 2004), we further examine the contribution of F409 and F430 in stabilizing the open state.

We converted all three aromatic amino acids, including W401, F409, and F430 to glycine in the E1371S background and examined current relaxations of the W401G/F409G/F430G/E1371S (or triple/E1371S). Compared with the current relaxation of W401G/ E1371S (Fig. II.3 B), the triple/E1371S mutation further shortens the time course of current decay. Thus the relaxation time constants show a graded change as additional mutations in NBD1's ATP binding pocket were introduced (Fig. II.3 C). The simplest interpretation of these results is that these three aromatic amino acids contribute to the stability of the open state by stabilizing ATP binding at the NBD1 site.

To further examine the role of ligand binding in stabilizing the open state, we considered nucleoside triphosphates that have been characterized previously, such as GTP, CTP, UTP (Zeltwanger, 1998), and P-ATP (Zhou et al., 2005). Unlike GTP, CTP,

and UTP, which only change the apparent affinity modestly, P-ATP has an apparent affinity >50-fold of that for ATP. We thus consider P-ATP an ideal ATP analogue for this type of energetic analysis. If the hypothesis that ligand binding energy can contribute to the stability of the open state is correct, one would expect that P-ATP should prolong the open time constant (Fig. II.4 A). Fig. II.4 B shows experiments examining current relaxations upon removal of ATP or P-ATP for E1371S, W401G/E1371S, Y1219G/ E1371S, and triple/E1371S. As demonstrated previously (Zhou et al., 2005), the relaxation time course upon washout of P-ATP for E1371S is approximately twofold longer than that with ATP. P-ATP also increases the relaxation time constant of Y1219G/E1371S by approximately twofold. However, this prolongation effect of P-ATP is significantly larger for W401G/E1371S (2.7-fold) and triple/E1371S (greater than fourfold; Fig. II.4 C). These data suggest an energetic coupling between mutations at the NBD1 site and alterations of the bound ligand. On the other hand, mutating the NBD2 residue and changing of the binding energy of the ligand are two independent events (see appendix for detailed analysis). We thus propose that ligand binding at the NBD1 site stabilizes the open state.

II.3 Discussion

II.3.1 Mutations (W401G and Y1219G) alter the ATP binding affinity without affecting ATP hydrolysis, thus are very useful tools to study the functional roles of the ATP binding.

Gating of the CFTR chloride channel is unique in that the ligand ATP, used for opening the channel, is hydrolyzed. Studies using different mutations that perturb ATP

hydrolysis (e.g., K1250A, E1371S) indicate that ATP hydrolysis drives channel closure. This input of the free energy of ATP hydrolysis into gating transitions poses great challenges in understanding CFTR's gating mechanism since it is often difficult to separate the functional roles of ATP binding and ATP hydrolysis in CFTR gating. Previous mutagenesis approaches to studying ATP-dependent gating focus on amino acid residues located in the well-conserved motifs (e.g., K464, K1250 in Walker A and D572, D1370, E1371 in Walker B motifs). These residues are conserved because they interact with the phosphate groups and Mg ions in the ATP binding pockets. Although these studies have provided significant insight into the role of ATP hydrolysis in CFTR gating, this kind of approach does not provide a distinct advantage in understanding the role of ATP binding since altering the ligand binding affinity with these mutations is often complicated by the mutational effect on ATP hydrolysis (e.g., K1250A in Vergani et al., 2003).

Recent successes in solving the crystal structures of CFTR's NBD1 (Lewis et al., 2004, 2005) have laid the foundation for a new era of gating studies using structure-guided mutagenesis approaches. The crystal structure of human CFTR's NBD1 reveals that the side chain of the W401 residue forms ring–ring stacking interaction with the adenine ring of the bound ATP molecule. Previous studies of other ATP binding proteins (MacLeod et al., 1998; Zhao and Chang, 2004; compare with Shyamala et al., 1991) suggest that aromatic amino acids that interact with the adenine ring of ATP may be the ideal candidates for investigating the role of ATP binding. A preliminary crystal structure of CFTR's NBD2 (Zhao et al., 2008) also shows that the side chain of the Y1219 residue forms ring-ring stacking interaction with the adenine ring of the bound nucleotide.

Furthermore, using sequence analysis and homology modeling, we identified the Y1219 residue as the equivalent amino acid at the NBD2 site that interacts with the adenine ring of ATP (Fig. II.1). A model by H. Senderowitz and collaborators from Predix Pharmaceuticals also reveals the same role of Y1219 in ATP binding (personal communication). Structural models (Serohijos et al., 2008; Mornon et al., 2008) of the entire CFTR protein based on SAV1866 crystal structure also show the same interaction. Functional studies of the Y1219 mutations indeed suggest a critical role of this residue in channel opening (Figs. II.1 and 2). The Y1219I mutation lowers the sensitivity of the opening rate to [ATP] without altering the maximal opening rate (Fig. II.2), indicating that this mutation indeed decreases the binding affinity for ATP at the NBD2 site. Interestingly, although the Y1219G mutation causes a drastic shift of the ATP dose–response relationship (Figs. II.1 and 2), it does not affect the mean open time. If we accept the idea that the open time is determined by the rate of ATP hydrolysis (Gadsby et al., 2006), this latter result suggests that the mutations at the Y1219 residue preferentially decrease ATP binding affinity without a significant effect on ATP hydrolysis. Thus, these novel mutations investigated in this work could be useful tools to discern the roles of ATP binding for future CFTR gating studies.

II.3.2 ATP binding at ABP2 is crucial to channel opening, while ATP binding at ABP1 modulates the channel closing rate by stabilizing the open conformation.

Although the crystal structure of human CFTR's NBD1 reveals the importance of W401 in ATP binding at the NBD1 site, the W401 mutation does not affect the ATP dose–response relationship, an inexact but direct way to estimate changes of ATP binding

affinity. This negative result presents challenges for one to quantitatively gauge ATP–NBD1 interactions. Our energetic analysis shown in the supplemental material, albeit imperfect and with its own assumptions, provides a potential quantitative assay to assess the functional consequence of mutations that decrease ATP binding affinity at the NBD1 site. Using this analysis, we show that two additional aromatic amino acids (F409 and F430) also play a role in determining the closing rate. It should be noted that F409 and F430 are found to interact with ATP in the crystal structure of mouse NBD1, but not human NBD1. The reason for this discrepancy is unclear. But X-ray crystallography provides only static snapshots of protein structures. Moreover, the numerous artificial mutations introduced into human CFTR's NBD1 for optimal crystallization may cause distortion of the structure. A more interesting possibility is that these minor differences in the binding pocket for the adenine ring of ATP may reflect different NBD1 structures in different functional states. Future studies of CFTR gating using these mutations may provide definitive answers.

The current studies of mutations in CFTR's ATP binding pockets suggest that the two ATP binding sites differ in their gating functions both kinetically and energetically. Since the closed state of the channel represents NBDs in the monomeric configuration (Vergani et al., 2005), the relationship between [ATP] and the opening rate reflects the ATP binding affinity at the site that controls channel opening. Our results with the Y1219 and W401 mutations (Fig. II.2 C) suggest that ATP binding at the NBD2 site, but not the NBD1 site, is critical for channel opening. However, whether ATP binding at the NBD1 site is essential for channel opening (e.g., Vergani et al., 2003) remains unknown. On the other hand, although both ATP binding sites play a role in channel closing, each site

utilizes ATP differently. During normal hydrolysis- driven gating, it appears that it is the ATP hydrolysis at the NBD2 site that catalyzes channel closing (Carson et al., 1995; Zeltwanger et al., 1999; Vergani et al., 2003; Bompadre et al., 2005b), whereas ATP binding at the NBD1 site modulates the closing rate by stabilizing the open channel conformation.

II.3.3 Structural and biochemical implications of the asymmetry of the two ABPs.

The kinetic and energetic asymmetry in CFTR's NBDs described above imparts several structural and biochemical implications. First, we propose an asymmetrical molecular motion of NBDs during gating. Our results suggest that channel opening is initiated by ATP binding at the NBD2 site. Indeed, the critical pair of amino acids (R555 and T1246 in Vergani et al., 2005) identified for lowering the transitional state energy for NBD dimerization is absent in the NBD1 site (T460 and L1353). Thus, it is possible that the molecular motion of NBD dimerization that leads to opening of the gate may not proceed as a simple symmetrical movement of two ATP-bound NBDs. We propose that NBD dimerization is triggered by ATP binding at the NBD2 site and subsequently progresses to close the gap at the NBD1 site. Since the open state represents a head-to-tail dimer of CFTR's two NBDs with two ATP molecules sandwiched in between, the ligand ATP now becomes part of the whole protein molecule in the open channel configuration. Thus, the ligand binding energy is expected to be part of the overall energetics of the open channel conformation. This idea predicts that manipulating the ligand binding energy with mutations or alterations of ligands can affect the stability of the open state. It seems puzzling that mutations at the NBD1 site, but not the NBD2 site, affect the open

time. However, these results are consistent with the idea that separation of the NBD dimer at the NBD1 site is coupled to channel closing (compare Vergani et al., 2003). Taking one step further, we speculate that the molecular motion that couples NBD dimerization and opening of the gate resides in the NBD1 site.

Second, it is known that NBD1 does not hydrolyze ATP (Szabo et al., 1999; Aleksandrov et al., 2002; Basso et al., 2003). Unlike the NBD2 site, the ATP binding pocket at NBD1 lacks the crucial glutamate residue that serves as a catalytic base for ATP hydrolysis (Lewis et al., 2004, 2005). In addition, the Walker A lysine (K464 in human CFTR) is not perfectly conserved across species. If the hypothesis that the free energy of ATP binding at the NBD1 site is used to stabilize the open channel configuration is correct, it is perhaps not surprising that the NBD1 site is not designed to hydrolyze ATP.

Third, to harvest a high binding energy at NBD1, it is necessary to construct a binding pocket that binds ATP tightly. It is interesting to note that the two aromatic residues, F409 and F430, in the ATP binding pocket of the NBD1 site, are located in the regulatory insertion that is unique to CFTR's NBD1. The existence of multiple aromatic residues in ATP binding pockets have been reported previously in many ATP binding proteins with high affinity to nucleotides, such as phosphodiesterases (Huai et al., 2003, 2004) and myosin isozymes (Gillespie et al., 1999). It is tempting to speculate that the higher affinity for nucleotides in NBD1 compared with NBD2 (Szabo et al., 1999; Aleksandrov et al., 2001; Aleksandrov et al., 2002; Basso et al., 2003; Zhou et al., 2005) is at least partly due to the existence of multiple aromatic residues in the ATP binding pocket of NBD1.

Regardless of how NBD1 assumes a high affinity for ATP, given the fact that the intracellular [ATP] is nearly always maintained in the millimolar range, it seems puzzling why one of CFTR's two NBDs (i.e., NBD1) exhibits a higher affinity for ATP, while most of the other ABC family members have two very similar NBDs. If we accept that CFTR is evolved from a primordial ABC transporter that functions as an ATP hydrolysis–driven pump, this structural modification of CFTR's NBD1 may serve a teleological purpose. For a pump molecule to transport its substrate efficiently, it is preferable for most of the intermediate states during a transport cycle to be short-lived. This basic design principle for efficient pumps may not be ideal for a channel because only the open state of the channel conducts ions. It seems possible that the purpose of rendering NBD1 with a high affinity for ATP is to allow the channel to stay in the open state longer so that more Cl^- ions can go through the channel during each gating cycle.

II.4 Summary

The general accepted scenario for CFTR gating cycle is as following. The R domain needs to be first phosphorylated to activate the channel. ATP binding and NBD dimer formation lead to channel opening. ATP hydrolysis closes the channel. In this work, we conclude that ATP binding at NBD2 is crucial for channel opening, while ATP binding at NBD1 modulates the channel closing rate. We distinguished the residues ATP interact with and we also demonstrated that how this interaction affect channel gating. However, a detailed mechanism is still to be elucidated. For example, how is the conformational change in NBDs transduced to the physical gate? On one side of each ABP, the residues

involved in ATP binding are from Walker A and B motifs. Functional studies addressing the roles of these residues were carried out extensively. On the other side of the ABP, the residues are mainly from the signature sequences (LSGGQ). The functional role of these residues, however, is not clear. We thus studied the role of residues in the signature sequences in the following chapters.

Chapter III: Mutations at the Signature Sequence of CFTR Create a Cd^{2+} -gated Chloride Channel

This chapter has been revised and modified from my manuscript published in J. Gen Physiol. 133:69-77, 2009, by Wang, X., Bompadre, S.G., Li, M. & Hwang, T.-C.. According to their web site, http://jgp.rupress.org/misc/terms.shtml, I retain the copyright for this work and am allowed to alter and build upon this work.

The goal of this chapter is to study the role of the signature sequences in NBD1 in channel gating. In this series of studies, we found that the signature sequence of NBD1 serves as a switch to transmit the signal of ATP binding at NBDs to channel opening. The importance of the signature sequence is attested by the fact that a Glycine to Aspartate mutation (i.e., G551D) in cystic fibrosis transmembrane conductance regulator (CFTR) results in a severe phenotype of cystic fibrosis. We previously showed that the G551D mutation completely eliminates ATP-dependent gating of the CFTR chloride channel. Here, we report that micromolar [Cd^{2+}] can dramatically increase the activity of G551D-CFTR in the absence of ATP. This effect of Cd^{2+} is not seen in wild-type channels or in G551A. Pretreatment of G551D-CFTR with the cysteine modification reagent 2-aminoethyl methane thiosulfonate hydrobromide (MTSEA) protects the channel from Cd^{2+} activation, which can be rescued by DTT washout. This suggested an involvement of endogenous Cysteine residue(s) in mediating this effect of Cd^{2+}. The mutants G551C, L548C, and S549C, all in the signature sequence of CFTR's NBD1, show robust response to Cd^{2+}. On the other hand, negligible effects of Cd^{2+} were seen with T547C, Q552C, and R553C, indicating that a specific region of the signature sequence is

involved in transmitting the signal of Cd^{2+} binding to the gate. Collectively, these results suggest that the effect of Cd^{2+} is mediated by a metal bridge formation between a Cysteine residue and the engineered Aspartate or Cysteine in the signature sequence. We propose that the signature sequence serves as a switch that transduces the signal of ligand binding to the channel gate.

III.1 Introduction

The CFTR is an ATP-gated chloride channel, whose malfunction leads to Cystic Fibrosis, the most common lethal genetic disease among Caucasians. Being a member of the ATP-Binding Cassette (ABC) transporter superfamily (Riordan et al., 1989), CFTR consists of two Membrane-Spanning Domains (MSD1 and MSD2) and two Nucleotide-Binding Domains (NBDs; NBD1 and NBD2). Like other members of this family, two NBDs dimerize in a head-to-tail configuration upon ATP binding, and these dimerized NBDs represent the open channel conformation of CFTR (Vergani et al., 2005). Recently, we showed that ATP opens the channel by binding to the binding pocket formed by the Walker A sequence of NBD2 and the signature sequence of NBD1 (Zhou et al., 2006). Under normal conditions, hydrolysis of this bound ATP closes the channel presumably by breaking the dimer apart (for review see Chen and Hwang, 2008).

Although operationally CFTR can be classified as a ligand- gated channel, unlike classical ligand-gated channels, CFTR's ligand (ATP) is consumed during the gating cycle. ATP hydrolysis at NBD2 provides an input of free energy so that CFTR's gating is not a process in thermodynamic equilibrium (Chen and Hwang, 2008). However, CFTR may work as a classical ligand-gated ion channel when ATP hydrolysis is abolished

(either by mutations or by using non-hydrolyzable ATP analogues). In this case, binding and unbinding of the ligand gates the CFTR channel and channel open time is often prolonged.

Recently we found that the disease-associated mutation G551D (the single – amino acid substitution of Glycine to Aspartate in the signature sequence of NBD1) abolishes the ATP-dependent gating of the channel (Bompadre et al., 2007). The importance of the signature sequence is attested by how dramatically the G551D mutation affects the gating of the channel and by the severity of the disease phenotype associated with this mutation, but little is known about its specific role in CFTR gating. Although the signature sequence is part of the ATP-binding pocket in a dimerized configuration, the crystal structure of isolated NBD1 of CFTR shows that ATP binds to the Walker A region (Lewis et al., 2004), and it is presumed that the signature sequence of the partner NBD may contact the bound ATP molecule when the two NBDs approach each other to form a dimer (Fig. III.1). The G to D mutation either completely abolishes ATP binding at this site, ABP2, or blocks the conformational changes following ATP binding. Evidence for the latter are biochemical studies of other ABC transporter protein that demonstrate that this G to D mutation in the signature sequence of either NBD have little effect on ATP binding (Ren et al., 2004). Taking together our work (Zhou et al., 2006) that ATP binding at ABP2 initiates channel opening, we think G551D mutation likely hampers the conformational changes at ABP2 that facilitate NBD dimerization, thus channel opening.

Since the G551D mutation introduces a negatively charged residue at the ATP binding pocket, our strategy is to use cations to artificially induce dimerization. Cations has been used to link two protein subdomains together previously (Webster et al., 2004).

A good example is Cd^{2+}, which has been used as a high affinity metal bridge to link two residues together to lock the protein structure. Base on all these information, we want to investigate the possibility that cations help two NBDs to form a dimer and thus induce channel opening. Cd^{2+}, Ca^{2+}, Ni^{2+}, and Zn^{2+} are the candidates, which might interact with the residues within 10 Å from the mutation position 551. It is well known that, Cd^{2+} coordinates with cystine, and histidine; Zn^{2+} coordinates with cystine; Ca^{2+} interacts with aspatate and glutamate, and Ni^{2+} can coordinate with histidine. These residues around the mutation site present interesting targets for using these divalent cations to understand channel gating.

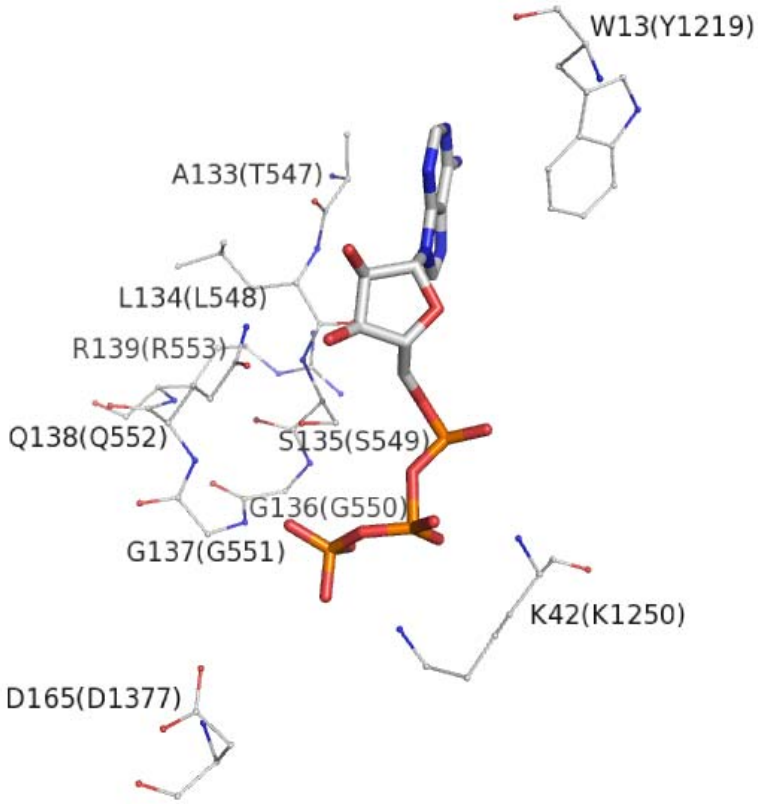

Chapter III Figure III.1: Schematic presentation of the interactions of ATP with key residues in the ATP binding pocket of an NBD dimer. The crystal structure of E. coli Malk NBD dimer (pdb code: 1Q12) was used to demonstrate these interactions. The ATP molecule is represented by the stick model. Selective residues are shown and represented by thin lines, including residues of the signature sequence, the Walker A lysine, the D-loop aspartate and the aromatic residue that strongly interacts with the adenine ring of ATP. These residues are colored by their atom types and labeled by their residue numbers as they appear in the amino acid sequence of E. coli Malk. The corresponding residues in CFTR are labeled in the parentheses.

We found that "soft" metal ions such as Cd^{2+} and Zn^{2+} can dramatically increase the activity of G551D-CFTR with a micromolar-apparent affinity. This effect of Cd^{2+} was negligible with the Wild-Type (WT) channels or the equivalent mutation, G1349D, at the signature sequence of NBD2 (data not shown). The apparent affinity for Cd^{2+} was further increased when glycine 551 was converted to cysteine. Cd also increase little current on G551E and G551H mutations, but the effect of Cd^{2+} was mostly abolished when the G551 residue was substituted by an alanine or lysine. (Figure not shown). Engineering a cysteine residue at position 548 or 549, but not at 547, 552, and 553, also creates channels that can be effectively gated by Cd^{2+} (Figure III.6, D). These data strongly support the notion that, like in ATP-dependent gating of CFTR, the signature sequence of genetically modified NBD1 also plays a key role in mediating Cd^{2+} - dependent gating, presumably because the mutations craft a multi-dentate Cd^{2+} -binding site. Consistent with this idea, pretreatment of the G551D-CFTR with the sul-hydryl reagent 2-aminoethyl methane thiosulfonate hydrobromide (MTSEA) abolished the effect of Cd^{2+} , suggesting that Cd^{2+} ions are coordinated by 551C/D and some other partner cysteine(s). The protection of the MTS reagent can only be washed out using a reducing agent. Identifying the responsible cysteine residue(s) will provide molecular insight into the gating mechanism of CFTR and the pharmacological target residues for CFTR treatment.

III.2 Results

III.2.1 Cd^{2+} Increases the Activity of G551D-CFTR

We studied the effect of different divalent cations, including Cd^{2+} , Ca^{2+} , Ni^{2+} , and Zn^{2+} , alone or in combination, on G551D-CFTR channels in excised inside-out

membrane patches from transiently transfected Chinese hamster ovary cells. Fig. III.2 A shows a real-time recording of G551D-CFTR channels in an excised patch that have been activated with 1 mM ATP and PKA (not depicted) before being exposed to different metal ions. Application of 10 μM Zn^{2+} or 10 μM Cd^{2+} in the absence of ATP increased the channel activity by 5.0 ± 0.4-fold (n = 6) and 12.2 ± 1.2- fold (n = 6), respectively, but neither 1 mM Ca^{2+} nor 10 μM Ni^{2+} had significant effects (n = 10). As a control, we applied the same metal ions to patches containing WT-CFTR channels. None of these cations, when applied in the absence of ATP, had any effect on WT-CFTR (n = 10) (Fig. III.2 B). Because CFTR channels can only be opened by ATP after they have been phosphorylated by PKA, we tested whether the effect of Cd^{2+} on G551D-CFTR is also phosphorylation dependent. We applied the same [Cd^{2+}] before and after PKA-dependent phosphorylation. As shown in Fig. III.3 A, Cd^{2+} only increased the current of G551D-CFTR after the channels had been pre- phosphorylated by PKA (n = 5).

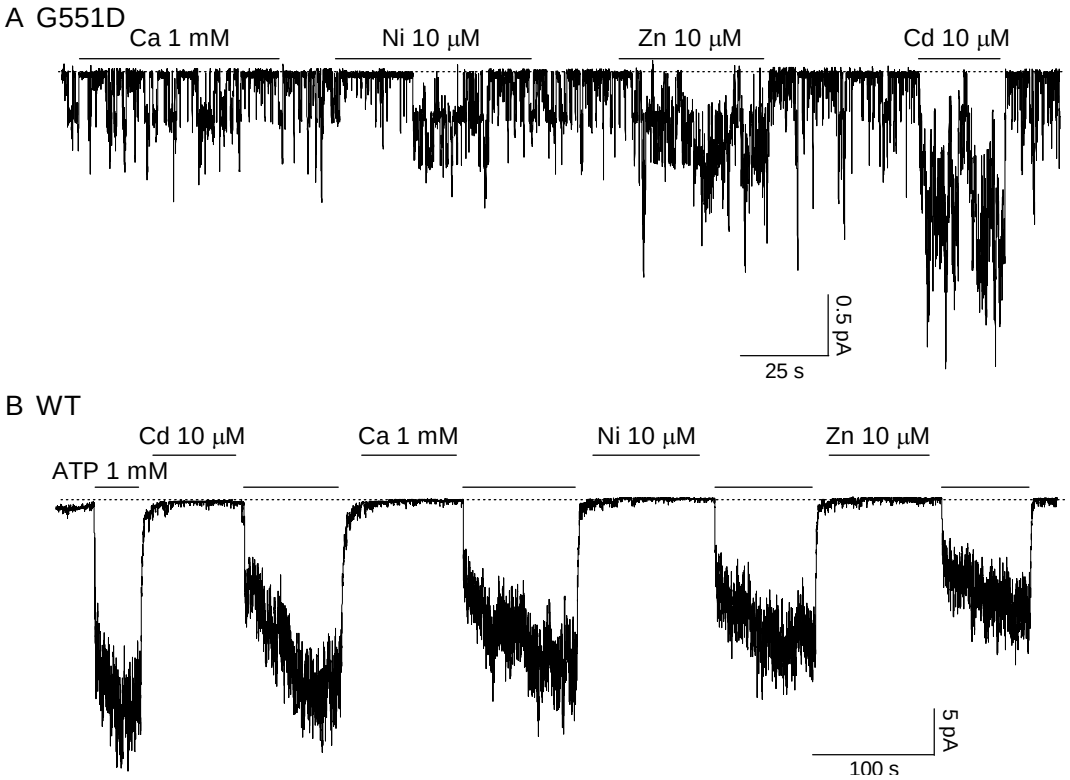

Chapter III Figure III.2. Effect of different metal ions on G551D- and WT-CFTR currents. (A) 10 μM Cd^{2+} and 10 μM Zn^{2+} potentiate G551D-CFTR ATP-independent currents, but 1 mM Ca^{2+} and 10 μM Ni^{2+} have little effect on the currents. (B) WT-CFTR currents are not affected by any of these cations. Dashed lines in all figures represent the baseline.

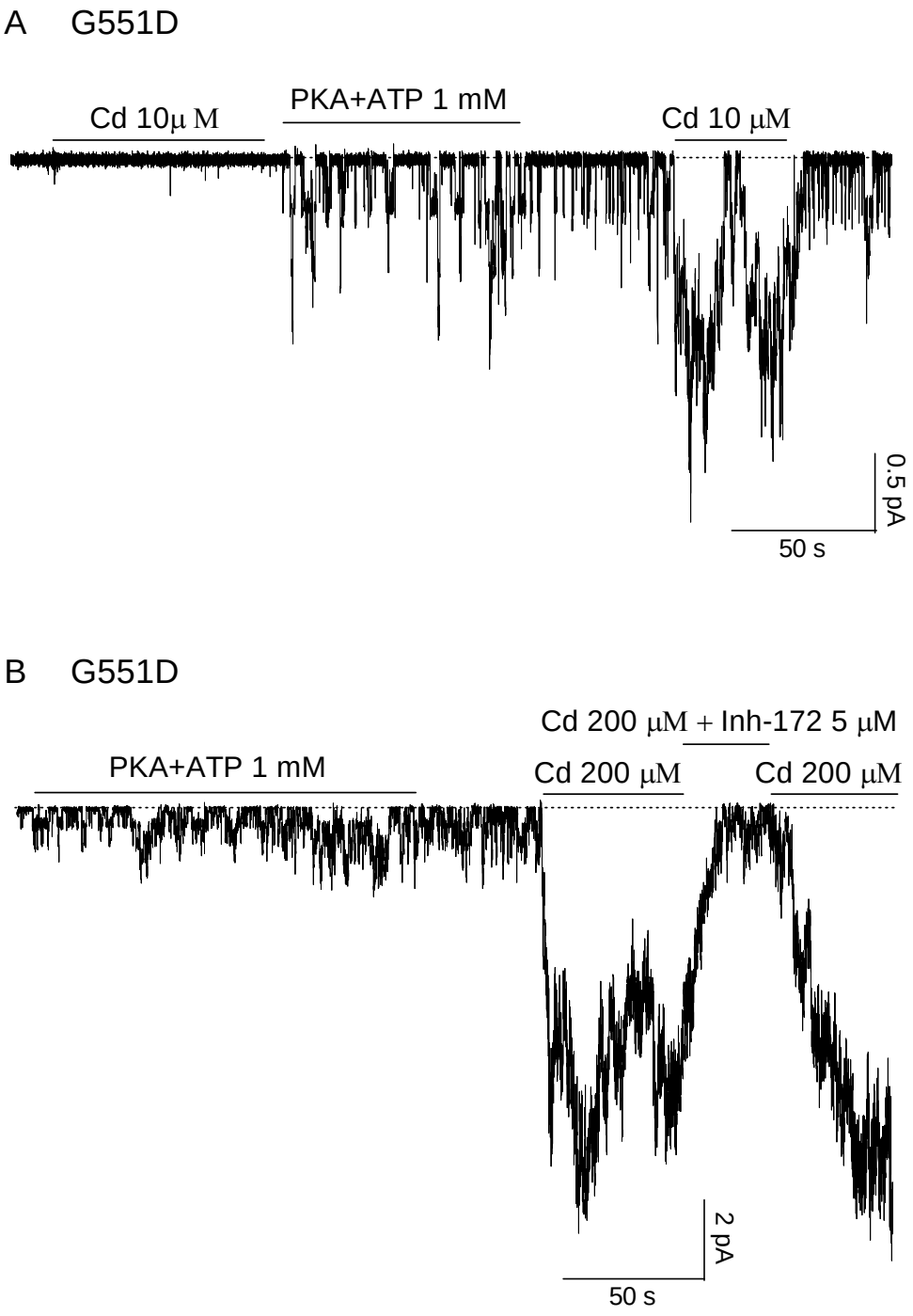

Chapter III Figure III.3**.** Functional characterization of the Cd^{2+}-dependent effect in G551D-CFTR. (A) Activation of G551D-CFTR by Cd^{2+} is phosphorylation-dependent. Note that in the same patch Cd^{2+} only increases the activity of G551D-CFTR after the channels are activated by PKA and ATP. (B) A CFTR specific blocker, inh-172, can inhibit the G551D-CFTR current induced by 200 μM Cd^{2+}.

Previously, we estimated the Po of G551D channels to be 100-fold smaller than the maximal Po of WT channels at saturated concentration of ATP, ~ 0.004 ± 0.001 with a mean open time of 367 ± 42 ms (Bompadre et al., 2007). A quick calculation gives us an opening rate of 0.010 ± 0.003 s^{-1} (from $P_o = \tau_o/ (\tau_o+\tau_c)$, where τ_o is the open time of the channel, $\tau_c = 1/r_{co}$ is the closed time of the channel and r_{co} is the opening rate) Because 100 μM Cd^{2+} potentiates G551D activity by ~ 20-fold, we estimate that the Po of G551D-CFTR is 0.08 ± 0.03 under this condition. From patches with fewer than five simultaneous channel opening steps, we calculated the open time of G551D channels in the presence of 100 μM Cd^{2+} to be 2.4 ± 0.4 s (n = 10). Then the opening rate of G551D-CFTR in the presence of 100 μM Cd^{2+} is ~ 0.036 ± 0.015 s^{-1}, a near fourfold increase (3.6 ± 1.8) of the opening rate of G551D-CFTR in the absence of Cd^{2+}.

We also tested the effect of combining these cations together on the G551D mutant. We first apply Ca^{2+}, and then Cd^{2+}. The Cd^{2+} effect was reduced. If Ca^{2+} and Cd^{2+} are applied simultaneously, the Cd^{2+} effect was also reduced. The induced current is about 0.67 fold less than Cd^{2+} alone (n=3, traces not shown). We interpret this decrease by a competition effect between Ca^{2+} and Cd^{2+}, since Ca^{2+} might also interact with D551 as well. Meanwhile, Ni alone or combined with Cd^{2+} shows no effect both on G551D and G551H, which indicates that histidine residues may not involved.

Although Cd^{2+} increases the activity of G551D-CFTR, Cd^{2+} shows little effect on G1349D-CFTR (n = 5) (Figure not depicted), a mutation of the corresponding glycine residue in the signature sequence of NBD2, indicating that this effect of Cd^{2+} is specific for the glycine-to-aspartate mutation at signature sequence on NBD1. To ensure that the channels opened by Cd^{2+} were indeed CFTR, we tested Cd^{2+} in patches excised from

nontransfected cells and did not observe any channel activation (n = 5, data not shown). In addition, the channels opened by 200 μM Cd^{2+} could be inhibited by inhibitor- 172, a specific CFTR inhibitor that has been shown to modulate gating of WT-CFTR (Ma et al., 2002; Caci et al., 2008). As shown in Fig. III.3 B, the current induced by 200 μM Cd^{2+} was nearly abolished by 5 μM inh-172 (97.2 ± 0.8% inhibition; n = 7). Another CFTR specific inhibitor, Glibenclamide, also shows similar inhibition of the Cd induced current. Thus, like ATP-dependent gating for WT-CFTR, activation of G551D mutant channels by Cd^{2+} requires pre-phosphorylation of the channel by PKA, and the Cd^{2+} -induced currents can be readily and reversibly inhibited by inh-172 and Glibenclamide. Because the activation of G551D-CFTR channels by Cd^{2+} is more effective than Zn^{2+}, we focused our studies on this particular cation.

III.2.2 Cd^{2+} Is More Potent on G551C than on G551D

Since Cd^{2+} and Zn^{2+} can bind and affect channel activities in various ways, we considered two possible mechanisms for the effect of Cd^{2+} on G551D-CFTR. First, Cd^{2+} may directly interact with the side chain of the aspartate at position 551 and form a metal bridge between D551 and some other amino acids. Alternatively, the G551D mutation may induce some kind of protein conformational changes which abolished ATP effect, and these structural changes enable Cd^{2+} to enhance the activity of G551D-CFTR. In this case, Cd^{2+} may exert its effects by binding to somewhere else other than 551D and opening the channel in a nonspecific manner. To differentiate these two possibilities and identify the Cd binding specificity, we first mutated the glycine at position 551 to cysteine. We reasoned that if Cd^{2+} directly interacts with the side chain of the aspartate at

551, it will do so more effectively with a cysteine at that position because the thiol group of cysteines can better coordinate soft metal ions like Cd^{2+} (Rothberg et al., 2003). We predict the dose response will follow a Hill Equation. Fig. III.4 shows representative traces of G551D (A) and G551C (B) in the presence of different [Cd^{2+}]. Note that 5 μM Cd^{2+} induces a higher G551C-CFTR current than 1 mM ATP, despite that this mutation retains responsiveness to ATP. The normalized dose – response relationships of Cd^{2+} for these two mutants are shown in Fig. III.4 (C and D). For G551D-CFTR, 100 μM Cd^{2+} increases the current by 21.38 ± 4.19 fold (n = 6), but the current response is not quite saturated. On the other hand, 10 μM Cd^{2+} already generates a maximal response for G551C-CFTR, with a maximal fold increase of 7.4 ± 0.3 (n = 5) compared with the currents generated by 1 mM ATP. If compare with basal activity as we did with G551D, the Cd^{2+} induced increase is about 60 fold. Fitting the dose – response relationships with the Hill Equation yields a $K_{1/2}$ of 14.6 ± 6.3 μM and 3.29 ± 0.66 μM for G551D and G551C, respectively.

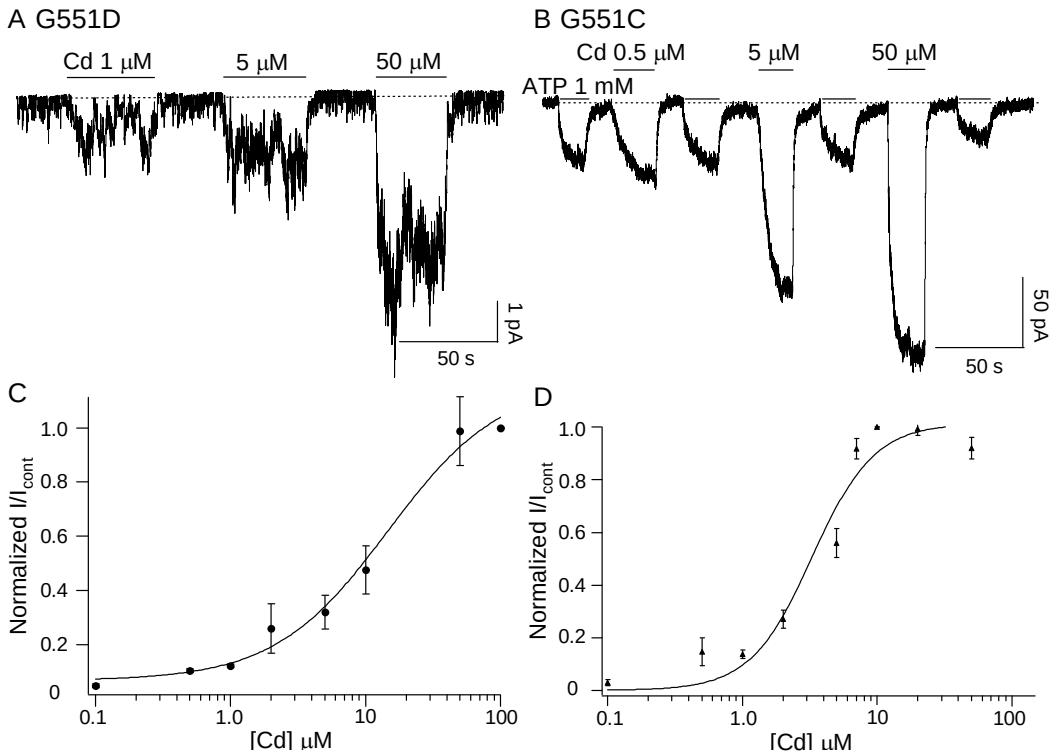

Chapter III Figure III.4. Representative current traces of G551D-CFTR (A) and G551C-CFTR (B) in the presence of different [Cd^{2+}]. The Cd^{2+} dose response relationships for G551D-CFTR (C) and G551C-CFTR (D) were fitted with the Hill equation, $y = min + (max - min)/ [1+ (K_{1/2}/[x])^n)]$ (smooth curves). The fold increase of the current in the presence of Cd^{2+} was normalized to the maximal fold increase for each mutant (21.38 ± 4.19 fold, 100 μM Cd^{2+} for G551D, and 7.4 ± 0.3, 10 μM Cd^{2+} for G551C). For G551D, $K_{1/2}$ = 14.6 ± 6.3 μM and n = 1.03 ± 0.34; for G551C, $K_{1/2}$ = 3.29 ± 0.66 μM and n = 1.89 ± 0.52.

To further test our hypothesis that the engineered aspartate or cysteine at position 551 is directly involved in coordinating Cd^{2+}, we mutated G551 to alanine, which Cd^{2+} should not be able to bind effectively. Like the G551C mutant, G551A-CFTR remains responsive to ATP. However, the effect of Cd^{2+} on G551A-CFTR is negligibly small compared with that of G551C-CFTR (Fig. III.5 A vs. Fig. III.4 B). This difference between G551A and G551C was quantified in Fig. III.5 B, where we compared the current generated by 1 mM ATP with the current generated by 10 μM Cd^{2+} for these two mutants. Because the side chains of aspartate and cysteine, but not alanine, are found in the multi-dentate coordinating geometries of metalloproteins that bind Cd^{2+} (Rulisek and Vondrasek, 1998), these results support the notion that Cd^{2+} interacts directly with the side chain of engineered aspartate or cysteine at position 551 despite the different apparent affinities. Also shown in Fig. III.5 (lower panel) is the ratio of currents induced by 10 μM Cd^{2+} and those in the absence of ATP (i.e., basal currents) for G551C- , G551D- and G551A-CFTR. This alternate data presentation again supports our idea that Cd^{2+} likely interacts directly with the side chain of the amino acid residue at the 551 position.

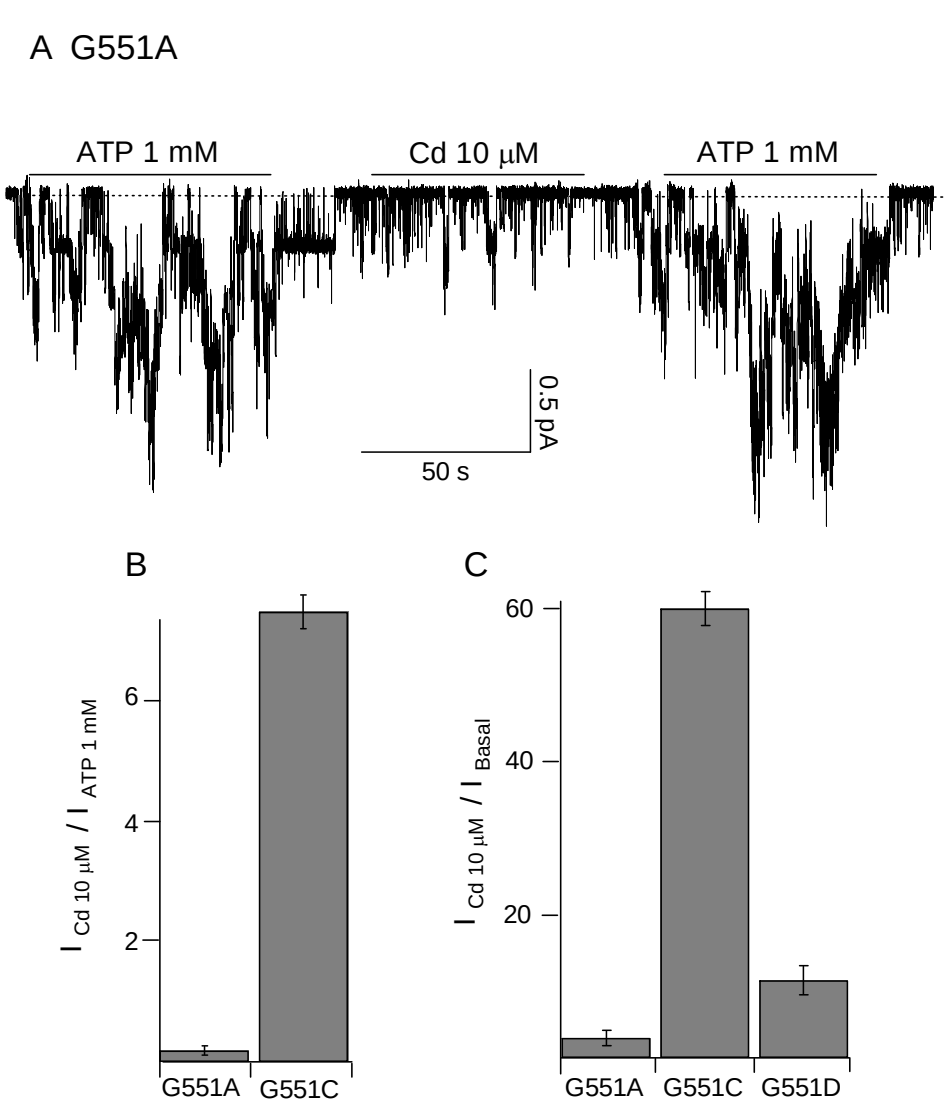

Chapter III Figure III.5**.** Comparison of Cd^{2+} and ATP induced currents between G551A and G551C mutants. (A) Representative current trace of G551A-CFTR. Although G551A-CFTR remains ATP-dependent, Cd^{2+} fails to increase the activity of the channels. (B) The ratio of currents induced by 10 μM Cd^{2+} and those with 1 mM ATP for G551C- and G551A-CFTR. (C): The ratio of currents induced by 10 μM Cd^{2+} and those in the absence of ATP (i.e., basal currents) for G551C- , G551D- and G551A-CFTR.

III.2.3 Cd^{2+} Increases the Activity of Other Signature Sequence Mutants

To further probe the Cd^{2+} -binding position and specificity, we introduced a cysteine at different positions in the signature sequence of NBD1 (LSGGQ), as well as the two amino acids framing the signature sequence. Specifically, we mutated amino acids T547, L548, S549, G551, Q552, and R553, one at a time, to cysteine. A representative S549C-CFTR current recording is shown in Fig. III.6 A. Cd^{2+} elicited macroscopic current even at sub-micromolar [Cd^{2+}]. At a concentration as low as 5 μM, Cd^{2+} already induced a maximal response that is 4.6 ± 0.4 fold (n = 6) larger than the currents generated by 1 mM ATP. Fitting the dose – response relationship with the Hill Equation yields a $K_{1/2}$ value of 2.4 ± 0.8 μM (Fig. III.6 C).

In contrast, 10 μM Cd^{2+} shows negligible effect on the T547C mutant (Fig. III.6 B). Fig. III.6 D , in which the relative efficacy of ATP (1 mM) versus Cd^{2+} (10 μM) is compared, summarizes data for all these mutations in or around the signature sequence. It appears that when cysteine is engineered outside the signature sequence (i.e., T547C and R553C) or at the C-terminal end of the signature sequence (i.e., Q552C), ATP remains a much better ligand than Cd^{2+} (e.g., Fig. III.6 B). However, for L548C, S549C, and G551C, the specificity of the ligand is altered so that Cd^{2+} becomes more effective at gating the channels than ATP. These results set apart amino acids 548 – 551 in the signature sequence in mediating the effect of Cd^{2+}. Similarly, when Cd^{2+} induced current was compared with basal current (without ATP), as shown in Fig. III.6 (lower panel), it singles out 548 - 551 as the critical region for mediating Cd^{2+} effects when they are converted to cysteine. It is interesting to note that S549 and G551 residues are involved in forming hydrogen bonds with the γ -phosphate of the bound ATP in several crystal

structures of NBD dimers (e.g., Fig. III.1) in the ABC transporters (Hopfner et al., 2000 ; Smith et al., 2002 ; Chen et al., 2003 ; Zaitseva et al., 2005). The significance of these overlapping regions of the signature sequence between ATP-dependent gating for WT-CFTR and Cd^{2+} - dependent gating of mutant channels is discussed below. The data also demonstrated that Cd can interact with multiple residues at the signature sequence rather than a single residue, which is the first effort in the CFTR field to study the role of signature sequence.

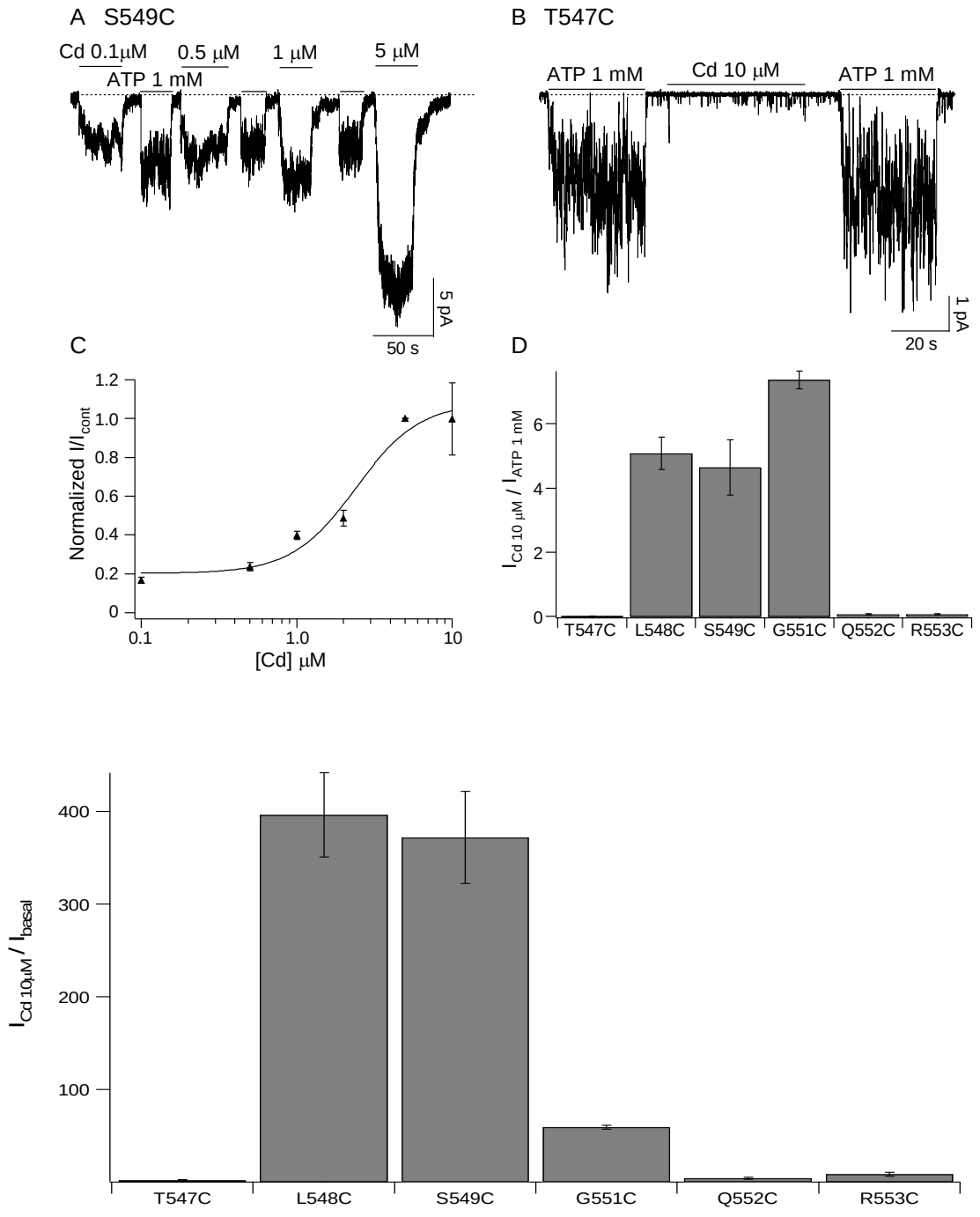

Chapter III Figure III.6. Comparison of Cd^{2+} and ATP induced currents or basal activity for different mutants in the signature sequence region of NBD1. (A) Representative S549C-CFTR current recording in the presence of different [Cd^{2+}]. (B) Representative T547C current recording in the presence of 1mM ATP or 10 μM Cd^{2+}. (C) Dose response relationship for S549C-CFTR fitted with the Hill Equation (solid line); $K_{1/2}$ = 2.4 ± 0.8 μM. The maximum fold increase is 4.6 ± 0.4. (D) Summary of the current ratios for different mutants with cysteine substituting amino acids in or around the signature sequence of NBD1. Lower panel: The Cd^{2+}-induced currents were compared to the basal current (i.e., current in the absence of ATP) for the same mutants in the NBD1 signature sequence region.

III.2.4 The Binding Partner of Cd^{2+} Is Likely To Be a Cysteine Residue

The micromolar affinity of Cd^{2+} in activating G551C or S549C mutants raises the possibility that some endogenous Cysteine(s) or Histidine(s) may participate in forming a high-affinity binding site for Cd^{2+}. Histidine is not the likely candidate since Ni^{2+} shows no current changes when we tested its effect on G551H and Ni^{2+} plus Cd^{2+} on G551D. To confirm cysteine as the best candidate for Cd^{2+} effect, we used the thiol-specific reagent MTSEA which can modify exposed cysteine by form covalent disulfide bond. Fig. III.7 shows a representative recording. The G551D-CFTR channels were exposed to 1 mM MTSEA for a short period of time (< 1 min), and MTSEA was subsequently washed out. Cd^{2+} no longer increased the channel activity after MTSEA pretreatment (n = 5). However, this effect of MTSEA can be reversed by 5 mM DTT. This result suggests that the binding partner of Cd^{2+} is likely a cysteine residue. To further test this hypothesis, we made a G551D-CFTR construct with 16 out of the 18 endogenous cysteine residues replaced with serines (the 2 Cysteine residues, C590 and C592, left unchanged are essential for protein expression) and another mutation with all the cysteines in G551D-CFTR have been replaced with serine, leucine with additional mutation V510A (Wang et al., 2007). Cd^{2+} can no longer activate this G551D/16-Cysless channel (not depicted) or G551D/V510A/ 18 Cysless channel. We therefore conclude that Cd^{2+} opens these CFTR mutants likely by forming a metal bridge between the introduced cysteine/aspartate and the endogenous cysteine(s) that has been identified later on.

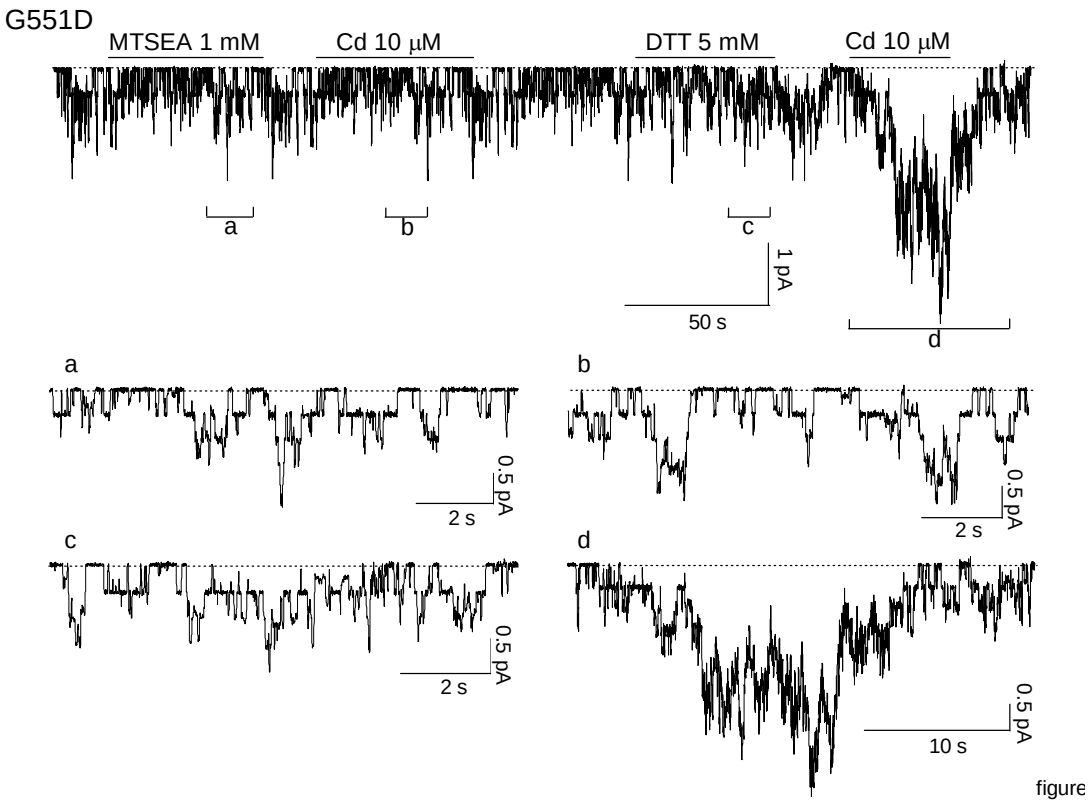

Chapter III Figure III.7. MESEA abolishes the effect of Cd^{2+} on G551D-CFTR. G551D-CFTR channels were activated with 1 mM ATP + PKA (not shown). Pretreatment of the patch with the thiol-specific reagent MTSEA abolished the potentiation effect of Cd^{2+}. 5 mM DTT can reverse the effect of MTSEA. Note that neither MESEA nor DTT by itself had discernable effects on the channel activity.

III.2.5 Cd with ATP together generate a profound increase in current for G551D-CFTR, which shows strong pharmacological prospects

Interestingly, we found that Cd^{2+} with ATP together can induce more than 30 fold (a representative trace is shown in Figure III.8) current increase compared with basal activity. If we use another higher binding affinity ATP analog, P-ATP, combined with Cd^{2+}, the current increase can be as much as 100-fold (a representative trace is shown in Figure III.9). If we accept that the G551D activity is 100 fold smaller than the activity of WT channels in the presence of saturating ATP (Bompadre et al, 2007), this results indicates that we can completely rescue the normal channel function by combining ATP with micromolar Cd^{2+}. Alternatively, Cd^{2+} and ATP together induce quite similar current on WT CFTR. The mechanism of these phenomena is not clear right now, but the fascinating result might extend our future research to pharmacological treatment of the G551D-CFTR.

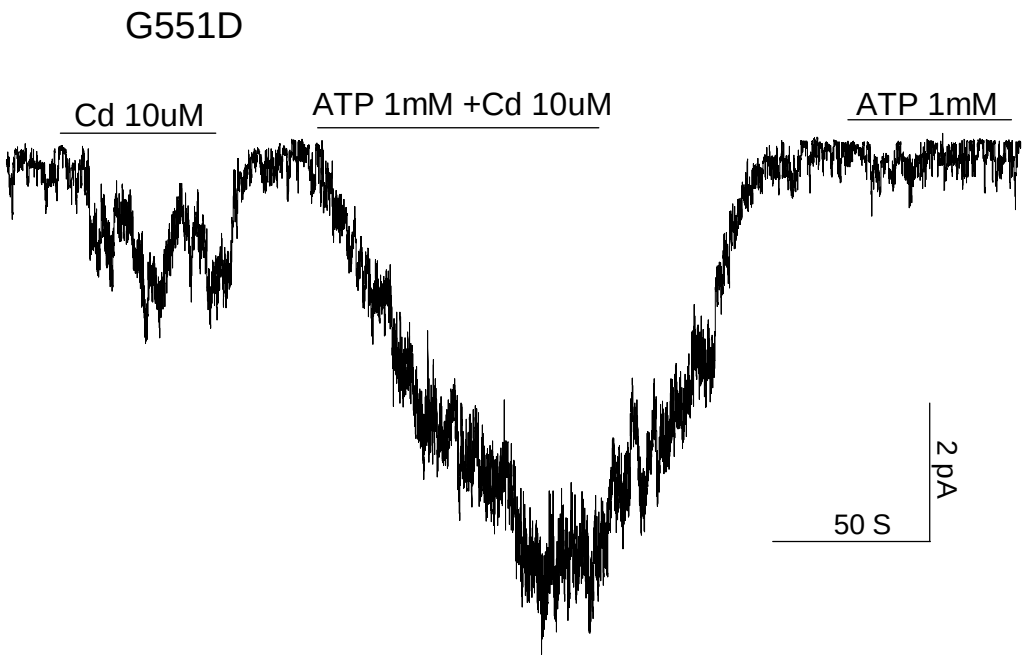

Chapter III Figure III.8. Cd^{2+} induces much more current in the presence of ATP than without ATP. The fold increase of current induced by 1mM ATP and 10 μM Cd^{2+} is 30 compared to basal activity of G551D-CFTR.

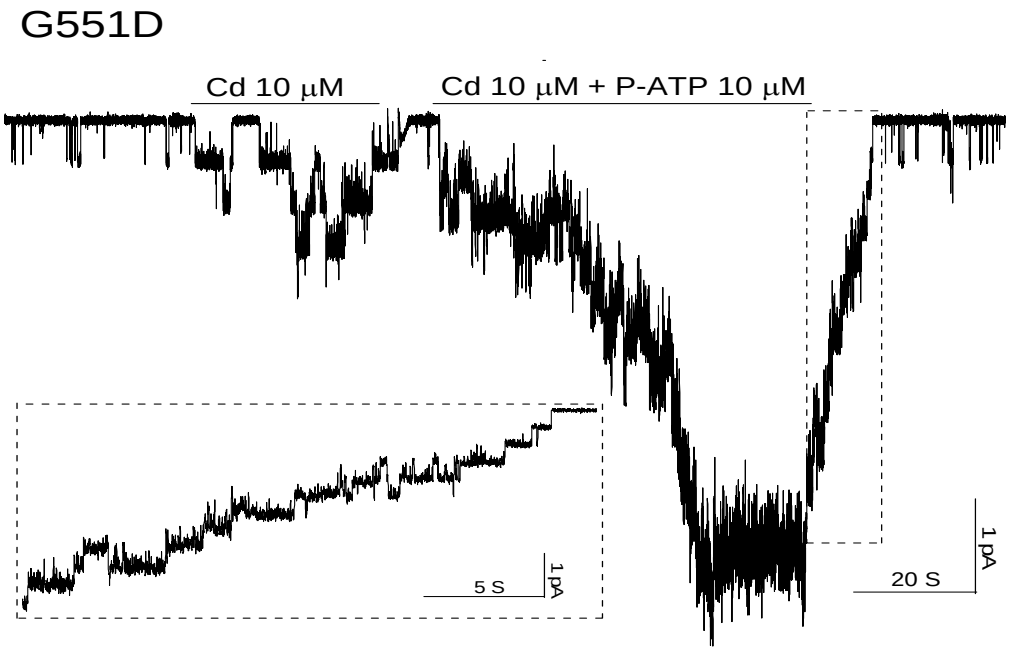

Chapter III Figure III.9. Cd^{2+} induced current can be further increased in the presence of P-ATP, an ATP analog with higher binding affinity. The fold increase of current induced by 10 μM P-ATP and 10 μM Cd^{2+} is ~200 compared to basal activity.

III.3 DISCUSSION

Here, we show that micromolar concentrations of Cd^{2+} can dramatically increase the activity of G551D-CFTR, a disease-associated mutant, as well as G551C-CFTR, L548C, and S549C-CFTR, in the absence of ATP. We speculate that this effect of Cd^{2+} is mediated by forming a metal ion bridge between the engineered aspartate or cysteine residue in the signature sequence of NBD1 (LSGGQ) and the yet to be identified cysteine residue(s) in another part of the CFTR protein.

III.3.1 Possible Kinetic Mechanism for the Action of Cd^{2+}

Before we discuss the possible biochemical/structural implications of our results, we will first look into the possible kinetic mechanism for the action of Cd^{2+}. It should be noted that this discussion on kinetics is meant to facilitate a better understanding of the action of Cd^{2+} and by no means suggest a definitive kinetic mechanism for Cd^{2+}, which will require extensive single channel studies. The simplest interpretation of Cd^{2+} -dependent activation of CFTR mutants shown here (SCHEME 1) is to consider Cd^{2+} as a ligand that increases the open probability (Po) of the channels. Two basic kinetic mechanisms are considered. Scheme 1 dictates that Cd^{2+}, by binding to the open state, induces another open state to increase the Po. This scenario can be envisioned if the Cd^{2+} binding site is exposed when the channel is in the open state.

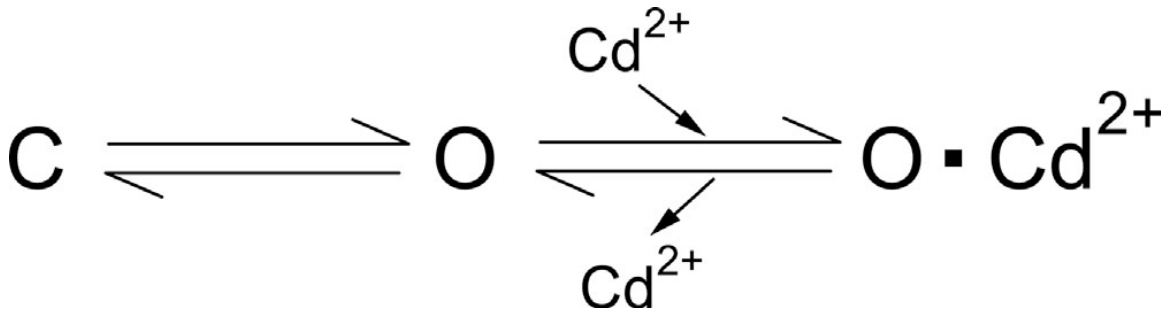

SCHEME 1

Scheme 2, a more generalized scheme for ligand-gated channels, proposes that Cd^{2+} can bind to both the open state and the closed state, but the Cd^{2+} -bound channel assumes a more favorable gating transition for the open state than the ligand-free channel.

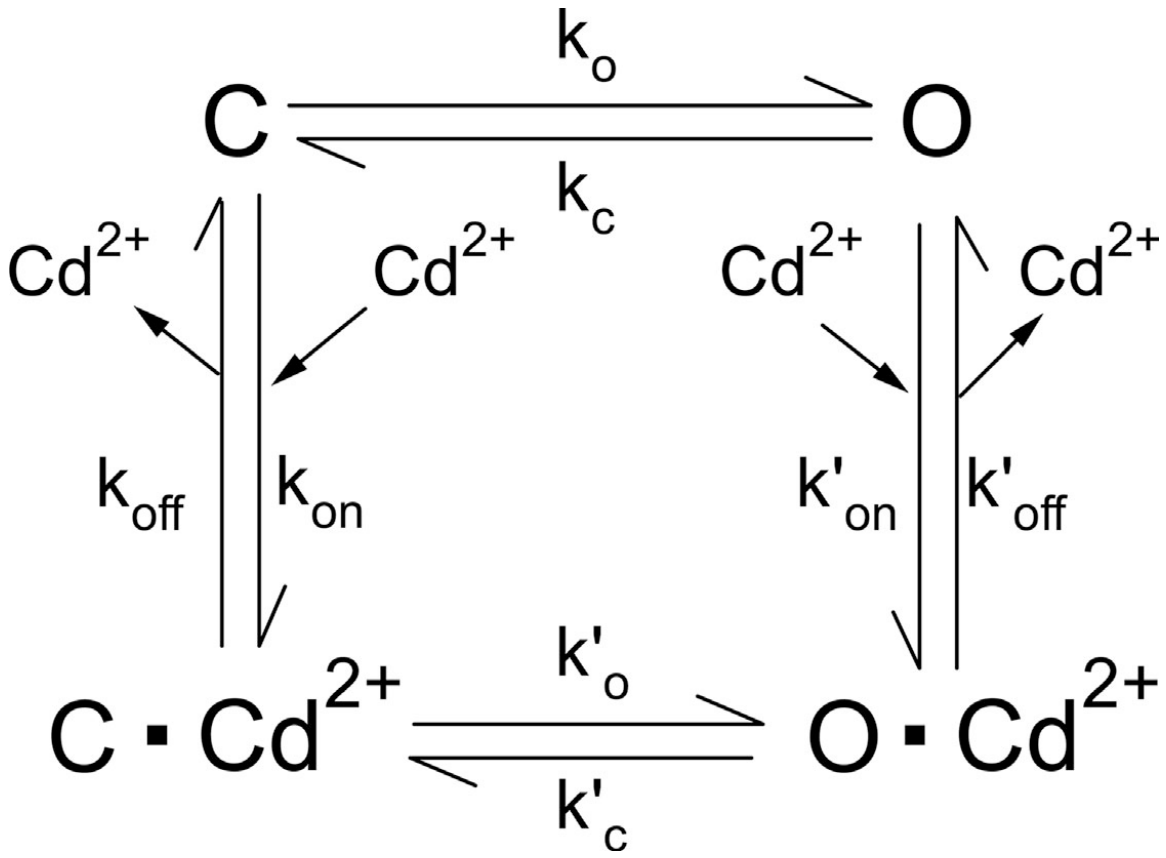

SCHEME 2

The major difference between these two schemes is that Scheme 1 predicts an unaltered opening rate in the presence of Cd^{2+}. As described above, the opening rate of G551D-CFTR is increased by Cd^{2+}. For G551C CFTR, this effect of Cd^{2+} on the opening rate likely also occurs. The open time for G551C-CFTR in the absence of ATP is 202.6 ± 29.6 ms (n = 3). In the presence of a saturating concentration of Cd^{2+} , the open time, estimated from the current relaxation upon removal of Cd^{2+} , is increased to 1.58 ± 0.21 s (n = 7). This approximately eightfold increase of the open time can hardly explain a ~ 40-fold (40.3 ± 2.5; n = 3) increase of the macroscopic current unless the opening rate is also increased significantly by Cd^{2+}. Although more complicated schemes are necessary to explain the full effect of Cd^{2+}, we consider Scheme 2, a generalized allosteric

mechanism for the modulation of protein function by ligand binding (Monod et al., 1965), as a simplistic model merely to aid this discussion.

III.3.2 Structure/Function Implications of the Effects of Cd^{2+} on CFTR Mutants

Although the signature sequence of ABC transporters is highly conserved, its functional role remains unclear despite numerous reports that mutations in this region perturb the function of the ABC proteins (Browne et al., 1996; Schmees et al., 1999; Chen et al., 2004; Ren et al., 2004; Szentpetery et al., 2004; Cai et al., 2006). Our previous studies have suggested that the ATP-binding pocket (i.e., ABP2 in Bompadre et al., 2007), formed by the Walker A region of NBD2 and the signature sequence of NBD1, plays a key role in the ATP-dependent opening of CFTR. Mutations of a conserved Tyrosine residue (Y1219) at NBD2 significantly reduce the potency of ATP to increase the opening rate of CFTR, likely because the mutations decrease ATP-binding affinity at ABP2 (Zhou et al., 2006). Alternatively, a mutation in the signature sequence of NBD1 (i.e., G551D) renders a channel completely irresponsive to ATP further supports the critical role of ABP2 in catalyzing channel opening (Bompadre et al., 2007). The current finding that Cd^{2+} can gate CFTR channels through an interaction with 551D/C, 548C, or 549C not only reinforces the role of ABP2 in channel gating, but also provides mechanistic insights into the functional role of the signature sequence in NBD1. We propose that the signature sequence of NBD1 may serve as a "switch" that, when activated by a ligand (ATP or Cd^{2+}), transmits the signal to the channel gate presumably located in the membrane-spanning domains that form the anion-selective pore.

The idea that ATP and Cd^{2+} gate the channel through a common structural motif of the signature sequence is supported by several pieces of evidence. First, as shown in Fig. III.3 A, gating of G551D-CFTR by Cd^{2+}, like ATP dependent gating of WT-CFTR, requires prior phosphorylation of the channels by PKA. Second, G551D-CFTR currents induced by Cd^{2+} can be inhibited by inhibitor- 172 or Glibenclamide, a gating modifier that has been shown to inhibit ATP-dependent gating of WT-CFTR (Ma et al., 2002 ; Caci et al., 2008). Third, normal gating of WT-CFTR channels involves interactions of ATP with the signature sequence of NBD1, as exemplified by the G551D mutation that completely eliminates the ATP-dependent gating (Bompadre et al. 2007). Fig. III.6 demonstrates that the Cd^{2+} -dependent gating also involves the signature sequence because engineering cysteine residues framing the signature sequence (i.e., T547C and R553C) did not confer this effect of Cd^{2+}. It should be noted that crystal structures of NBD dimers (e.g., Fig. III.1) reveal that γ -phosphate, a critical component for ATP being a successful ligand for CFTR gating, forms hydrogen bonds with the side chain of serine (S549 in CFTR) and the main chain of nitrogen of glycine (G551 in CFTR). These two positions coincide with the region involved in Cd^{2+} -dependent gating (Fig. III.6 D). Although we cannot definitively rule out the possibility that Cd^{2+} -dependent gating of CFTR mutants bears no relationship to normal gating of WT channels by ATP, collectively, our data support the idea that a defined region of the signature sequence transduces the signal of ligand (ATP or Cd^{2+}) binding to the gate of CFTR.

III.3.3 Chemical Mechanism for the Action of Cd^{2+}

Several lines of evidence suggest that the effect of Cd^{2+} reported here is mediated though a metal bridge formation between at least two coordinating residues. First, the apparent affinities for G551C and S549C are at low micromolar range, supporting the idea that multiple cysteines are involved in coordinating Cd^{2+}. Second, a thiol-specific reagent, MTSEA, can abolish the effect of Cd^{2+} on G551D. Third, based on the Monod-Wyman- Changeux model (Scheme 2) for allosteric modulation of protein function by ligand binding (Monod et al., 1965), we can conclude that when Cd^{2+} binding yields a ~30-fold increase of the gating constant (i.e., $K'/K = 30$ where $K' = k'_o/k'_c$ and $K = k_o/k_c$) as in the case of G551D, thermodynamics dictates that the binding affinity for the open state has to be 30-fold higher than that for the closed state (i.e., $Kd/Kd' = 30$ where $Kd = k_{off}/k_{on}$ and $Kd' = k'_{off}/k'_{on}$). One can imagine that in the closed state, the coordinating residues (aspartate or cysteine) are too far apart to form an ideal coordinate for Cd^{2+} binding. However, if the side chains of these residues move closer to each other after the conformational changes during channel opening, the open state could assume a higher affinity for Cd^{2+} simply because of a better coordination.

Our data have pointed to an involvement of partner cysteine(s) in mediating the effect of Cd^{2+}, and there are 18 cysteines in human CFTR (14 cysteines in the cytoplasmic domains). We identified the partner cysteine by systematically removing cysteines in different parts of CFTR in next chapter.

III.3.4 Pathophysiological Implications

The disease-associated mutant G551D has a ~ 100-fold smaller Po than WT channels. Many compounds (Amaral and Kunzelmann, 2007) and ATP analogues (Cai et

al., 2006 ; Bompadre et al., 2007) have been found to potentiate the activity of G551D-CFTR channels, but none of them could increase the activity of G551D-CFTR to WT levels. The binding site for only a very limited number of these CFTR "potentiators" has been identified (Bompadre et al., 2008). Interestingly, the 20- fold increase of the G551D-CFTR current by Cd^{2+} is by far the most effective potentiation demonstrated for this disease-associated mutant. Unfortunately, because of its toxicity, Cd^{2+} cannot be used therapeutically. Although Zn^{2+} may be an interesting alternative, its low potency and efficacy also prohibit a possible therapeutic application. Nevertheless, our findings open the door for rational drug design that can greatly benefit Cystic Fibrosis patients carrying the G551D mutation. These studies suggest that the signature sequence of NBD1 can be a drug target for rescuing the dysfunctional G551D channels. The more interesting data is 10 μM Cd^{2+} combined with ATP generate enough current increase to rescue the G551D current to WT level. It is worth noting that the significance of our results in future drug design should hold even if this Cd^{2+} -dependent gating for G551D-CFTR and normal ATP-dependent gating of WT channels turn out to use different gating machinery.

III.4 Summary

In this chapter, we demonstrated that micromolar [Cd^{2+}] can dramatically increase the activity of G551D-CFTR in the absence of ATP. Since Cd^{2+} fails to increase the current of G551D/cysless and thiol reactive reagent (MTSEA) protects the G551D from Cd^{2+} effect, the Cd^{2+} acts on the G551D and G551C –CFTR by serving as a metal bridge connecting G551D/C to an unknown cysteine residue in CFTR. Furthermore, the effect is not limited to position 551 only. When L548, S549 are mutated to cysteine, Cd^{2+} can also

exerts its effect. We thus proposed that the signature sequence serves as a switch to transduce the signal of ligand binding to the gate opening.

After the cysteine that coordinates with Cd^{2+} is identified, we might get a better understanding of this switch function. Based on our preliminary data that Cd^{2+} still increases the current of the CFTR mutant of S549C that all six cysteines in NBD2 are removed, we suspected that the cysteine is not located in NBD2, which did not support our hypothesis that the Cd^{2+} increases mutant CFTR current by enhancing the NBD dimerization. Moreover, the results raise the possibility that NBDs dimerization might not be an absolutely requirement of CFTR gating. We identified the cysteine in the next chapter and more detailed mechanistic information will be provided.

Chapter IV: The signature sequence carries a switch function for CFTR channel gating

The goal of this chapter is to identify the cysteine(s) that mediates the switch function of the signature sequence. The identified cysteines are located in the R domain and NBD2, both of these cysteines' effect can not be explained by NBDs' dimerization. Further studies will look into the mechanism of how the R domain interacts with NBD1 and the functional role of the signature sequence at NBD2.

Our studies described in Chapter III show that metal ions like Cd^{2+} and Zn^{2+} can increase the activity of G551D-CFTR and this effect is most likely due to metal bridge formation between 551D and an endogenous cysteine in CFTR. To identify the cysteine(s) which interact with Cd^{2+} and the signature sequence on NBD1, we first systematically removed cysteine residues in different parts of CFTR under the G551D background. We then reengineered individual cysteine back to the cysless G551D construct, in which all cysteine are replaced under G551D background. Our results finally point to two cysteines, one is 832C in the R domain, and the other one is 1344C in NBD2. Interestingly, the effect of Cd^{2+} on G551D/Cysless/832C or on G551D/Cysless/1344C can not be explained by NBDs dimerization. Because 832C is located on a flexible area of the R domain, it may interact with NBD1 through the signature sequence to lead the channel opening. We will further study the amino acids around this position and try to identify the interaction range. From the homology structure, 1344C is located too far away from 551D to coordinate with Cd^{2+}, and how it is involved remains unclear. G551D-Cysless-CFTR shows no effect with Cd^{2+}, but

returning 832C alone on this construct rescue one third of the Cd^{2+} effect compared to G551D-CFTR. This result suggests that interactions of the signature sequence on NBD1 with 832C and Cd^{2+} can lead to channel opening . In other words, we presume that the signature sequence carries the switch function for CFTR channel opening, and the R domain, especially around 832, mediates the signal transmission of ligand binding to channel opening. Our findings not only provide structural information for CFTR channel gating, but also open a new area of research that focuses on the interaction between the R domain and NBDs.

IV.1 Introduction

The gating and structure function relationship of the CFTR had been extensively studied; however, the gating mechanism is still unknown. In order to better understand the relationship between the dimerization of NBDs and the gating of CFTR at the molecular level, it is essential to know how the CFTR domains are coupled together and how the signal of dimerization is transmitted to the gate. Understanding how these ABC transporters work at the molecular level is one of the issues actively pursued in many research fields.

A single replacement of glycine to aspartate makes G551D-CFTR irresponsive to its natural ligand, ATP. We proposed (Bompadre et al., 2007) that the G to D mutation blocks the conformation change after ATP binding. More recently, we (Wang et al., 2009) demonstrated that micromolar [Cd^{2+}] can dramatically increase the activity of G551D-CFTR in the absence of ATP. The effect of Cd^{2+} is mediated by a metal bridge formation between 551D and a cysteine, the result has been shown in last chapter. We proposed that

the signature sequence might serve as a switch to transmit the ligand biding signal to channel opening. Our preliminary studies also suggested that the cysteine is not likely located at the other side of the ATP binding pocket (ABP2). This raises the possibility that the NBDs dimerization might not be a requirement for channel opening. The cysteine might be located in the R domain, NBD1 or MSDs. Identification of this cysteine will likely provide new insights into our understanding of CFTR gating, especially into better understanding of the switch function of the signature sequence.

In this study, we continue our work of identifying the cysteine. We mutated all the cysteines in CFTR to serine or leucine in G551D background (hereafter referred as cysless G551D). We then reengineered cysteine one by one back to this cysless G551D construct to test the Cd^{2+} effect. We found that by bringing 832C or 1344C back to the cysless G551D-CFTR, positive Cd^{2+} response can be observed. The effect of Cd^{2+} can not be explained by the formation of a NBD dimer mediated by Cd^{2+}. 832C is located in the R domain, and 1344C is located in NBD2 but too far away from 551D to coordinate with Cd^{2+}. We proposed that 832C in the R domain mediates this signal transmission by interacting with the signature sequence of NBD1, which serves as switch function to transmit ligand binding to channel opening. In addition, the enhancement of G551D currents in the presence of divalent cations led us to study the mechanism of coupling process from NBDs dimerization to opening of the channel gate. The answer to our proposed experiments will shed light on these issues.

In this chapter, we present our results by first describing our strategy to identify the cysteine. Our efforts of searching for the cysteine and the resulting constructs shows positive Cd^{2+} response are followed. In the section of discussion and future direction, we

proposed several lines of experiments designed to help us further look into the gating mechanism of CFTR.

IV.2 Results

IV.2.1 Strategy for identifying the cysteine(s)

There are 18 cysteines in CFTR. To find the cysteine(s) that coordinates with Cd^{2+}, we divide them into four groups. By removing groups of cysteines, the searching procedure is fastened. These four groups are denoted as F1, F2, F3 and F4. F1 segment includes 5 cysteines in MSD1. F2 segment includes 5 cysteines in NBD1, we kept 590C and 592C untouched for good protein expression level in F2 cysless constructs. F3 segment includes 2 cysteines in the R domain and MSD2. F4 segment includes 6 cysteines in NBD2 and C-terminal of CFTR. (Figure IV.1)

A

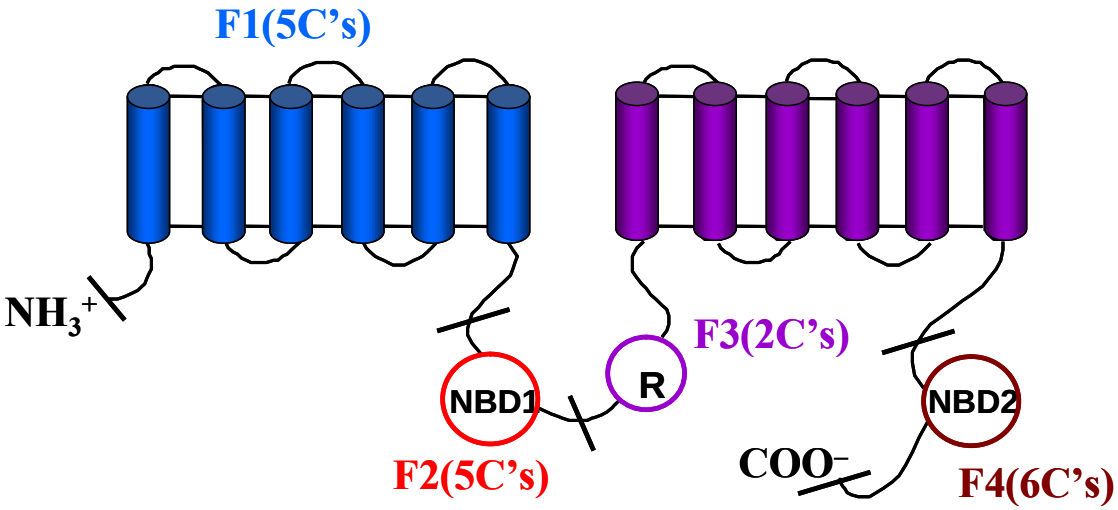

B

F1	76S, 128S, 225S, 276S, 343S
F2	491S, 524S, 590C, 592C, 647S
F3	832S, 866S
F4	1344S, 1355S, 1395S, 1400S, 1410S, 1458S

Chapter IV Figure IV.1: Simplified topological model emphasizing the five domains of a CFTR chloride channel. The 18 cysteines in CFTR are grouped into 4 segments. (A) the topological model of CFTR. Blue colored MSD1 represents F1 segment, red colored NBD1 represents F2 segment, purple colored R domain and MSD2 represents F3 segment and brown colored NBD2 represents F4 segment. (B) The table of cysteines in each segment. F1 segment includes C76, C128, C225, C276, and C343, F1 cysless construct means mutating all these 5 cysteines to serines. F2 segment includes C491, C524, C590, C592, and C647, F2 cysless means mutating C491, C524 and C647 to serine but keep C590 and C592 as cysteines because these two cysteines are essential to maintain the channel expression level. F3 segment includes C832 and C866, F3 cysless means mutating these two cysteines to serines. F4 segment includes C1344, C1355, C1395, C1400, C1410 and C1458, F4 cysless means mutating all of these 6 cysteines to serines.

IV.2.2 Cd^{2+} fails to induce current increase on G551D/Cysless mutant

Our studies show that Cd^{2+} increases G551D current, and this Cd^{2+}-dependent current can be inhibited by a CFTR specific blocker, Inh-172. We further tested the Cd^{2+} effect on a G551D construct where all the cysteines were mutated to serine or leucine with an additional mutation, valine 510 to alanine (V510A, which will maintain enough channel expression level for experiment, Wang et al., 2007), Cd^{2+} both 10 μM and 100 μM failed to induce any current increase on this construct. The trace is shown in Figure IV 2. The data again support our idea that an endogenous cysteine is involved in coordinating with Cd^{2+} to increase the G551D current.

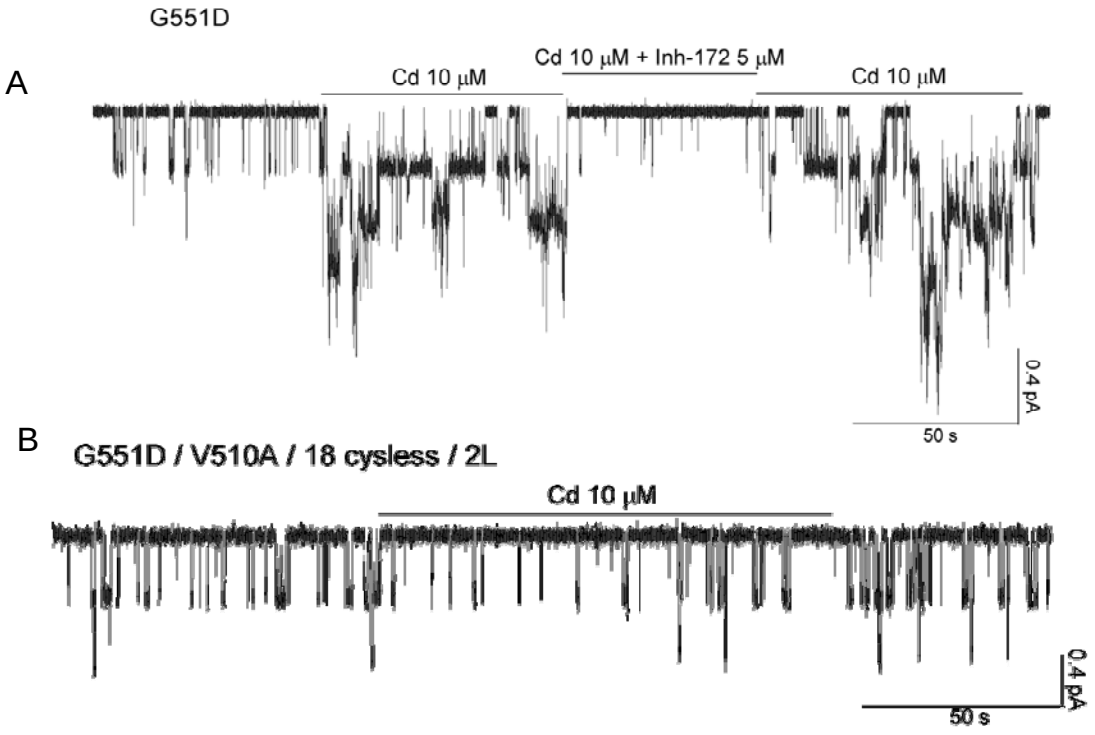

Chapter IV Figure IV.2: Cd^{2+} effect on G551D-CFTR and G551D-cysless-CFTR. (A). Cd^{2+} 10μM induce 10.18 (±1.89) (n=10) fold current increase compare with basal current. The current induced by Cd^{2+} 10μM can be inhibited by 5μM CFTR specific blocker inh-172. (B). Meanwhile, Cd^{2+} 10μM fails to affect G551D/V510A/18 cysless/2L-CFTR (n=6).

IV.2.3 The cysteine is located in the R domain, MSD2 and NBD2

We first divided all the cysteines into two parts, by introducing two mutants, G551D/F1+F2 Cysless and G551D/F3+F4 Cysless, in which the cysteines in F1+F2 and F3+F4 are removed, respectively. We first investigated the effect of Cd^{2+} on G551D/F1+F2 cysless (cysteines in both F1 and F2 segments are mutated to serines) and G551D/F3+F4 cysless (Figure IV.3). Cd^{2+} can increase current on G551D/F1+F2 cysless but shows negligible effect on G551D/F3+F4 cysless. Furthermore, we tested the effect of different [Cd^{2+}]. The Cd^{2+} dose response curve of G551D/ F1+F2 cysless is very similar to that of G551D itself (Figure IV.7). With these results, we first excluded the cysteines in the F1 and F2 segments, 10 cysteines in NBD1 and MSD1. We thus focused our search in the F3 and F4 segments, i.e., in the R domain, MSD2 and NBD2.

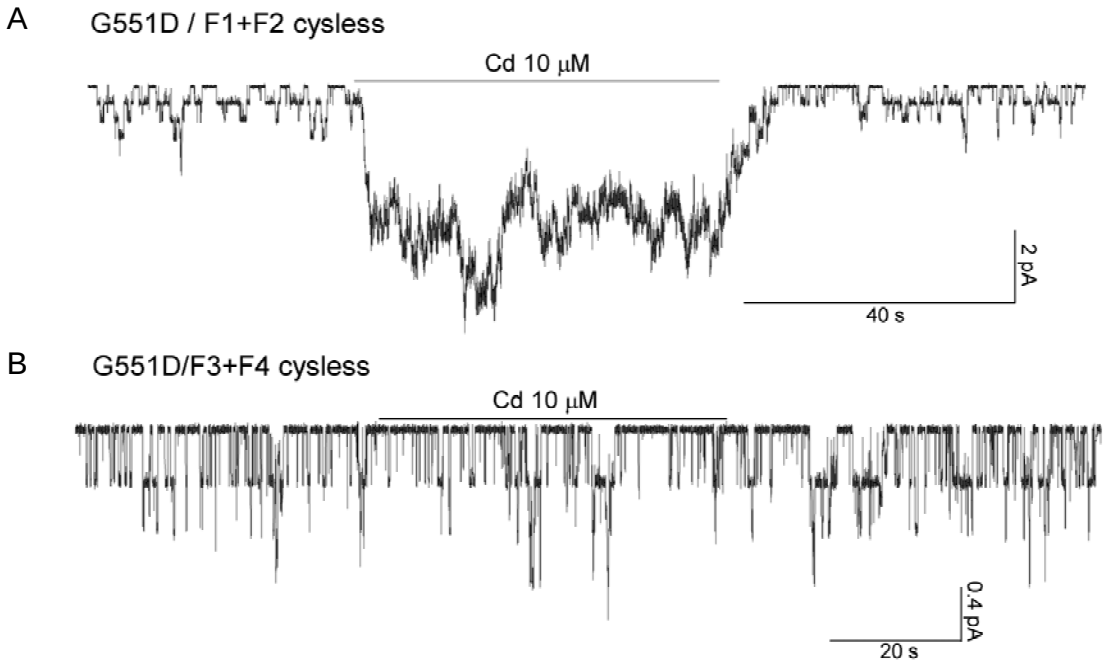

Chapter IV Figure IV.3: Looking for the cysteines which interact with Cd^{2+} in different areas of CFTR by dividing 18 cysteines in CFTR into two groups. (A). Cd^{2+} (10μM) induces a 7.8 ± 0.8 fold increase in the current and Cd^{2+} (200μM) induces a 21.45 ± 3.2 fold increase in the current compared with the basal activity on G551D/F1+F2 cysless-CFTR (cysteines in transmembrane domain 1 and nucleotide binding domain 1 have been mutated to serines, n = 6). (B). Cd^{2+} shows no effect on G551D/F3+F4 cysless-CFTR (cysteines in transmembrane domain 2, nucleotide binding domain 2 and regular domain have been replaced by serine) at both 10μM and 200μM (n = 6).

IV.2.4 Cysteines in both F3 and F4 segments are involved.

We then investigated the effect of 10 μM Cd^{2+} on G551D/F3 cysless and G551D/F4 cysless. Traces are shown in Figure IV.4. Cd^{2+} can increase current in both of these two mutants. By analyzing the Cd^{2+} dose response (Figure IV.7, Cd^{2+} $K_{1/2}$ for G551D/F4 cysless is about 10μM) and the magnitude of current fold increase (Table 1 and Figure IV.8, compared with basal activity, Cd^{2+} 100 μM induces 2.11 ± 0.45 fold increase in current on G551D/F3 cysless and 9.95 ± 0.81 fold increase in current on G551D/F4 cysless), we concluded that both of them may be involved in Cd^{2+} interaction, and that the cysteines in F3 play a major role to assist the Cd^{2+} effect.

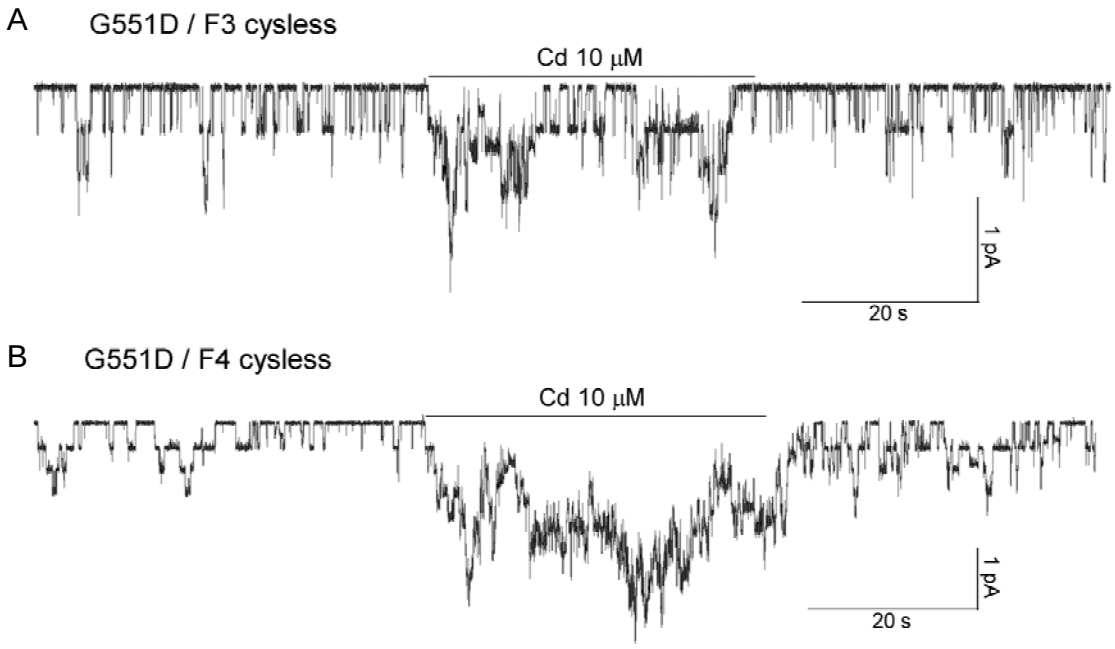

Chapter IV Figure IV.4: Comparison of Cd^{2+} 10 μM induced currents between G551D/F3 cysless (mutating cysteines in regular domain and transmembrane domain 2 to serine) and G551D/F4 cysless (mutating cysteines in nucleotide binding domain 2 to serine) CFTR. (A). Cd^{2+} 10 μM induces 1.03 ± 0.11 fold increase in the current (n = 8) compared with the basal activity. (B). Cd^{2+} (10 μM) induces 4.2 ± 0.58 (n = 4) fold current compare with basal activity.

IV.2.5 C832, not C866 in F3 segment when introduced to G551D/Cysless mutant, showed Cd^{2+} response.

Since there are two cysteines in the F3 segment and 6 cysteines in F4 segment, we thus chose an alternative way to search for the cysteines. Under the background of G551D/V510A/18 cysless, we reintroduced these 8 cysteines back one by one. In these constructs, only one cysteine is present.

In the F3 segment, there are only two cysteines, 832C and 866C. The traces of Cd^{2+} effect on G551D/V510A/18 cysless/832C and 866C are plotted in Figure IV.5. Only one of them showed positive Cd^{2+} effect. As seen in Figure IV.5, upper panel, when 832C was introduced back to the G551D/18 cysless background, Cd^{2+} can increase the current.

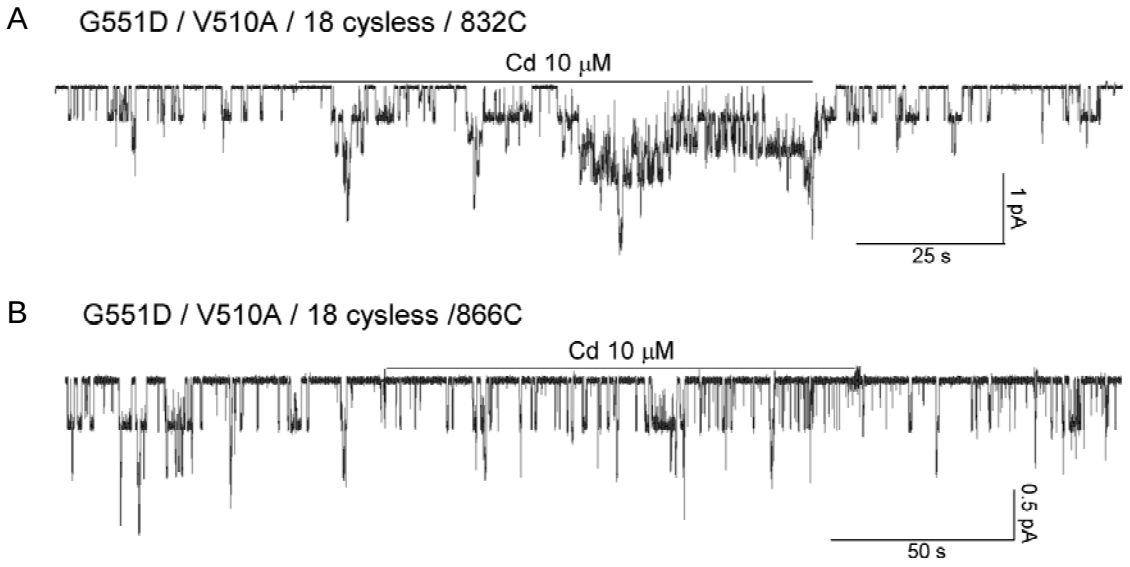

Chapter IV Figure IV.5:Representative trace about Cd^{2+} effect on R domain cysteines. (A).Cd^{2+} 10 μM induces 3.06 ± 0.287 fold (n = 27) increase in the current when there is only one cysteine-832C on the R domain remain on G551D/18 cysless background. (B). Another cysteine on the R domain, 866C, did not show positive Cd^{2+} effect (n = 5).

IV.2.6 Bringing back 1344C in F4 segment gave positive Cd^{2+} response.

Similarly, we tested 6 mutants, in which only one cysteine in F4 segment is brought back to the G551D/Cysless background. Among these 6 cysteines, only bringing back 1344C shows the ability to induce current when Cd^{2+} is applied. For constructs bringing back all other individual cysteines in F4 segment, Cd^{2+} fails to induce a current increase. Representative traces of positive and negative Cd^{2+} responses are plotted in Figure IV.6, in which Cd^{2+} increases the current on G551D/V510A/18 cysless/1344C, but fails to do so on G551D/V510A/18 cysless/1400C.

By systematically examining all 18 cysteines in CFTR, we identified two cysteines that gave positive Cd^{2+} responses when reintroduced into the G551D/Cysless background. They are 832C in the R domain and 1344C in NBD2. The dose responses of Cd^{2+} on G551D, G551D/F1+F2 cysless, G551D/F4 cysless, G551D/V510A/18cysless/832C and G551D/V510A/18 cysless/1344C are shown in Figure IV.7. Table IV.1 and Figure IV.8 summarize the magnitude of current fold increase by Cd^{2+} 10 μM and 100 μM on different mutants we have tested.

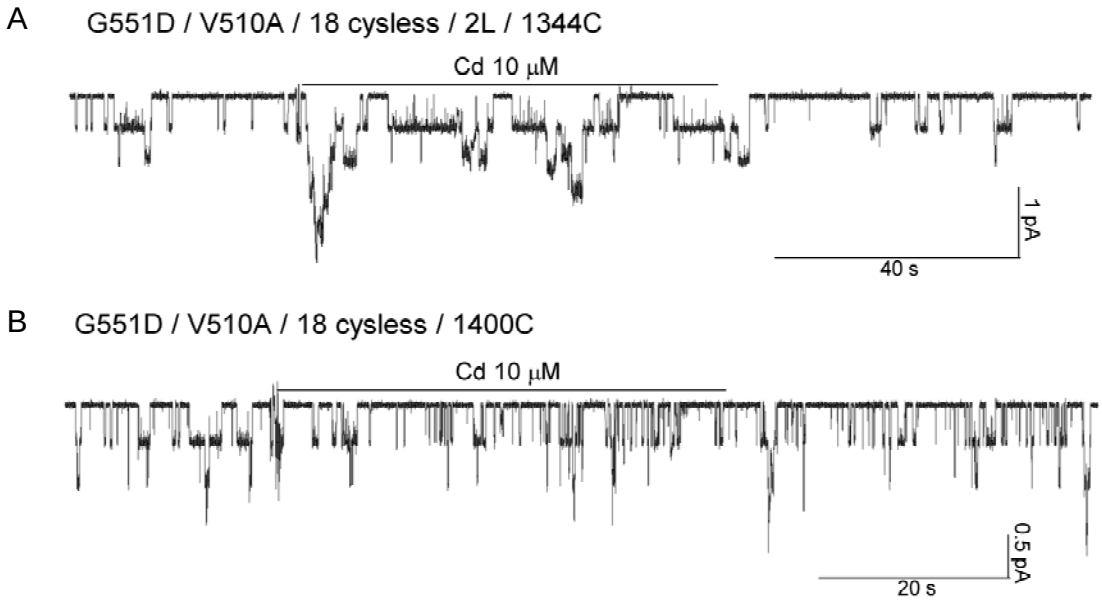

Chpater IV Figure IV.6: Representative trace about Cd^{2+} effect with the cysteines on NBD2. (A). With 551D and only one cysteine, 1344C-CFTR, Cd^{2+} 10 μM induces 3.934 ± 0.69 (n = 17) fold current compare with basal activity. (B) Cd^{2+} 10 μM induces 0.809 ± 0.189 (n = 7) current on G551D/V510A/18 cysless/1400C.

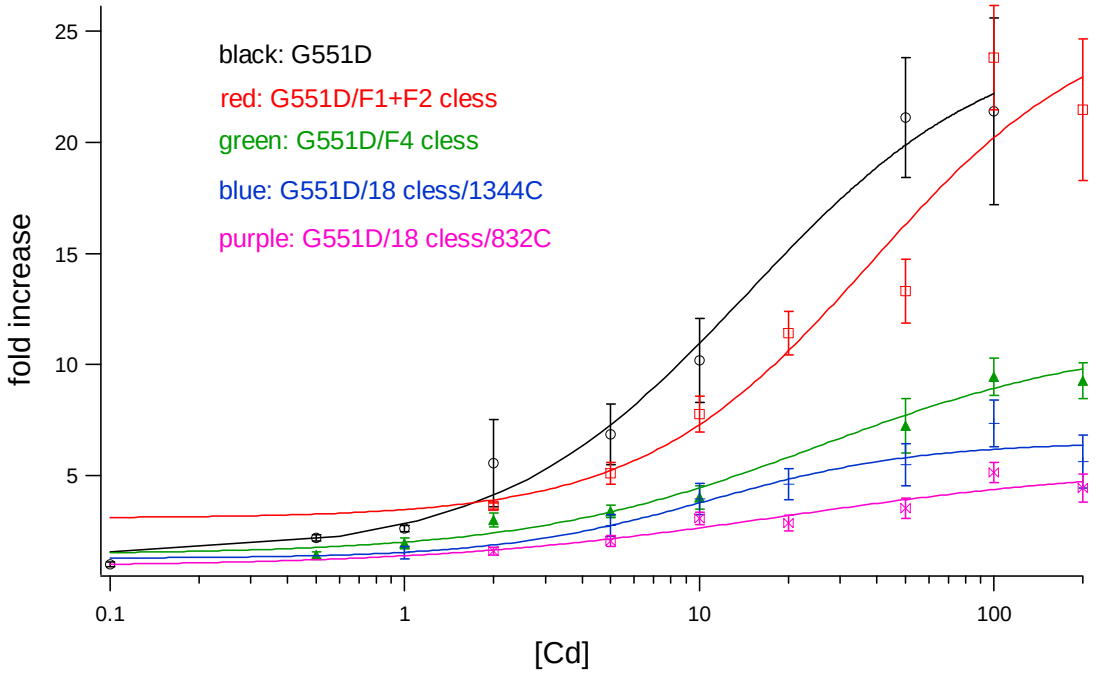

Chapter IV Figure IV.7: Fold increase of current induced by Cd^{2+} at different concentrations.

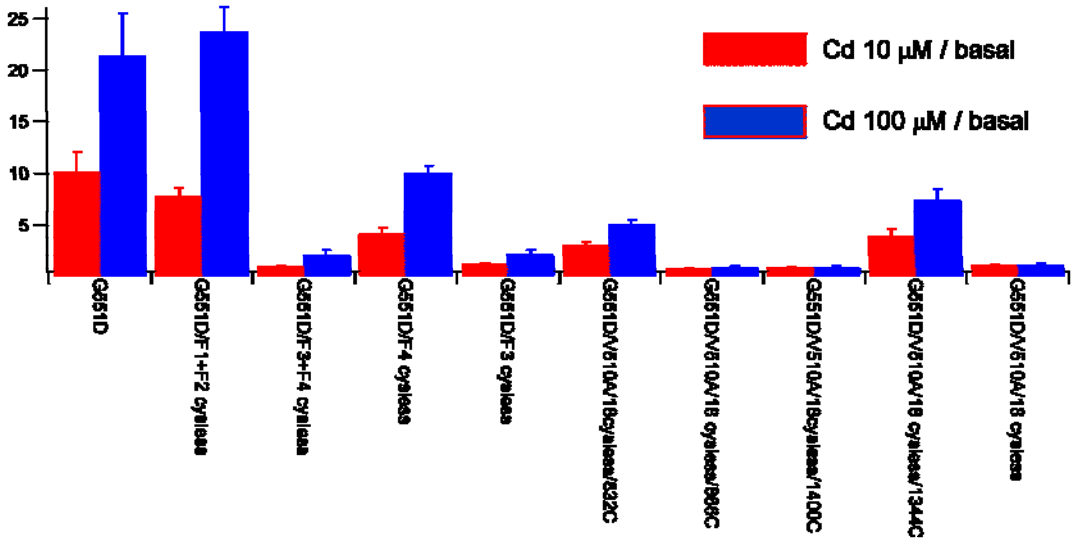

Chapter IV Figure IV.8: Summary of fold increase of current by 10 and 100 µM of Cd^{2+} on mutants tested.

Table IV.1: Summary of fold of current increase by 10 and 100 μM of Cd^{2+} on mutants we tested.

CFTR mutants	Fold of increase by Cd^{2+} 10 μM	Standard error for 10μM	Fold of increase by Cd^{2+} 100 μM	Standard error for 100μM
G551D	10.18	1.89	21.38	4.19
G551C	58.88	2.24		
G551D/F1+F2 cysless	7.77	0.82	23.81	2.35
G551D/F3+F4 cysless	1.03	0.07	2.06	0.50
G551D/F3 cysless	1.19	0.12	2.11	0.45
G551D/F4 cysless	4.20	0.58	9.95	0.82
G551D/F4 cysless/C832S	1.22	0.09	1.24	0.11
G551D/F4 cysless/C866S	3.58	0.44	6.46	0.93
G551D/F3 cysless/C1400S	4.48	0.52	5.87	0.34
G551D/V510A/18cysless/832C	3.06	0.29	5.12	0.44
G551D/V510A/18 cysless/866C	0.69	0.06	0.87	0.10
G551D/V510A/18cysless/1400C	0.81	0.08	0.82	0.19
G551D/V510A/18cysless/1344C	3.93	0.69	7.34	1.05
G551D/V510A/18 cysless	1.08	0.14	1.09	0.26
G551D/C832S	2.37	0.21	4.31	0.81
G551C/C832S	6.73	2.03		
G551D/V510A/18cysless/832C	3.06	0.29	5.12	0.44
G551D/V510A/18cysless/866C	0.69	0.06	0.87	0.10
G551D/V510A/18cysless/1344C	3.93	0.69	7.34	1.05
G551D/V510A/18cysless/1355C	1.55	0.47	1.52	0.42
G551D/V510A/18cysless/1395C	0.99	0.10	1.23	0.11
G551D/V510A/18cysless/1400C	0.81	0.08	0.82	0.19
G551D/V510A/18cysless/1410C	1.17	0.41	1.09	0.08
G551D/V510A/18cysless/1458C	1.47	1.41	1.11	0.48
G551C/V510A/18cysless	2.42	0.95	2.12	0.68
G551C/V510A/18cysless/832C	5.61	2.29		
WT/V510A/18cysless	0.91	0.13		
WT/V510A/18cysless/832C	2.11	0.63	4.32	0.68
WT/V510A/18cysless/1344C	3.50	1.08	3.13	1.76

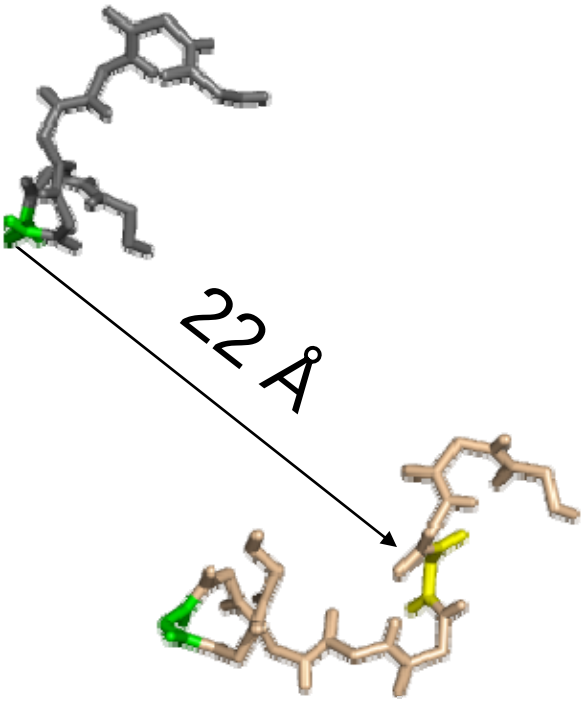

Chapter IV Figure IV.9: Modeled CFTR NBD dimer structure showing residue at position 1344 is far away from 551.

IV.3 Discussion

IV.3.1 Mechanism for the involvement of C1344 is not clear

The results that Cd^{2+} can enhance the current on G551D/Cysless/1344C are unexpected. Although located in NBD2, 1344C is in a different ATP binding pocket from 551. In the so-called head-to-tail arrangement of NBD dimers, the ATP binding pocket consists of residues from the Walker A and B motifs of one NBD and the signature sequence of the other NBD. 551 is located in the signature sequence of NBD1, thus in ABP2, while 1344 is located near the signature sequence of NBD2, just 5 residues upstream of 1349, the equivalent position of 551 in NBD2, in ABP1. Thus, the side chains of 551 and 1344 are physically very far from each other in an NBD dimer. Based on the structure model of the CFTR dimer, the distance between them is estimated to be 22 Å (figure IV.9). In the crystal structures of proteins that contain Cd^{2+}, the distance between the residues that coordinate Cd^{2+} is less than 10 Å (Rulisek and Vondrasek, 1998). Thus, the current increase by Cd^{2+} on G551D/Cysless/1344C can not be explained by the formation of a metal bridge between 1344C and 551D, due to the physical constrain. We suspect that there is another Cd^{2+} working site around 1344, forming by similar metal bridge between 1344C and other negatively charged residues. We will look into this issue in the future. The modeled dimer structure will be used as a guide to search for the negatively charged residues. We will adopt a similar strategy to identify residues that are involved, by removing the candidate residue to test if the Cd^{2+} effect is gone.

Chapter V: Future directions and thesis summary

We have identified the Cysteines that mediate Cd effect on G551D and the identified cysteines are located in the R domain and NBD2. Both of these cysteines' effect can not be explained by NBDs' dimerization. Further studies will look into the mechanism of how the R domain interacts with NBD1 and the functional role of the signature sequence at NBD2.

V.1 Studying Cd effects on the mutant channels by switching from G551D to G551C.

When designing our future experiments, we will change from G551D to G551C. Cysteines provide better Cd^{2+} coordination than aspartates, an idea supported by our previous data that Cd^{2+} has a higher binding affinity on G551C than on G551D (Wang et al., 2009). The advantage of changing to G551C is a bigger response to Cd^{2+}, which allows us to study the kinetics of Cd^{2+} action.

V.2 Experiments to provide evidence that 551C and 832C are interacting with each other directly.

We need to show that 551C and 832C interact with each other directly when Cd^{2+} enhances the channel activity. Several experiments are underway.

1. Compare the Cd^{2+} effect on WT/18 cysless/551C, WT/18 cysless/832C, and WT/18 cysless/551C/832C. In these constructs, all cysteines in CFTR are removed by mutating them to serine or leucine. Cysteines either at 551 or 832 or both are engineered

back, respectively. The fold of current increase induced by Cd^{2+} is expected to be small when only a single cysteine is present, but large when both cysteines are present. Indeed, our preliminary data show exactly as we predicted. In figure V.1A, representative traces of Cd^{2+} effect are plotted. Also shown is the bar representation of fold increase of current induced by Cd^{2+} on these mutants (Figure V.1B).

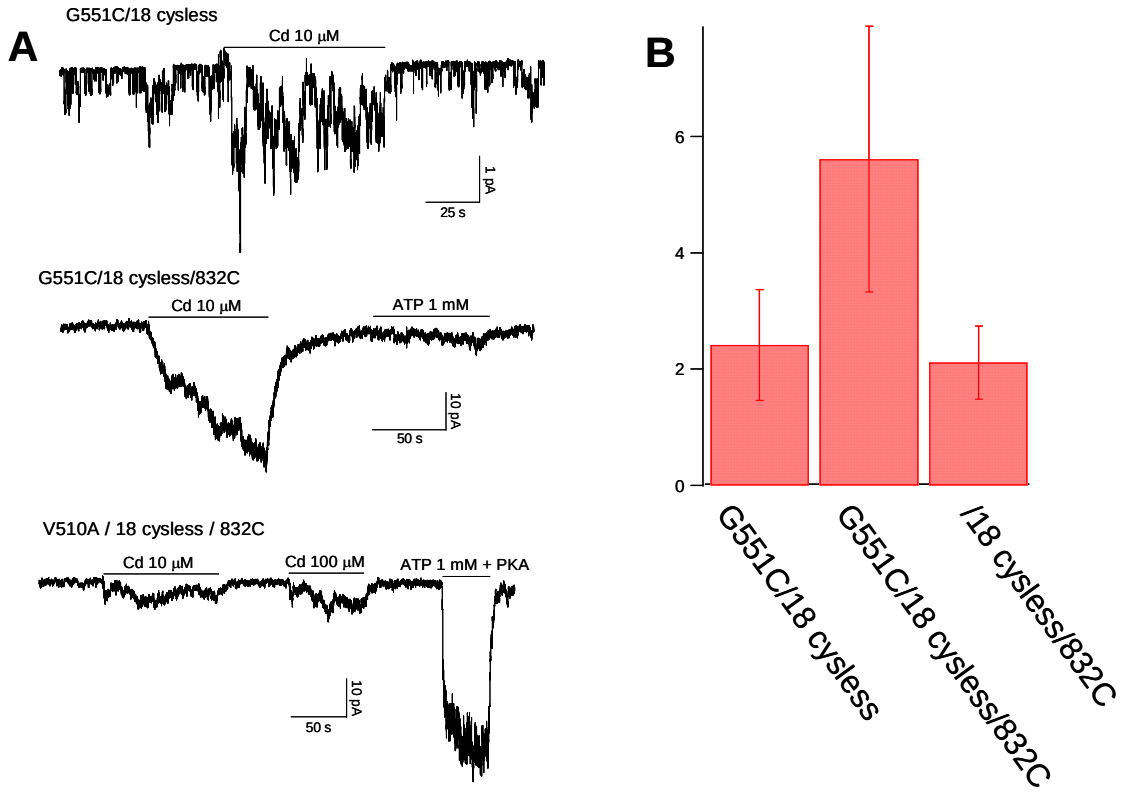

Chapter V. Figure V.1: Cd^{2+} effect on constructs with engineered cysteines at desired positions. (A) Representative recordings. Top: G551C/18 cysless: single cysteine is brought back at 551. Middle: G551C/18 cysless/832C: both cysteines at 551 and 832 are brought back. Bottom: single cysteine is brought back at 832. (B) Fold increase of current by Cd^{2+} 10 µM on the constructs that cysteine was engineered back to the mutant with all cysteines removed. 2.11 ± 0.63 (n = 6) when single cysteine is brought back at 551 (G551C/18 cysless), 2.40 ± 0.95 (n = 4) when single cysteine is brought back at 832 (18 cysless/832C), 5.61±2.29 (n = 6) when both cysteines are brought back at 551 and 832 (G551C/18 cysless/832C).

2. Change the ligand from Cadmium to Nickel. We want to demonstrate that this coordination site physically exists. Cd^{2+} coordinates with both cysteines and histidines, it also interacts with negatively charged residues such as aspartate and glutamate. Ni^{2+}, on the other hand, specifically coordinates with histidines. We thus propose to change the Cd^{2+} binding site to a Ni^{2+} binding site. Correspondently, we will engineer a histidine at 551 or 832 or both. If our hypothesis that the distance between the position 551 and 832 is physically close enough, we predict that Ni^{2+} will enhance the current slightly when a single histidine is introduced, but greatly when both histidines are introduced. However, we are aware that we might get negative results. The possible reasons are first the binding site might not be in perfect distance and orientation for Ni^{2+}, since the coordination of Ni^{2+} with histidines might be different from Cd^{2+} with cysteines. Besides, two histidine residues might not provide a strong Ni^{2+} binding site. If in this case, we might introduce more histidine residues at this site. For example, we will introduce one more histidine residue around 551H and 832H, the resulting mutants will have four histidine residues at this site. We will first start with G551H/S549H/C832H/F834H.

3. Test the effect of a crosslinker on WT/18 cysless/551C/832C. We will apply a crosslinker that has thiol reactive groups at both ends of molecule. The two ending groups are connected by different lengths. MTS reagents are highly specific thiol modification chemicals. There are commercially available reagents that connect two MTS group by various lengths. They are denoted as MTS-n-MTS, with n represents the number of methyl group that connecting two MTS groups. If the crosslinker with the correct length is applied, we expected that the WT/18 cysless/551C/832C can be locked into an open state. The open channel can only be closed by DTT, the reducing agent that

breaks the disulfide bond formed by the crosslinker. We will start with MTS-4-MTS, since the length is around 10 Å. This kind of experiments can also define the physical distance constrain by using crosslinkers with different length.

V.3 Define the physical range of 551C and 832C by mutants around these two residues.

After the direct interaction between 551 and 832 is established, we will next show that the interaction is not limited to these two positions only. If our idea that the signature sequence serves as a switch and the R domain may mediate the signal transduction is correct, the contact between the signature sequence and the R domain around the 832 region should not be limited to 551 and 832 only. We will first fix position 551. Under the cysless background with 551 mutated to cysteine, we will engineer one cysteine each around the 832 position. Since the structure of the R domain is not known, we have to start a blind search by scanning all the residues around this region. We will begin with a 10 residue window, with residues 827 to 837 mutated to cysteine one at a time. Similarly, we will fix C832 and scan the residues 546 to 555 by mutating them to cysteine one by one. If a pattern of residue pair emerges, we may design more residue pairs to test if they give positive Cd^{2+} response. This series of experiments will provide insights into the physical constrain of these two interacting regions.

V.4 Functional evidence for an interaction between the R domain and NBD1

Our previous data (Wang et al., 2009) provide the strongest evidence that the signature sequence of NBD1 serves as a switch to transmit the ligand binding to channel

opening. We also suggested that dimerization might not be required for channel opening. In this work, we showed that most likely 832C is the cysteine that coordinates with Cd^{2+}, together with 551C to explain the positive Cd^{2+} response. Since C832 is located in the R domain, our data provide the first piece of evidence for the involvement of R domain in the CFTR channel gating, after it was phosphorylated. We proposed that the R domain can mediate the signal transduction by switching on the signature sequence.

The interaction between the R domain and NBDs demonstrated in our work will significantly impact the field. Previously, the functional role of the R domain is vague. For example, Winter & Welsh (1997) showed that phosphorylation of the R domain by PKA accelerates the rate of channel opening and Li et al. (1996) demonstrated that PKA-dependent phosphorylation is a prerequisite for the ATPase activity of purified wild-type human CFTR. Only recently, Baker et al. (2007) used NMR spectroscopy to investigate interactions between the R domain and NBD1. They found interaction between the R domain and NBD1, and phosphorylation of the R domain promoting the dissociation of the R domain from NBD1. However, where and how does the R domain interact with NBD are not clear. Our data provide the first piece of evidence that the R domain interacts with NBD1 and can play a role in channel gating. The interaction is via position around 551 in NBD1 and 832 in the R domain. The signature sequence serves as a switch to transmit ligand binding to channel opening, while the R domain can mediate the signal transduction.

V.5 Thesis summary

In this thesis, we studied the gating mechanism of the CFTR. The role of NBD dimerization in channel gating is intensively investigated. We first dissected the roles of ATP binding at each site. Because dimerization induces conformational changes and provides two ATP binding sites, two critical aromatic amino acids (W401 in NBD1 and Y1219 in NBD2) were identified as interacting with the adenine ring of the bound ATP. By modifying these two aromatic residues in the two binding pockets, we studied the roles of these two binding sites, without disturbing the ATP hydrolysis. Mutations of these two equivalent residues result in two channels with totally different gating behavior. W401G has little effect on the sensitivity of the opening rate to [ATP], but Y1219G dramatically lowers the apparent affinity for ATP by more than 50-fold. However, W401G shortens the open time constant and this shorting can be compensated by a higher binding affinity ATP analog, P-ATP, while Y1219G has little impact on the channel open time. These results demonstrated that opening of the channel is initiated by ATP binding at the NBD2 site, and tighter binding at W401 at the NBD1 site prolongs channel open time.

In each ATP binding pocket, residues from both NBDs are involved. On one side, residues from Walker A and B motifs were studied extensively. In contrast, the aromatic residues interacting with ATP's adenine ring are first studied in this thesis. On the other side of the binding site, residues are from the signature sequence. However their roles are less clear. We then studied the mutants of the signature sequence on NBD1 with cations. We found that micromolar [Cd^{2+}] can dramatically increase the activity of G551D-CFTR, whose activity is insensitive to ATP, but this current increase is not due to enhanced dimerization of two NBDs. By mutating individual residues from the signature sequence

to cysteine, a specific region of the signature sequence is found to result in positive response to Cd^{2+}. We thus conclude that the signature sequence on NBD1 serves as a switch that transmits the signal of ligand binding to the gate opening. The Cd^{2+} effect is found to work through forming a metal bridge connecting G551D/C to another cysteine residue in CFTR.

We identified two cysteines to be responsible for the Cd^{2+} effect. One of the cysteine is 832C in the R domain, and the other one cysteine is 1344C in NBD2. These data suggest that NBD dimerization per se is not responsible for channel opening, challenging the prevailing concept that NBD dimerization is coupled to channel gating. It is proposed that residues in the R domain, specifically around the 832 region, may mediate the signal transmission of ligand binding to channel opening.

Our data thus provide the first piece of evidence that the R domain can replace NBD2 in the CFTR channel opening after the channel is phosphorylated. The studies on the mechanism of the interactions between the signature sequence and the R domain are ongoing. Our findings of the roles of two ATP binding pockets and of the signature sequence on NBD1 also offer very interesting targets for future drug design.

Appendix

Materials and Methods

Site-directed mutagenesis and cell culture

Mutations were introduced into WT-CFTR, as previously described (Bompadre et al., 2007), using QuickChange XL kit (Stratagene, La Jolla, CA) following the manufacturer's protocol. All mutations were confirmed by sequencing (DNA core, University of Missouri-Columbia). The cDNA of WT or mutant CFTR were co-transfected with pEGFP-C3 (Clontech, Palo, Alto, CA) to Chinese hamster ovary (CHO) cells, using Superfect transfection reagent (Qiagen, Valencia, CA) according to the manufacturer's protocols. Cells were used for patch clamp experiments at least two days after transfection.

Electrophysiological experiments and data analysis

All data were recorded at room temperature (23-25°C), using an EPC10 patch-clamp amplifier (Heka Electronic, Lambrecht, Germany). Inside-out membrane patches were excised from the transfected cells, and held at -50mV. The currents were filtered at 100 Hz with a built-in 4-pole Bessel filter and digitized online at 500 Hz. A 50/60 Hz noise eliminator (Quest Scientific, Vancouver, BC, Canada) was used to reduce 60 Hz noise. Cells were perfused with a bath solution containing (in mM): 145 NaCl, 5 KCl, 2 $MgCl_2$, 1 $CaCl_2$, 5 glucose, 5 Hepes and 20 sucrose (pH 7.4 with NaOH). The pipette solution contained (in mM): 140 NMDG-Cl, 2 $MgCl_2$, 5 $CaCl_2$ and 10 Hepes (pH 7.4 with NMDG). After establishing the inside-out configuration, the patch was perfused with a standard perfusion solution containing (in mM): 150 NMDG-Cl, 2 $MgCl_2$, 10

EGTA and 8 Tris (pH 7.4 with NMDG). The perfusion solution with the metal ions contained (in mM): 150 NMDG-Cl, 2 $MgCl_2$, 8 Tris (pH 7.4 with ~18 mM Hepes). Measurements of the steady state mean current amplitude and the fits to the dose response relationships were carried out using Igor software (Wavemetrics, Lake Oswego, OR).

Recordings with up to five channel opening steps were used for single channel kinetic analysis. Mean open times were calculated using a program developed by Dr. Csanady (Csanady, 2000) as previously described (Zhou et al, 2006). All averaged data are presented as mean ± SEM.

The Cd^{2+} dose response relationships were calculated as the ratio between the steady-state current in the presence of different [Cd^{2+}] to the current under control conditions. For the G551D mutant, since it does not respond to ATP, we used as control the current in the absence of ATP (which is the same as in the presence of 1mM ATP). For the G551C and S549C mutants, since they are ATP-dependent, we used the current in the presence of 1 mM ATP as control. The fold increase of the current in the presence of Cd^{2+} was normalized to the maximal fold increase for each mutant (100 μM for G551D, 10 μM G551D, and 5 μM for S549C).

Reagents

Mg-ATP was purchased from Sigma-Aldrich (St Louis, MO, USA), PKA was purchased from Promega (Madison, WI, USA) and Sigma (St Louis, MO, USA), and (2-

aminoethyl) methane thiosulfonate hydrobromide (MTSEA) was purchased from Toronto Research Chemicals (North York, On., Canada).

Energetic analysis of the closing rate

The idea that ligand binding energy contributes to the overall energetics of the open state allows us to analyze quantitatively the effects of ligands with different binding affinities and mutations at the ligand binding pocket on the closing rate of the channel (also known as mutant cycle analysis). Since the E1371S mutation abolishes ATP hydrolysis, gating of this mutant CFTR can be reduced to a simple closed-open transition (for example, see Vergani et al., 2005). Here we use an energetic scheme like the one shown below to differentiate effects of ligand binding at CFTR's two NBDs on the stability of the open state.

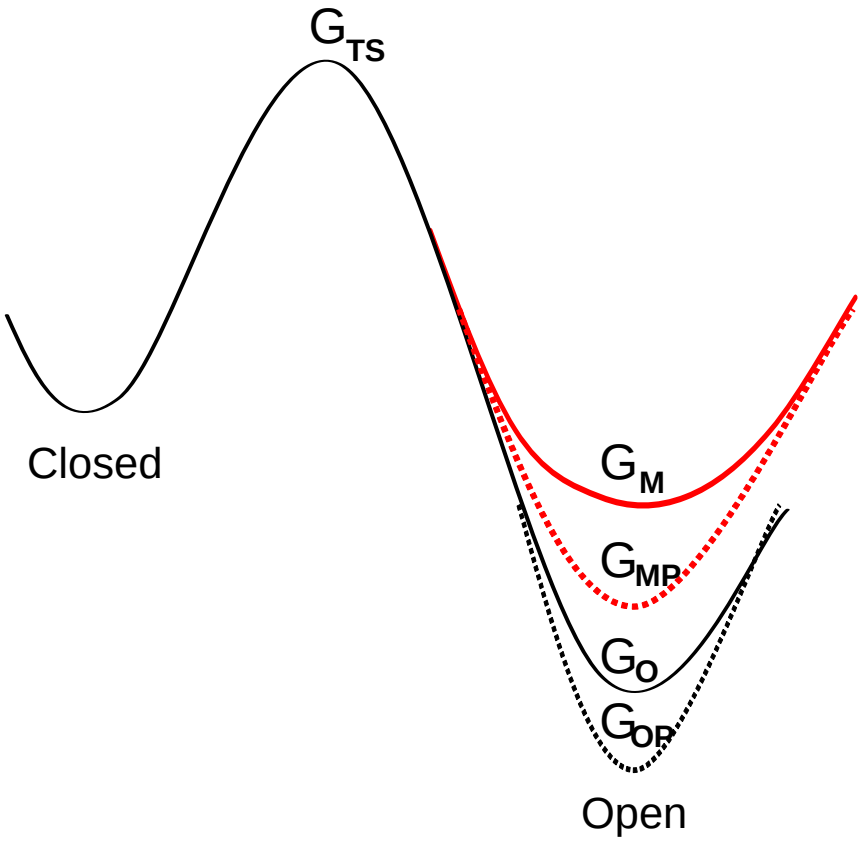

This figure shows a simplified free energy coordinate for the closed-open transition of E1371S. The open state (O) of the channel needs to overcome the activation energy ($G_{TS} - G_O$) to sojourn to the closed state. When a mutation, M, at the NBD1 site (e.g., triple glycine substitution at W401, F409, and F430 residues) destabilizes the open state to a state with the free energy of G_M, the closing rate (k_c) is increased.

$$k_c (O) = A \exp (-(G_{TS} - G_O)/RT)$$

$$k_c (M) = A \exp (-(G_{TS} - G_M)/RT)$$

A single prefactor is used in the equation since we are not using any single equation to determine ΔG. Instead, ratios of two rate constants will be calculated for comparison (see below). On the other hand, when a high affinity ATP analog (e.g., P-ATP) stabilizes the open state by providing extra binding energy, the closing rate for P-ATP-opened channels will be decreased.

$$k_c (OP) = A \exp (-(G_{TS} - G_{OP})/RT) = A \exp (-((G_{TS} - G_O) + (G_O - G_{OP}))/ RT)$$

$$k_c (MP) = A \exp (-(G_{TS} - G_{MP})/RT) = A \exp (-((G_{TS} - G_M) + (G_M - G_{MP}))/RT)$$

The ratios of the closing rates between ATP-opened and P-ATP-opened channels for O and M are:

$$k_c (O)/k_c (OP) = \exp ((G_O - G_{OP})/ RT)$$

$$k_c (M)/k_c (MP) = \exp ((G_M - G_{MP})/ RT)$$

If P-ATP stabilizes the open state by binding to the NBD2 site, the free energy gained should be the same for O and M if we assume that the binding site at NBD2 is not altered by the mutation at the NBD1 site (i.e., $G_O - G_{OP} = G_M - G_{MP}$). Then, the ratio of the closing rate between ATP-opened and P-ATP-opened channels should remain constant (i.e., k_c (O)/k_c (OP) = k_c (M)/k_c (MP)).

Data shown in Fig. II.4b contradict this prediction since k_c(O)/k_c(OP) = ~2 whereas k_c (M)/k_c (MP) = ~4. Therefore, it is likely that P-ATP's effect on the closing rate is not through its binding at the NBD2 site. On the other hand, if P-ATP stabilizes the open state by binding to the NBD1 site, the free energy gained by P-ATP binding will vary with the mutations introduced into the NBD1 binding pocket (i.e., $G_O - G_{OP} \neq G_M - G_{MP}$). Thus, the ratio of the closing rate between ATP-opened and P-ATP-opened O will be different from that of M as seen in Fig. II.4b.

The hypothesis that P-ATP binding at the NBD1 site stabilizes the open state predicts that mutations decreasing the binding affinity at the NBD2 binding pocket (e.g., Y1219G) will not affect the free energy gained by P-ATP binding. Indeed, the ratio of the closing rate between ATP-opened and P-ATP-opened Y1219G/E1371S is nearly the same as that for E1371S (Fig. II.4b). Thus, based on the mutant cycle analysis described above, we conclude that P-ATP stabilizes the open channel conformation by binding to the NBD1 site. This result together with the observation that only the mutations of the aromatic amino acids at the NBD1 site, but not the NBD2 site, affect the open time

strongly support the hypothesis that ligand binding at the NBD1 site affects the stability of the open state.

References

Aleksandrov, L., Aleksandrov, A.A., Chang, X.B., Riordan, J.R.. (2002) The first nucleotide binding domain of cystic fibrosis transmembrane conductance regulator is a site of stable nucleotide interaction, whereas the second is a site of rapid turnover. *J Biol Chem* 277: 15419–15425.

Aleksandrov, L., A. Mengos, X.-B., Chang, A., Aleksandrov, and J.R. Riordan. (2001) Differential interactions of nucleotides at the two nucleotide binding domains of CFTR. *J. Biol. Chem.* 276: 12918-12923.

Amaral, M.D., K. Kunzelmann. (2007) Molecular targeting of CFTR as a therapeutic approach to cystic fibrosis. *Trends in Pharmacological Sciences*. 28: 334-341.

Ambudkar, S.V., Kim, I.W., Xia, D., Sauna, Z.E. (2006) The A-loop, a novel conserved aromatic acid subdomain upstream of the Walker A motif in ABC transporters, is critical for ATP binding. *FEBS Lett* 580: 1049–1055.

Baker, J.M.R., Hudson, R.P., Kanelis, V., Choy, W.-Y., Thibodeau, P.H., Thomas, P.J. & Forman-Kay, J.D. (2007) CFTR regulatory region interacts with NBD1 predominantly via multiple transient helices. *Nat Struct Mol Biol* 14: 738-745.

Basso, C., Vergani, P., Nairn, A.C., Gadsby, D.C. (2003) Prolonged nonhydrolytic interaction of nucleotide with CFTR's NH2-terminal nucleotide binding domain and its role in channel gating. *J Gen Physiol* 122: 333–348.

Baukrowitz, T., Hwang, T. C., Nairn, A. C. & Gadsby, D. C. (1994) Coupling of CFTR ClK channel gating to an ATP hydrolysis cycle. *Neuron* 12, 473–482.

Berger, A.L., M. Ikuma, and M.J. Welsh. (2005). Normal gating of CFTR requires ATP binding to both nucleotide-binding domains and hydrolysis at the second nucleotide-bing domain. *Proc. Natl. Acad. Sci. USA*. 102: 455-460.

Bompadre, S.G., M. Li, T.-C. Hwang. (2008). Mechanism of G551D-CFTR potentiation by a high affinity ATP analog. *J. Biol. Chem.* 283: 5364-5369.

Bompadre, S.G., Ai, T., Cho, J.H., Wang, X., Sohma, Y., Li, M. & Hwang, T.C. (2005a) CFTR gating I: Characterization of the ATP-dependent gating of a phosphorylation-independent CFTR channel (DeltaR-CFTR). *J Gen Physiol.* 125: 361-75.

Bompadre, S.G., Cho, J.H., Wang, X., Zou, X., Sohma, Y., Li, M. & Hwang, T.C. (2005b) CFTR gating II: Effects of nucleotide binding on the stability of open states. *J Gen Physiol.* 125: 377-94.

Bompadre, S.G., Y. Sohma, M. Li, T.-C. Hwang. (2007). G551D and G1349D, two CF-associated mutations in the signature sequence of CFTR, exhibit distinct gating defects. *J. Gen. Physiol.* 129: 285-298.

Browne, B.L., V. McClendon, D.M. Bedwell. (1996) Mutations within the first LSGGQ motif of Ste6p cause defects in **a**-factor transport and mating in *Saccharomyces cerevisiae*. *Journal of Bacteriology*. 178: 1712-1719.

Caci, E. A., Caputo A., Hinzpeter N., Arous P., Fanen N.D., Sonawane A.S., Verkman R., Ravazzolo O., Zegarra-Moran L.J., Galietta. (2008) Evidence for direct CFTR inhibition by CFTR(inh)-172 based on Arg347 mutagenesis. *Biochem J*. 413: 135-142.

Cai, Z. A., Taddei, D.N., Sheppard. (2006) Differential sensitivity of the cystic fibrosis (CF)-associated mutants G551D and G1349D to potentiators of the cystic fibrosis transmembrane conductance regulator (CFTR) Cl- channel. *J. Biol. Chem.* 281: 1970-1977.

Carson, M.R., Winter, M.C., Travis, S.M. & Welsh, M.J. (1995) Pyrophosphate stimulates wild-type and mutant cystic fibrosis transmembrane conductance regulator Cl- channels. *J Biol Chem* 270: 20466-20472.

Chen, J. G., Lu, J., Lin, A.L., Davidson, F.A., Quiocho. (2003). A tweezers-like motion of the ATP-binding cassette dimer in an ABC transport cycle. *Molecular Cell*. 12: 651-661.

Chen, M. R., Abele, R., Tampe. (2004). Functional non-equivalence of ATP-binding cassette signature motifs in the transporter associated with antigen processing (TAP). *J. Biol. Chem.* 279: 46073-46081.

Chen, T.-Y., T.-C. Hwang. (2008) CLC-0 and CFTR: Chloride channels evolved from transporters. *Physiol. Rev.* 88: 351-387.

Cotton, J.F., Ostedgaard, L.S., Carson, M.R., Welsh, M.J. (1996) Effect of cystic fibrosis-associated mutations in the fourth intracellular loop of cystic fibrosis transmembrane conductance regulator. *J Biol Chem* 271: 21279–21284.

Csanady, L. (2000). Rapid kinetic analysis of multichannel records by a simultaneous fit to all dwell-time histograms. *Biophys. J.* 78: 785-799.

Csanády, L., K.W. Chan, D. Seto-Young, D.C. Kopsco, A.C. Nairn, and D.C. Gadsby. (2000) Severed channels probe regulation of gating of cystic fibrosis

transmembrane conductance regulator by its cytoplasmic domains. J. Gen. Physiol. 116: 477–500.

Csanády, L., K.W. Chan, A.C. Nairn, and D.C. Gadsby. (2005). Functional roles of nonconserved structural segments in CFTR's NH2-terminal nucleotide binding domain. J. Gen. Physiol. 125: 43-55.

Cui, L., Aleksandrov, L., Hou, Y. X., Gentzch, M., Chen, J. H., Riordan, J. R. & Aleksandrov, A. A. (2006) The role of cystic fibrosis transmembrane conductance regulator phenylalanine 508 side chain in ion channel gating. *J. Physiol.* 572: 347–358.

Davidson, A.L., Chen, J. (2004) ATP-binding cassette transporters in bacteria. *Annu Rev Biochem*. 73: 241-68.

Dawson, R.J. & Locher, K.P. (2006) Structure of a bacterial multidrug ABC transporter. *Nature*.443: 180-5.

Dean, M., Rzhetsky, A. & Allikmets, R. (2001) The human ATP-binding cassette (ABC) transporter superfamily. *Genome Res.* 11: 1156–1166.

Diederichs, K., Diez, J., Greller, G., Muller, C., Breed, J., Schnell, C., Vonrhein, C., Boos, W. & Welte, W. (2000) Crystal structure of MalK, the ATPase subunit of the trehalose/maltose ABC transporter of the archaeon Thermococcus litoralis. *EMBO J*. 19: 5951-5961.

Gadsby, D.C., Vergani, P. & Csanady, L. (2006) The ABC protein turned chloride channel whose failure causes cystic fibrosis. *Nature*. 440: 477-83.

Gadsby, D.C., Nairn, A.C.. (1999) Control of CFTR channel gating by phosphorylation and nucleotide hydrolysis. *Physiol Rev* 79 *Suppl*: S77–S107.

Gaudet, R. & Wiley, D.C. (2001) Structure of the ABC ATPase domain of human TAP1, the transporter associated with antigen processing. *EMBO J*. 20: 4964-4972.

Gillespie, P.G., S.K.H. Gillespie, J.A. Mercer, K. Shah, and K.M. Shokat. (1999) Engineering of the myosin-Ib nucleotide-binding pocket to create selective sensitivity to N6-modified ADP analogs. *J. Biol. Chem.* 274: 31373-31381.

Gunderson, K. L. & Kopito, R. R. (1994) Effects of pyrophosphate and nucleotide analogs suggest a role for ATP hydrolysis in cystic fibrosis transmembrane regulator channel gating. *J. Biol. Chem.* 269, 19 349–19 353.

Gunderson, K.L., Kopito, R.R. (1995) Conformational states of CFTR associated with channel gating: the role ATP binding and hydrolysis. *Cell* **82**, 231-239.

Hanrahan, J.W., Wioland, M.A.. (2004) Revisiting cystic fibrosis transmembrane conductance regulator structure and function. *Proc Am Thorac Soc* 1: 17–21.

Higgins, C.F., Linton, K.J. (2004) The ATP switch model for ABC transporters. *Nat Struct Mol Biol* 11: 918–926.

Hollenstein, K., Frei, D.C., Locher, K.P. (2007) Structure of an ABC transporter in complex with its binding protein. *Nature* 446: 213–216.

Hopfner, K.P., Karcher, A., Shin, D.S., Craig, L., Arthur, L.M., Carney, J.P., Tainer, J.A. (2000) Structural biology of Rad50 ATPase: ATP-driven conformational control in DNA double-strand break repair and the ABC-ATPase superfamily. *Cell* 101: 789-800.

Huai, Q., J. Colicelli, and H. Ke. (2003) The crystal structure of AMP-bound PDE4 suggests a mechanism for phosphodiesterase catalysis. *Biochemistry*. 42: 13220-13226

Huai, Q., Y. Liu, S.H. Francis, J.D. Corbin, and H. Ke. (2004) Crystal structures of phosphodiesterases 4 and 5 in complex with inhibitor 3-isobutyl-methylxanthine suggest a conformation determinant of inhibitor selectivity. *J. Biol. Chem.* 279: 13095-13101.

Huang, S.-Y., Bolser, D., Liu, H.-Y., Hwang, T.-C. & Zou, X. (2009) Molecular modeling of the heterodimer of human CFTR's nucleotide-binding domains using a protein-protein docking approach. *J Mol Graph Model* **27**, 822-828.

Hung, L.W., Wang, I.X., Nikaido, K., Liu, P.Q., Ames, G.F. & Kim, S.H. (1998) Crystal structure of the ATP-binding subunit of an ABC transporter. *Nature* 396: 703-707.

Hwang, T. C., Nagel, G., Nairn, A. C. & Gadsby, D. C. (1994) Regulation of the gating of cystic fibrosis transmembrane conductance regulator Cl channels by phosphorylation and ATP hydrolysis. *Proc. Natl Acad. Sci. USA* 91, 4698–4702.

Hwang, T.C. and Sheppard, D.N. (2009) Gating of the CFTR Cl- channel by ATP-driven nucleotide-binding domain dimerisation. *J. Physiol.* 587: 2151-2161.

Karpowich, N., Martsinkevich, O., Millen, L., Yuan, Y.R., Dai, P.L., MacVey, K., Thomas, P.J. & Hunt, J.F. (2001) Crystal structures of the MJ1267 ATP binding cassette reveal an induced-fit effect at the ATPase active site of an ABC transporter. *Structure (Camb).* 9: 571-586.

Lewis, H.A., S.G. Buchanan, S.K. Burley, K. Conners, M. Dickey, M. Dorwart, R. Fowler, X. Gao, W.B. Gruggino, W.A. Hendrickson, J.F. Hunt, M.C. Kearins, D. Lorimer, P.C. Maloney, K.W. Post, K.R. Rajashankar, M.E. Rutter, J.M. Sauder, S. Shriver, P.H. Thibodeau, P.J. Thomas, M. Zhang, X. Zhao, S. Emtage. (2004)

Structure of nucleotide-binding domain 1 of the cystic fibrosis transmembrane conductance regulator. *EMBO J.* 23: 282-293.

Lewis, H.A., Zhao, X., Wang, C., Sauder, J.M., Rooney, I., Noland, B.W., Lorimer, D., Kearins, M.C., Conners, K., Condon, B., Maloney, P.C., Guggino, W.B., Hunt, J.F. & Emtage, S. (2005) Impact of the deltaF508 mutation in first nucleotide-binding domain of human cystic fibrosis transmembrane conductance regulator on domain folding and structure. *J Biol Chem.* 280: 1346-53.

Li, C., Ramjeesingh, M., Wang, W., Garami, E., Hewryk, M., Lee, D., Rommens, J.M., Galley, K. & Bear, C.E. (1996) ATPase activity of the cystic fibrosis transmembrane conductance regulator. *J. Biol. Chem.* 271: 28463-28468.

Locher, K.P., Lee, A.T. & Rees, D.C. (2002) The E. coli BtuCD structure: a framework for ABC transporter architecture and mechanism. *Science.* 296: 1091-8.

Lu, G., Westbrooks, J.M., Davidson, A.L., Chen, J. (2005) ATP hydrolysis is required to reset the ATP-binding cassette dimer into the restingstate conformation. *Proc Natl Acad Sci USA* 102: 17969–17974.

Ma, T., J.R. Thiagarajah, H. Yang, N.D. Sonawane, C. Folli, L.J. Galietta, A.S. Verkman. (2002) Thiazolidinone CFTR inhibitor identified by high-throughput screening blocks cholera toxin-induced intestinal fluid secretion. *The Journal of Clinical Investigation*. 110: 1651-1658.

MacLeod, K.J., E. Vasilyeva, J.D. Baleja, and M. Forgac. (1998) Mutational analysis of the nucleotide binding sites of the yeast vacuolar proton-translocating ATPase. *J. Biol. Chem.* 273: 150-156.

Mathews, C.J., J.A. Tabcharani, X.-B. Chang, T.J. Jensen, J.R. Riordan, and J.W. Hanrahan. (1998) Dibasic protein kinase A sites regulate bursting rate and nucleotide sensitivity of the cystic fibrosis transmembrane conductance regulator chloride channel. *J. Physiol.* 508: 365-377

Monod, J., J. Wyman, J.P. Changeus. (1965) On the nature of allosteric transitions: A plausible model. *J. Mol. Biol.* 12: 88-118.

Moody, J.E., Millen, L., Binns, D., Hunt, J.F. & Thomas, P.J. (2002) Cooperative, ATP-dependent association of the nucleotide binding cassettes during the catalytic cycle of ATP-binding cassette transporters. *J. Biol. Chem.* 277: 21111-21114.

Mornon, J.-P., Lehn, P. & Callebaut, I. (2008) Atomic model of human cystic fibrosis transmembrane conductance regulator: membrane-spanning domains and coupling interfaces. *Cell Mol Life Sci* 65, 2594-2612.

Muallem D., and Vergani P. (2009) ATP hydrolysis-driven gating in cystic fibrosis transmembrane conductance regulator. *Phil. Trans. R. Soc. B* 364: 247–255.

Pinkett, H.W., Lee, A.T., Lum, P., Locher, K.P., Rees, D.C. (2007) An inwardfacing conformation of a putative metal-chelate-type ABC transporter. *Science* 315: 373–377.

Powe, A.C.Jr., L. Al-Nakkash, M. Li, and T.-C. Hwang. (2002) Mutation of Walker-A lysine 464 in cystic fibrosis transmembrane conductance regulator reveals functional interaction between its nucleotide-binding domains. *J. Physiol.* 539: 333-346.

Ramaen, O., Leulliot, N., Sizun, C., Ulryck, N., Pamlard, O., Lallemand, J.Y., Tilbeurgh, H., Jacquet, E.. (2006) Structure of the human multidrug resistance protein 1

nucleotide binding domain 1 bound to Mg2_/ATP reveals a non-productive catalytic site. *J Mol Biol* 359: 940–949.

Ramjeesingh, M., Li, C., Garami, E., Huan, L.J., Galley, K., Wang, Y. & Bear, C.E. (1999) Walker mutations reveal loose relationship between catalytic and channel-gating activities of purified CFTR (cystic fibrosis transmembrane conductance regulator). *Biochemistry* **38**, 1463-1468.

Ren, X.Q., T. Furukawa, M. Haraguchi, T. Sumizawa, S. Aoki, M. Kobayashi, S. Akiyama. (2004) Function of the ABC signature sequences in the human multidrug resistance protein 1. *Mol. Pharmacol.* 65: 1536-1542.

Riordan, J.R., J.M. Rommens, B. Kerem, N. Alon, R. Rozmahel, Z. Grzelczak, J. Zielenski, S. Lok, N. Plavsic, J.-L. Chou, M.L. Drumm, M.C. Iannuzzi, F.S. Collins, L.-C. Tsui. (1989) Identification of the cystic fibrosis gene: cloning and characterization of complementary DNA. *Science*. 245: 1066-1073.

Rothberg, B.S., K.S. Shin, G. Yellen. (2003) Movements near the gate of a hyperpolarization-activated cation channel. *J. Gen. Physiol.* 122: 501-510.

Rowe, S.M., Miller, S., Sorscher, E.J. (2005) Cystic fibrosis. *N Engl J Med* 352:1992–2001.

Rulisek, L. J. Vondrasek. (1998) Coordination geometries of selected transition metal ions (Co^{2+}, Ni^{2+}, Cu^{2+}, Zn^{2+}, Cd^{2+}, and Hg^{2+}) in metalloproteins. *Journal of inorganic biochemistry*. 71: 115-127.

Schmees, G., A. Stein, S. Hunke, H. Landmesser, E. Schneider. (1999) Functional consequences of mutations in the conserved 'signature sequence' of the ATP-binding- cassete protein MalK. *Eur. J. Biochem.* 266: 420-430.

Schmitt, L., Benabdelhak, H., Blight, M.A., Holland, I.B. & Stubbs, M.T. (2003) Crystal structure of the nucleotide-binding domain of the ABC-transporter haemolysin B: identification of a variable region within ABC helical domains. *J. Mol. Biol*. 330: 333-342.

Scott-Ward, T.S., Cai, Z., Dawson, E.S., Doherty, A., Da, Paula, A.C., Davidson, H., Porteous, D.J., Wainwright, B.J., Amaral, M.D., Sheppard, D.N. & Boyd, A.C. (2007). Chimeric constructs endow the human CFTR Cl- channel with the gating behavior of murine CFTR. *Proc Natl Acad Sci U S A* 104: 16365-16370.

Seibert, F.S., Linsdell, P., Loo, T.W., Hanrahan, J.W., Riordan, J.R. & Clarke, D.M. (1996) Cytoplasmic loop three of cystic fibrosis transmembrane conductance regulator contributes to regulation of chloride channel activity. *J Biol Chem.* 271: 27493-9.

Seibert, F.S., Linsdell, P., Loo, T.W., Hanrahan, J.W., Clarke, D.M. & Riordan, J.R. (1996) Disease-associated mutations in the fourth cytoplasmic loop of cystic fibrosis transmembrane conductance regulator compromise biosynthetic processing and chloride channel activity. *J Biol Chem.* 271: 15139-45.

Seibert, F. S., Jia, Y., Mathews, C. J., Hanrahan, J. W., Riordan, J. R., Loo, T. W.& Clarke, D. M. (1997) Disease-Associated Mutations in Cytoplasmic Loops 1 and 2 of Cystic Fibrosis Transmembrane Conductance Regulator Impede Processing or Opening of the Channel. *Biochemistry*; 36: 11966-74.

Seibert, F.S., Chang, X.B., Aleksandrov, A.A., Clarke, D.M., Hanrahan, J.W., Riordan, J.R. (1999) Influence of phosphorylation by protein kinase A on CFTR at the cell surface and endoplasmic reticulum. *Biochim Biophys Acta* 1461: 275–283.

Serohijos, A.W.R., Hegedús, T., Aleksandrov, A.A., He, L., Cui, L., Dokholyan, N.V. & Riordan, J.R. (2008). Phenylalanine-508 mediates a cytoplasmic-membrane domain contact in the CFTR 3D structure crucial to assembly and channel function. *Proc Natl Acad Sci U S A* **105**, 3256-3261.

Shah, K., Y. Liu, C. Deirmengian, and K.M. Shokat. (1997). Engineering unnatural nucleotide specificity for Rous sarcoma virus tyrosine kinase to uniquely label its direct substrates. *Proc. Natl. Acad. Sci. USA*. 94: 3565-3570.

Sheppard, D.N., Welsh, M.J. (1999) Structure and function of the CFTR chloride channel. *Physiol Rev* 79 *Suppl*: S23–S45.

Shyamala, V., V. Baichwal, E. Beall, and G.F. Ames. (1991). Structure-function analysis of the histidine permease and comparison with cystic fibrosis mutations. *J. Biol. Chem.* 266: 18714-18719.

Smit, L.S., Wilkinson, D.J., Mansoura, M.K., Collins, F.S. & Dawson, D.C. (1993) Functional roles of the nucleotide-binding folds in the activation of the cystic fibrosis transmembrane conductance regulator. *Proc. Natl. Acad. Sci. USA* 90:9963-9967.

Smith, P., C.N. Karpowich, L. Millen, J.E. Moody, J. Rosen, P.J. Thomas, J.F. Hunt. (2002). ATP binding to the motor domain from an ABC transporter drives formation of a nucleotide sandwich dimer. *Mol Cell*. 10: 139-149.

Stratford, F.L., Ramjeesingh, M., Cheung, J.C., Huan, L.J. & Bear, C.E. (2007). The Walker B motif of the second nucleotide binding domain (NBD2) of CFTR plays a key role in ATPase activity of the NBD1-NBD2 heterodimer. *Biochem J* 401: 581-586.

Sugita, M., Y. Yue, and J.K. Foskett. (1998). CFTR Cl^- channel and CFTR-associated ATP channel: distinct pores regulated by common gates. *EMBO J.* **17:** 898-908.

Szabo, K., G. Szakacs, T. Hegedus, and B. Sarkadi. (1999). Nucleotide occlusion in the human cystic fibrosis transmembrane conductance regulator: Different patterns in the two nucleotide binding domains. *J. Biol. Chem.* 274: 12209-12212.

Szentpetery, Z., A. Kern, K. Liliom, B. Sarkadi, A. Varadi, E. Bakos. (2004). The role of the conserved glycines of ATP-binding cassette signature motifs of MRP1 in the communication between the substrate-binding site and the catalytic centers. *J. Biol. Chem.* 279: 41670-41678.

Tombline, G., L.A. Bartholomew, I.L. Urbatsch, and A.E. Senior. (2004). Combined mutation of catalytic glutamate residues in the two nucleotide binding domains of P-glycoprotein generates a conformation that binds ATP and ADP tightly. *J. Biol. Chem.* **279**: 31212-31220.

Vankeerberghen, A., Cuppens, H., Cassiman, J.J. (2002). The cystic fibrosis transmembrane conductance regulator: an intriguing protein with pleiotropic functions. *J Cyst Fibros* 1: 13–29.

Venglarik, C. J., Schultz, B. D., Frizzell, R. A. & Bridges, R. J. (1994) ATP alters current fluctuations of cystic fibrosis transmembrane conductance regulator: evidence for a three-state activation mechanism. *J. Gen. Physiol.* 104, 123–146.

Verdon, G., Albers, S.V., Dijkstra, B.W., Driessen, A.J. & Thunnissen, A.M. (2003) Crystal structures of the ATPase subunit of the glucose ABC transporter from Sulfolobus solfataricus: nucleotide-free and nucleotide-bound conformations. *J. Mol. Biol.* 330: 343-358.

Vergani, P., Nairn, A.C. & Gadsby, D.C. (2003) On the mechanism of MgATP-dependent gating of CFTR Cl^- channels. *J. Gen. Physiol.* 121: 17-36.

Vergani, P., S.W. Lockless, A.C. Nairn, D.C. Gadsby. (2005). CFTR channel opening by ATP-driven tight dimerization of its nucleotide-binding domains. *Nature*. 433: 876-880.

Walker, J.E., Saraste, M., Runswick, M.J. and Gay, N.J. (1982) Distantly related sequences in the alpha- and beta-subunits of ATP synthase, myosin, kinases and other ATP-requiring enzymes and a common nucleotide binding fold. *EMBO J.*, 1, 945–951

Wang, F., Zeltwanger, S., Yang, I.C.H., Nairn, A.C. & Hwang, T.-C. (1998). Actions of genistein on cystic fibrosis transmembrane conductance regulator channel gating: evidence for two binding sites with opposite effects. *J Gen Physiol* **111**, 477-490.

Wang, X., Bompadre, S.G., Li, M. & Hwang, T.-C. (2009). Mutations at the signature sequence of CFTR create a Cd^{2+}-gated chloride channel. *J Gen Physiol* **133**, 69-77.

Wang, Y., Loo, T.W., Bartlett, M.C., Clarke, D.M. (2007) Correctors promote maturation of cystic fibrosis transmembrane conductance regulator (CFTR)-processing mutants by binding to the protein. *J Biol Chem.* 282: 33247-51

Webster, S.M., Del Camino, D., Dekker, J.P. & Yellen, G. (2004) Intracellular gate opening in Shaker K^+ channels defined by high-affinity metal bridges. *Nature* 428: 864-8.

Welsh, M.J. & Smith, A.E. (1993) Molecular mechanisms of CFTR chloride channel dysfunction in cystic fibrosis. *Cell* 73: 1251-1254.

Winter, M. C., Sheppard, D. N., Carson, M. R. & Welsh, M. J. (1994) Effect of ATP concentration on CFTR ClK channels: a kinetic analysis of channel regulation. *Biophys. J.* 66, 1398–1403.

Winter, M.C. & Welsh, M.J. (1997). Stimulation of CFTR activity by its phosphorylated R domain. *Nature* 389, 294-296.

Yuan, Y.R., Blecker, S., Martsinkevich, O., Millen, L., Thomas, P.J. & Hunt, J.F. (2001) The crystal structure of the MJ0796 ATP-binding cassette. Implications for the structural consequences of ATP hydrolysis in the active site of an ABC transporter. *J. Biol. Chem.* 276: 32313-32321.

Zaitseva, J., S. Jenewein, A. Wiedenmann, H. Benabdelhak, I.B. Holland, L. Schmitt. (2005). Functional characterization and ATP-induced dimerization of the isolated ABC-domain of the haemolysin B transporter. *Biochemistry*. 44: 9680-9690.

Zeltwanger, S., Wang, F., Wang, G.T., Gillis, K.D. & Hwang, T.-C. (1999). Gating of cystic fibrosis transmembrane conductance regulator chloride channels by adenosine triphosphate hydrolysis: quantitative analysis of a cyclic gating scheme. *J Gen Physiol* **113,** 541-554.

Zhang, K.Y.J., G.L. Card, Y. Suzuki, D.R. Artis, D. Fong, S. Gillette, D. Hsieh, J. Neiman, B.L. West, C. Zhang, M.V. Milburn, S.-H. Kim, J. Schlessinger, G Bollag. (2004). A Glutamine Switch Mechanism for Nucleotide Selectivity by Phosphodiesterases. *Mol.Cell*. 15: 279-286.

Zhao, Q. and X. B. Chang. (2004). Mutation of the aromatic amino acid interacting with adenine moiety of ATP to a polar residue alters the properties of multidrug resistance protein 1. *J. Biol. Chem*. 279: 48505-48512.

Zhao, X., Conners, K., Emtage, S., Lu, F. & Atwell, S. (2008). The crystal structure of the second nucleotide binding domain (NBD2) of CFTR suggests NBD2 subdomain movements are involved in channel opening. *Pediatr Pulmonol Suppl* **31**, 205.

Zhou, Z., Hwang, T.C.. (2009) Gating of cystic fibrosis transmembrane conductance regulator (CFTR) chloride channels. *Adv Mol Cell Biol.* In press.

Zhou, Z., Wang, X., Li, M., Sohma, Y., Zou, X. & Hwang, T.-C. (2005). High affinity ATP/ADP analogues as new tools for studying CFTR gating. *J Physiol* **569**, 447-457.

Zhou, Z., Wang, X., Liu, H.-Y., Zou, X., Li, M. & Hwang, T.-C. (2006). The two ATP binding sites of cystic fibrosis transmembrane conductance regulator (CFTR) play distinct roles in gating kinetics and energetics. *J Gen Physiol* **128**, 413-422.

Zou, X. & Hwang, T.-C. (2001) Gating of CFTR by ATP hydrolysis: Structure and Function. *Biochemistry* 40: 5579-5586.

VITA

Xiaohui Wang was born in June 13, 1971, in Henan, China. Between year 1991 and 1995, she attended Wuhan University where she received her B. S. degree in physics. From 1995 to 2001, she worked as government officer in Department of education and information center, Bureau of environment protection in Guangzhou, Guangdong. In January 2002, she came to the Unites States of America. In December 2003, she started to work as research specialist in Dalton Cardiovascular Research Center. In August 2004, she enrolled the Ph.D. program in Medical physiology and pharmacology department in Medical school at the University of Missouri-Columbia. She had been working in CFTR gating since then in Dalton Cardiovascular Research Center, Columbia, Missouri.